UNIVERSITY OF VERONA

DEPARTMENT OF

Medicine, Section of General Pathology

GRADUATE SCHOOL OF

Life and Health Sciences

DOCTORAL PROGRAM IN

Inflammation, Immunity and Cancer

WITH THE FINANCIAL CONTRIBUTION OF

Italian Multiple Sclerosis Foundation

Cycle XXIX

TITLE OF THE DOCTORAL THESIS

Role of integrins in the trafficking of Th1 and Th17 cells in the central nervous system during experimental autoimmune encephalomyelitis

S.S.D. MED/04

Coordinator: Prof./ssa Gabriela Constantin

Signature

Tutor: Prof./ssa Gabriela Constantin

Signature

Co-tutor Dott./ssa Barbara Rossi

Signature

Doctoral Student: Dott./ssa Silvia Dusi

Signature

Role of integrins in the trafficking of Th1 and Th17 cells in the central nervous system during experimental autoimmune encephalomyelitis

Silvia Dusi

PhD thesis

Verona, 20th february 2017

Table of Contents

Riassunto

La Sclerosi Multipla (SM) è una patologia infiammatoria autoimmune cronica, disabilitante e demielinizzante, del sistema nervoso centrale (SNC). La migrazione di cellule T autoreattive e la loro riattivazione attraverso la presentazione antigenica effettuata dalle locali cellule presentanti l'antigene, rappresentano due eventi critici nella patogenesi della SM e nel suo modello animale, l'encefalite autoimmune sperimentale (EAE). Le risposte ai potenziali antigeni all'interno del SNC richiedono una migrazione a lungo raggio, comunicazione a corto raggio e contatti cellula-cellula diretti con le cellule presentanti l'antigene.

Il principale obiettivo di questo studio è indagare il ruolo delle integrine αLβ2 (LFA-1) e α4 (VLA-4 and α4β7) nella migrazione e nella motilità delle cellule autoreattive Th1 e Th17 in corso di EAE all'interno del midollo spinale utilizzando le moderne tecniche di microscopia intravitale.

La microscopia intravitale permette di visualizzare questi processi dentro il midollo spinale, il quale rappresenta il principale sito di infiammazione durante l'EAE. Mediante la microscopia intravitale in epifluorescenza abbiamo prima di tutto investigato il ruolo delle integrine α4 e LFA-1 nella migrazione delle cellule autoreattive Th1 e Th17 all'interno dei vasi piali del midollo spinale durante la fase preclinica, l'esordio e la fase cronica di EAE. Abbiamo utilizzato un modello di EAE immunizzando topi C57BL/6 con il peptide MOG_{35-55}. Le cellule Th1 e Th17 MOG-specifiche sono state prodotte *in vitro* da topi TCR-transgenici 2D2, marcate con label fluorescenti e iniettate in endovena nei topi immunizzati direttamente prima dell'acquisizione.

I nostri risultati pongono l'accento su un ruolo selettivo per l'integrina LFA-1 nella migrazione delle cellule Th1 in particolare durante le prime fasi di malattia. Ruolo che invece non è svolto in fase cronica di malattia.

Inoltre, il blocco della subunità α4, ma non dell'integrina α4β7 inibisce fortemente sia il rotolamento sia l'adesione stabile delle cellule Th1 all'endotelio infiammato. Questo suggerisce l'integrina VLA-4 come principale mediatrice della migrazione delle Th1 nel SNC infiammato in corso di EAE. Di notevole interesse è inoltre il selettivo ruolo per l'integrina α4β7 evidenziato in particolare

nell'adesione stabile esclusivamente delle cellule Th17 all'esordio ed in fase cronica di malattia.

Successivamente, per studiare la motilità intraparenchimale delle cellule Th1 e Th17 nel midollo spinale durante la fase preclinica della patologia, il picco di malattia e la fase cronica abbiamo utilizzato la microsocopia laser a due fotoni.

I nostri risultati dimostrano una massiva infiltrazione di Th1 e Th17 nel parenchima del SNC al picco di malattia, mentre la migrazione di queste cellule durante le altre fasi della malattia è significativamente minore.

In seguito, il nostro studio si è focalizzato sulla fase clinica della malattia e abbiamo osservato che le cellule Th1 e le cellule Th17 mostrano differenze significative nelle componenti direzionali, con le cellule Th1 che si muovono velocemente in direzione rettilinea, coprendo lunghe distanze nel parenchima del midollo spinale, mente le cellule Th17 girano intorno in un volume specifico del tessuto facendo stop and go. In particolare, il blocco dell'integrina LFA-1 influenza drasticamente le dinamiche delle cellule, portando ad una riduzione nella velocità e interferendo con il loro pattern di motilità rettilinea. Inoltre, in presenza di un anticorpo bloccante anti-LFA-1, le cellule Th17 mostrano una riduzione di velocità drastica. Diversamente, l'anticorpo anti-α4 non ha nessun effetto sul comportamento motile delle Th1, ma riduce fortemente la velocità delle Th17 suggerendo che l'integrina VLA-4 non sia richiesta per la motilità intraparenchimale durante l'EAE. Tuttavia, alla luce dei risultati ottenuti in precedenza mediante microscopia intravitale, va preso in considerazione un selettivo ruolo esercitato dall'integrina $\alpha4\beta7$ nella motilità intraparenchimale delle Th17. Complessivamente, i nostri risultati suggeriscono che l'LFA-1 sia la principale integrina che controlla la motilità delle cellule Th1 e Th17 e che $\alpha4\beta7$ sia invece selettivamente coinvolta nella motilità delle cellule Th17 nel midollo spinale in condizioni infiammatorie al picco di malattia. A sostegno di questi risultati abbiamo testato un trattamento terapeutico mediante blocco locale, a livello intratecale, delle integrine LFA-1 e $\alpha4\beta7$ nel nostro modello murino di EAE cronica. Entrambi i trattamenti hanno evidenziato una riduzione nello sviluppo della malattia che suggerisce l'importanza di interferire direttamente con le dinamiche delle cellule pro infiammatorie a livello del SNC.

Approfondire dunque la conoscenza dei meccanismi molecolari che controllano la motilità intratissutale di cellule T attivate nel SNC potrebbe aiutarci a identificare nuove strategie terapeutiche per le patologie autoimmuni cerebrali croniche.

Abstract

Multiple sclerosis (MS) is a chronic disabling autoimmune inflammatory demyelinating disease of the central nervous system (CNS). The migration of autoreactive T cells from the blood into the CNS and their reactivation through antigen presentation by local antigen presenting cells (APCs) represent critical events in the pathogenesis of MS and its animal model, the experimental autoimmune encephalomyelitis (EAE). The responses to potential antigens inside the CNS require long-range migration of cells, short-range communication and direct cell-cell contact with APCs.

The **main goal** of this study was to investigate the role of αLβ2 (LFA-1) and α4 (VLA-4 and α4β7) integrins in the migration and motility behavior of Th1 and Th17 cells, which represent key players in the induction of EAE, using intravital microscopy approaches.

Intravital microscopy techniques allow the visualization of T cell migration and reactivation in the spinal cord (SC), which represents the main inflammation site during EAE. By using epifluorescence intravital microscopy (IVM) we first studied the roles of α4 and LFA-1 integrins in Th1 and Th17 cell adhesion in the pial vessels of spinal cord (SC) venules in mice immunized with MOG_{35-55} peptide during the preclinical phase, disease onset and chronic phase of disease. We used an EAE model by immunization of C57BL/6 mice with MOG_{35-55} peptide. MOG_{35-55}-specific Th1 and Th17 cells were produced *in vitro* from 2D2 TCR transgenic mice, labeled with fluorescent dyes and intravenously injected in immunized mice before imaging. Our results underlined a selective role for LFA-1 integrin in Th1 cell recruitment in inflamed SC vessels during the early phases of the disease but not during the chronic phase. Moreover, blocking antibodies against the α4 subunit, but not blockade of α4β7 integrin greatly inhibited rolling and firm adhesion of Th1 cells in the SC venules during all disease phases, suggesting that VLA-4 is the major molecule involved in Th1 cell adhesion in the SC venules during EAE. Interestingly, blockade of α4β7 integrin led to a significant reduction of firm adhesion in Th17 cells at the onset and chronic phase of EAE indicating a selective role of α4β7 integrin in the recruitment of Th17 cells in the inflamed CNS.

Taking advantage of two-photon laser microscopy (TPLM) approach we next investigated the motility behavior of fluorescently labeled Th1 and Th17 cells within SC parenchyma during different disease phases. Our results showed a massive infiltration of Th1 and Th17 cells in the CNS parenchyma at disease peak, whereas the migration of these cells during other phases of disease was significantly lower. Furthermore, Th1 and Th17 cells displayed significant differences in the directional component, with Th1 cells moving faster in straight directions covering long distances deep in the SC parenchyma, whereas Th17 cells moved around in a specific volume of tissue in a stop and go mode. Notably, the blockade of LFA-1 integrin drastically affected the dynamics of Th1 cells leading to a reduction in velocity and interfering with their straight-line motility pattern. Moreover, Th17 cells displayed a drastic reduction of velocity in the presence of a blocking anti-LFA-1 antibody. The analysis of cellular morphology suggested that LFA-1 is actively involved in the cytoskeleton rearrangements necessary for T cell amoeboid migration inside the CNS, but had no role in the cytoskeleton dynamics in Th17 cells. Notably, $\alpha 4$ integrins had no role in Th1 cells motility, but drastically reduced the dynamics of Th17 cells inside the SC parenchyma. To check the therapeutic relevance of our intravital microscopy findings, we performed intrathecal injection of anti-LFA-1 or anti-$\alpha 4\beta 7$ antibodies at disease onset and observed a significant inhibition of EAE progression in mice immunized with MOG_{35-55} peptide. Collectively, our data demonstrate that LFA-1 integrin differently controls intraparenchymal Th1 and Th17 cells dynamics, whereas $\alpha 4\beta 7$ integrin is selectively involved in Th17 cell trafficking in the CNS during EAE. Furthermore, our results suggest that interfering with the molecular mechanisms controlling intraparenchymal dynamics of activated T cells may represent a new therapeutic strategy for CNS autoimmune diseases.

Introduction

Multiple sclerosis: the history of a disease

Multiple sclerosis (MS) is a chronic, often disabling autoimmune inflammatory disorder of the nervous system (CNS) mostly affecting the young adult population. Jean-Martin Charcot, neurologist at the Hôpital de Salpétrière, well defined for the first time the features of MS, as "le sclérose en plaque", in 1868 (Orrell RW, *J R Soc Med* 2005). MS is a disease affecting approximately 2.5 million people worldwide, counting 250,000 to 400,000 people in the United States (Noonan CW et al., *Neurology*, 2002; Ascherio A and Munger K, *Semin Neurol*, 2008) and similar rates in Europe (Pugliatti M et al., *Eur J Neurol*, 2006). As is in the case of many other autoimmune diseases, evidence suggests that the incidence of MS is increasing (Orton SM et al., *Lancet Neurol*, 2006).

The disease most often starts between 20 and 40 years of age, and affects women more frequently than man (Compston A and Coles A, *Lancet*, 2008). MS can follow different patterns of evolution and varying rates of disability. In 1996, the US National Multiple Sclerosis Society (NMSS) Advisory Committee on Clinical Trials defined the clinical subtypes of MS and provided standardized definitions for four MS clinical course: relapsing-remitting (RR), secondary progressive (SP), primary progressive (PP) and progressive relapsing (PR) At disease onset, 80% of patients show an acute episode affecting one or several sites, which is known as the clinically isolated syndrome (CIS), while 20% of patients display primary progressive MS (PPMS). This initial transient inflammation in CIS leads to successive episodes of neurological dysfunction (this form of disease is called relapsing-remitting MS, RRMS) at the early course of disease that usually recover and transient remyelination occurs. If these episodes were accompanied by whitematter abnormalities detected by magnetic resonance imaging (MRI) at clinically unaffected sites, the chance of a second attack of demyelination subsequently recurring, accomplishing the diagnostic criteria for relapsing-remitting multiple sclerosis. Over time symptoms accumulate leading to chronic progressive disability for the majority of people with the disorder (**Fig. 1**). Progressive forms of MS are associated with gradual loss of neurological function

and ascending paralysis and are thought to be in part independent of inflammation. In all these situations, progression starts at around 40 years of age. Although MS occurs most commonly in young adults, it is also diagnosis in children and adolescents. They take more years to reach from onset the secondary progressive stage than adults, but anyhow do so at a younger age. In all disease forms, the clinical course takes several decades to evolve (Confravreux C and Vukusic S, *Brain* 2005; Compston A and Coles A, *Lancet* 2008).

RRMS, which is the most common form of MS, is associated with acute inflammatory episodes resulting in a reduction in neurological function. Patients may experience some recovery between relapses, but the majority of patients with RRMS evolve to a more progressive form, termed secondary progressive MS (SPMS), which is associated with gradual loss of neurological function and ascending paralysis and is thought to be independent of inflammation.

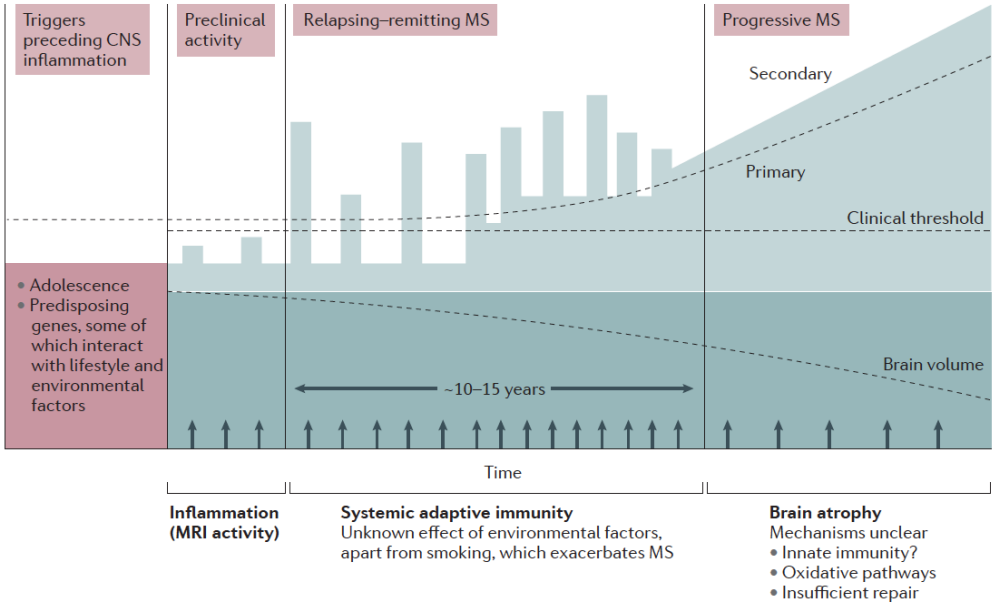

Figure. 1 Progression of multiple sclerosis. Different risk factors play a role during subclinical phase of disease triggering CNS inflammation (*red area*). Progression of MS takes several years (*green area*). Bars denote inflammatory events that cause damage to CNS, although some of which do not achieve clinical thresholds. Arrows show episodes of new inflammation detected by MRI, that results more frequent than clinical relapses (Picture adapted from Olsson T et al., *Nat Rev Neurol,* 2016).

MS is characterized by perivascular infiltration of mononuclear cells that includes lymphocytes and macrophages (Prineas JW, *Handbook of Multiple Sclerosis*,

1996). These inflammatory plaques, determined using magnetic resonance imaging (MRI), represent the pathological hallmark of MS (Frohman et al., *N Engl J Med*, 2006).

Although the precise etiology of MS remains not well understood and environmental factors are still unknown, recently the identification of genetic variants affecting the development of the disease has grown almost exponentially.

The cause of the recurrent inflammation in MS is now generally accepted to be autoimmune in nature. Studies demonstrating the presence of inflammatory cells and their products in the brain lesions of MS patients, in addition to reports from animal models, has led to the generally accepted hypothesis that disease is mediated by pathogenic T cell responses against myelin antigens, followed by a broader neurodegenerative process (Compston A and Coles A, *Lancet,* 2008). Leucocyte infiltration from peripheral circulation through the blood-barrier brain (BBB) causes the activation of microglia and astrocytes leading to the myelin sheath and the underlying axon damage.

Multiple sclerosis: the pathogenesis from peripheral side to the central nervous system

The pathogenesis leading to demyelination includes 3 major processes. The first step is establishment of autoimmunity to CNS myelin components, in which molecular mimicry between infectious agents and myelin antigens may play a role (Wucherpfenning KW and Strominger JL, *Cell*, 1995) (**Fig. 2**).

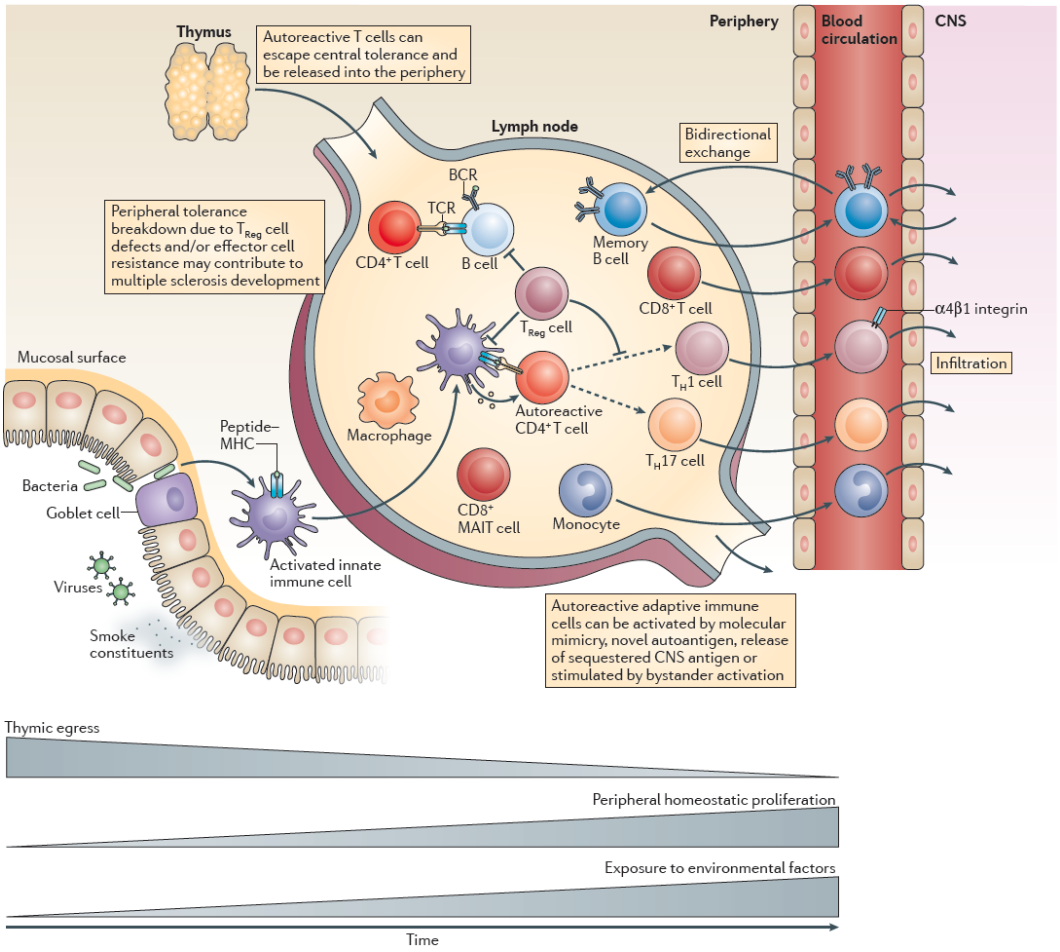

Figure 2. Pathogenesis of MS: the story begins on the peripheral side. Principal processes in the development of EAE or MS occur in a peripheric dysregulated immune system: once activated, autoreactive CD8+, CD4+ T cells such as Th1 and Th17 cells, B cells and innate immune cells can egress from lymphoid tissues and then migrate to the CNS. Genetic, life style and enviroment are risk factors in MS (Picture adapted from Dendrou C et al., *Nat Rev Immunol*, 2015)

The second step is the entry of immune cells into the CNS via the BBB. The third step consists of immune reactions occurring within the CNS when activated T cells encounter specific antigens presented by microglia. T helper (Th) cells, so

called for their ability to coordinate and fine-tune the immune response, initiate an attack against "self" antigens expressed mainly on oligodendrocytes leading to chronic inflammation (Comabella M and Khoury SJ, *Clinical Immunology*, 2012). Final demyelination is rendered either by macrophages recruited from the bloodstream across the BBB, or by tumor necrosis factor (TNF)-α and nitric oxide (NO), which are secreted by T cells and macrophages, and toxic to CNS myelin (**Fig. 3**). The inflammatory processes of MS are associated with a complex cascade of inflammatory molecules and mediators, including chemokines, adhesion molecules associated with activated endothelium of vessels wall and matrix metalloproteases (Cannella B and Raine CS, *Ann. Neurol*, 1995; Cuzner ML*, Neuropathol Exp Neurol*, 1996; Sørensen TL et al., *J Clin Invest*, 1999).

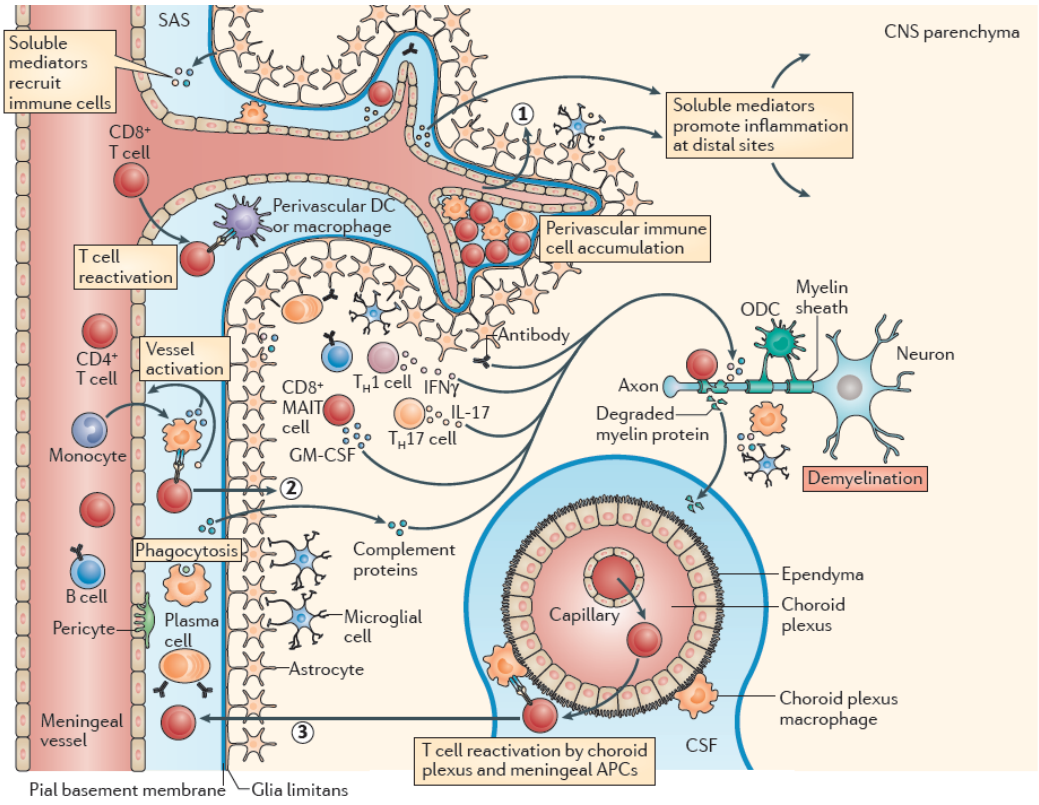

Figure 3. Pathogenesis of MS: what happens on the CNS side. Infiltration of immune cells from the periphery primarily occurs during early-stage of disease. Infiltrating cells can pass from the meningeal blood vessels through the BBB or the subarachnoid space or from the choroid plexus across the blood cerebrospinal fluid (CSF). Within CNS parenchyma these cells and activated resident microglia and astrocytes lead to demyelination and neuroaxonal injury with direct cell-contact mechanisms and the release of soluble inflammatory factors and

neurotoxic mediators (Picture adapted from Dendrou C et al., *Nat Rev Immunol*, 2015).

Leukocyte recruitment to sites of inflammation is the "*primu movens"* of the immune responses and consists of a multistep process regulated by adhesion molecules and chemoattactants. Classically, leukocyte adhesion cascade includes three main steps including rolling, activation and firm adhesion to the endothelia. The first contact between leukocyte and endothelial cells is named tethering, followed by rolling, which occurs as subsequent interaction. Among adhesion molecules, selectins and their carbohydrate ligands are associated with tethering and rolling steps. Rolling is mediated by E-selectin P-selectin and L- selectin which have as dominant ligand the P-selectin glycoprotein ligand (PSGL-1) for all three selectins. PSGL-1 is expressed on almost all leukocytes and certain endothelial cells. In addition to PSGL-1, E-sel binds to glycosylated CD44 (Ley K et al., *Nat Rev Immunol*, 2007). The adhesion molecule CD44 and the interaction with its main ligand the hyaluronic acid (HA), have also received attention in recent studies, in particular during autoimmune disease and cancers. As a primary adhesion receptor, CD44 can mediate leukocyte rolling on activated endothelium and extravasation. Moreover, CD44 may have a role in cell-matrix interactions, in particular can guide localization of cells within inflamed tissue (Puré E and Cuff CA, *Trends Mol Med*, 2001). Also α4 integrins may support the rolling step. Indeed, integrin activation triggered by chemoattractants is well acknowledged as key event in leukocytes arrest in blood vessels, but they also play a role during leukocyte rolling. Integrin activation requires a G-protein-coupled receptor engagement with an appropriate chemoattractant and include both clustering on cell membrane and modulation of the integrin conformation leading to reach a state of high affinity for binding to integrin endothelial counter receptor. Finally, the extravasation of leukocytes, also referred as diapedesis, depends on cytoskeleton rearrangement and represents the final step of the recruitment process (Ransohoff RM et al., *Nat Rev Immunol*, 2003; Ley K et al., *Nat Rev Immunol*, 2007).

Integrin family

Integrins are a large family of heterodimeric transmembrane glycoproteins composed of nonhomologous α and β transmembrane proteins of 100 kDa. Structurally, a large extracellular domain form a globular head in which sticks to a pair of short cytoplamatic tails connect each subunit. The α and β subunits are characterized by a large extracellular domain, a short transmembrane domain and a cytoplasmic region. The association of both subunits at N-terminal end forms the ligand-binding site, whereas the C-terminal region traverses the plasma membrane and interacts with cytoskeleton. The ligand-binding activity can be rapidly regulated by conformational changes as well as by transcriptional induction and redistribution from intracellular pools (Carman CV and Springer TA, *Curr Opin Cell Biol*, 2003). Integrin functions as bi-directional signaling molecules and binding to their ligands results in intracellular signals and conversely, cellular signaling events can modulate their affinity for extracellular ligands.

The most important β1-integrin expressed on leukocytes is the Very Late Antigen-4 (VLA-4, CD49d/CD29, α4β1), which binds to its ligand VCAM-1 (CD106), and is chiefly responsible for leukocyte rolling and firm adhesion to vascular endothelium and leukocyte recruitment to the inflamed area (Luster AD et al., *Nat Immunol*, 2005; Ley K et al., *Nat Rev Immunol*, 2007). β2-integrins include four different heterodimers: Lymphocyte Function-Associated Antigen-1 (LFA-1, CD11a/CD18), Mac-1 (CD11b/CD18), p150, 95 (CD11c/CD18), and CD11d/CD18. The most studied β2-integrin involved in leukocyte recruitment is LFA-1 (CD11a/CD18; αLβ2) which participates in rolling interactions but predominantly mediates the firm adhesion/arrest of leukocytes in the blood vessels of lymphoid organs or at sites of inflammation by binding the Ig superfamily ligands ICAM-1 (CD54) and ICAM-2 (CD102), expressed by the vascular endothelium (Luster AD et al., *Nat Immunol*, 2005; Ley K et al., *Nat Rev Immunol*, 2007).

LFA-1 integrin

LFA-1 has a heterodimeric structure with two subunits: CD18, which is common at all β2-integrins and CD11a, which is specific for LFA-1. As circulating leukocytes are continually exposed to ICAMs on the vasculature, therefore the ligand-binding activity of LFA-1 has to be kept under tight control to avoid inappropriate adhesion while these cells are flowing in blood or migrating through tissues and thus needs to be highly regulated. Integrin activation is achieved by signaling through other leukocyte receptors, termed "inside-out signaling". "Outside-in signaling" is generated when the active integrin signals back into the leukocyte on which it is expressed.

LFA-1 is found in three distinct conformational states (**Fig. 4**). The inactive low-affinity state shows a bent structure with the ligand-binding headpiece (αI domain) in close proximity to membrane-proximal stalk region. In the intermediate affinity state LFA-1 starts to extend the stalk regions shifting the molecule to the active higher-affinity conformation, where LFA-1 exhibits extended extracellular domain with the ligand-binding pocket for ICAM-1.

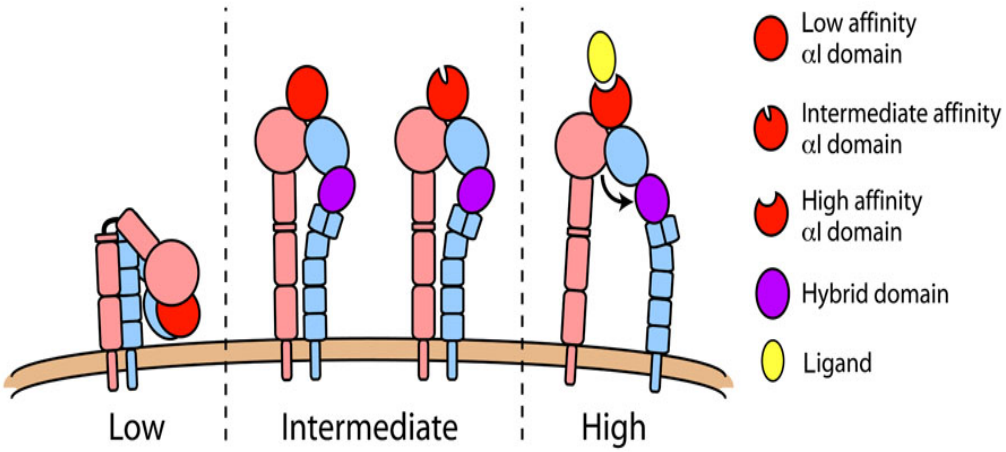

Figure 4. LFA-1 conformations. Three different conformations of LFA-1 integrin have been demonstrated. LFA-1 is in low affinity state extracellular domain with a bent structure shaped like an inverted V (*left*). Extended conformations (*middle*) have a different orientation of their hybrid domain (*purple*). The swingout of this domain lead to the conversion from intermediate to high affinity state (*right*) (Picture adapted from Lefort CT and Ley K., *Front Immunol*, 2012).

Several studies reported that the active conformation causes integrin activation allowing matrix interactions and mediating firm arrest on endothelium. A number of structural studies in recent years have provided better understanding of how signals may be transmitted from the intracellular integrin domains across the cell membrane to the ligand-binding domain. Two major modulation of integrin functions have been demonstrated, involving (1) increased receptor affinity by conformational changes of the heterodimer or (2) lateral mobility of the receptor on the plasma membrane leading to formation of clusters of heterodimers and increased avidity (Bazzoni G and Hemler ME, *Trends Biochem Sci*, 1998). For T cells, clustering appears to be the consequence of an initial high-affinity interaction of LFA-1 with multivalent ICAM-1. Clustering formation leads to cytoskeletal rearrangements that are essential for the adhesion and spreading of T cells on ICAM-1 (Porter JC et al., *J Immunol*, 2002). Moreover, once the T cell begins to migrate, the distribution of the membrane LFA-1 is changed. LFA-1 is organized into at least three different regions of activity in the migrating cell: the projecting lamellae at the leading edge where intermediate affinity LFA-1 functions, the mid cell zone containing high-affinity LFA-1, and the elevated uropod at the trailing edge with its high levels of LFA-1. More likely, the mid cell zone provides firm attachment to ICAM-1 that supports the cell's extensive leading edge as it scans other leukocytes and vascular surface. The membrane organization of LFA-1 into intermediate and high-affinity zone gives biological relevance to these different conformations and suggests that they operate together to regulate migration.

The ability of T cells to adhere and migrate is critical for a fully functional immune system. In response to inflammatory signals, T cells leave the blood stream by migrating along vascular endothelial surfaces, scanning for a suitable exit point into target tissue (Serrador J et al., *Trends Cell Biol,* 1999; Worthylake RA and Burridge K, *Curr Opin Cell Biol*, 2001). *In vitro* T cells are observed to move across the surface of APCs in a state of constant motility (Friedl P and Gunzer M*, Trends Immunol*, 2001), and *in vivo* T cells are highly motile deep in the lymph nodes (Miller MJ et al., *Proc Natl Acad Sci*, 2003) or in the inflamed target tissue such as in the SC during EAE (Bartholomäus I et al., *Nature*, 2009).

The ability of LFA-1 to act as a signaling receptor has not been extensively examined, as it has been chiefly associated with promoting cell-cell contacts, thereby optimizing signaling through other receptors. Cells move by coordinating the generation of lamellipodial protrusions at the front of the cell leading to new attachments, followed by the detachment of previous adhesions at the rear of the cell (Horwitz AR and Parson JT, *Science* 1999). LFA-1 is directly involved in leading to cell attachment, polarization and random migration. These events are critically dependent on dynamic changes in the acto-myosin cytoskeleton.

Even though an active role of LFA-1 in the cytoskeleton rearrangement during cellular migration was established, a potential role of α4 integrin in the cell plasticity during migration is still not well unknown. α4 integrin cytoplasmic domain is known to regulate cytoskeletal association and resistance to shear stress during adhesion event but their role in cellular migration was not established (Hyduk SI et al., *J Immunol, 2011*; Alon R et al., *J Cell Biol*, 2005).

Experimental animal model of multiple sclerosis and its features

The most widely used animal model of MS is experimental autoimmune encephalomyelitis (EAE) (Zamvil SS and Steinman L, *Annu Rev Immunol*, 1990; Gold R et al., *Brain*, 2006). EAE can be induced by immunization of susceptible experimental animal strains including primates and rodents with myelin autoantigens emulsified in complete Freund's adjuvant (CFA) or by adoptive transfer of brain antigen-specific T cells (Ben-Nun A et al., *Eur J Immunol*, 1981). This model was introduced by Rivers in the 1930 (Rivers TM and Schwentker FF, *J Exp Med*, 1935) and was substantially improved as an animal model for demyelinating inflammation of the CNS by adding Freund's adjuvant to emulsify myelin antigens (Kabat EA et al., *Science,* 1946).

A conceptual breakthrough was achieved in the 1980s by the groups of Wekerle and Cohen, who showed that myelin antigen-specific CD4+ T cell lines propagated *in vitro* could, upon adoptive transfer, induce demyelinating inflammation in the CNS parenchyma (Ben-Nun A et al., *Eur J Immunol*, 1981). This proved that EAE is induced by an autoimmune response to myelin antigens initiated by CD4+ T cells. In the following years, EAE became an invaluable tool

to study the activation of autoreactive T cells in the peripheral immune compartment, their migration into the CNS and their reactivation, and subsequent inflammation in the target tissue (**Fig. 2, 3**). In murine and primate EAE models, major immunogenic and encephalitogenic CNS autoantigens have been identified by isolation of antigen-specific major histocompatibility complex class II-associated peptides (MHC-II) restricted T cell clones. Most of these autoantigens are myelin antigens such as myelin basic protein (MBP), proteolipoprotein (PLP), myelin oligodendrocyte glycoprotein (MOG), and myelin-associated oligodendrocyte basic protein (MOBP) (Gold R et al., *Brain*, 2006).

Currently, the most common protocol for EAE induction is based on the injection of an encephalitogenic peptide, mostly MOG_{35-55} or $PLP_{139-151}$ peptide, which is emulsified in CFA containing mineral oil and *Mycobacterium tubercolosis* strain H37Ra, followed by injection of pertussis toxin. The resulting phenotype depends mainly on the antigen source and the genetic background of the animal species and strains used (**Fig. 5**). For example, $PLP_{139-151}$ peptide induces a relapsing-remitting EAE in SJL mice, with acute disease episodes followed by a remission phase (**Fig. 5A**). The grade of remission depends on disease severity: if mice develop a mild disease, remission can be complete, otherwise remission could be partial. Typically, several acute relapses and remission phases take place during disease progression.

MOG_{35-55} peptide, instead, triggers chronic-progressive EAE in C57Bl/6 mice that are the most favored mice for transgenic experiments (Gold R et al., *Brain*, 2006). C57Bl/6 mice typically develop a chronic form of the disease: after an initial peak, they partially recover and maintain a stable lower clinical score during disease chronicity (**Fig. 5B**).

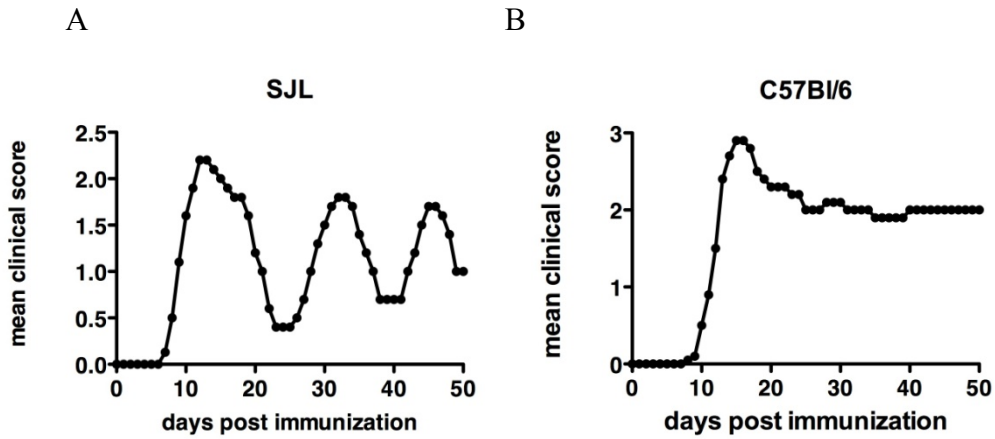

Figure 5. The resulting phenotype of disease. Comparison of disease progression between SJL and C57Bl/6 mice.

Helper T cells differentiation and functions during adaptive immune response and autoimmunity

Naïve CD4+ T cells, after being activated by antigen presentation and differentiated into distinct effector subsets, play a major role in mediating immune response through the secretion of subset-specific cytokines. Different types of cellular immune responses that have been identified are essential to understanding the mechanisms of the inflammatory process in MS and to devising strategies to control it. Depending on the cytokines they produce, these T cell subsets have very different properties. Helper T cells (Th cells) include the well-defined effector Th1, Th2 and Th17 subsets as well as the more recently described Th22 cells, but also regulatory subsets like regulatory T cells (Treg) (**Fig. 6**). Three signals are required for efficient T cell differentiation. The first is in the form of antigen presented by an antigen- presenting cell (APC), such as a dendritic cell (DC). The second signal comes in the form of costimulatory receptors on T cells engaging their cognate ligands on APCs. Small signaling protein molecules, such as cytokines, provide the third signal (Kapsenberg ML, *Nature Reviews Immunology*, 2003). Antigen presentation in the presence of interleukin (IL)-12 induces the expression of T-bet and production of interferon (IFN)-γ, therefore promoting naïve T cell polarization into the Th1 phenotype (**Fig. 6**). Th1 phenotype cell targets are macrophages and dendritic cells. Th1 type responses are

important in inflammation and tissue injury. IL-4 induces GATA3 expression and IL-4 production and is necessary for Th2 cell polarization. Th2 cells produce mainly IL-4, IL-13 and IL-5, and express the transcription factor GATA-3 (**Fig. 6**). Their cell targets are eosinophils and basophils (Miossec P et al., *N Engl J Med*, 2009). Th2-type responses are important in allergic reactions, helminth infections, and anti-inflammatory actions (Abbas AK et al., *Nature*, 1996). Th cells that produce IL-17 but not IFN-γ or IL-4 were named Th17 cells (Park H et al., *Nat Immunol*, 2005). Despite the dependence of Th17 cells on IL-23, their initial development from naïve T cells requires transforming growth factor (TGF)-β and IL-6 or IL-21 (**Fig. 6**), and this process is enhanced by TNF-α and IL-1β (Stockinger B and Veldhoen M, *Curr Opin Immunol*, 2007). IL-23 is required in the later stage of Th17 development for their terminal differentiation into mature effector cells (McGeachy MJ et al., *Nat Immunol*, 2009). Development of the Th17 lineage is directed by two transcription factors, RORγt and RORα (Ivanov II et al., *Cell*, 2006; Yang X et al., *Immunity*, 2008). Initial commitment to the Th17 lineage is antagonized by Th1 and Th2 cytokines, and both IFN-γ and IL-4 suppress Th17 differentiation (Harrington LE et al., *Nat Immunol*, 2005; Park H et al., *Nat Immunol*, 2005). Th17 cells express a range of pro-inflammatory mediators including IL-17A, IL-17F, IL-22, and IL-21 (Ghilardi N and Ouyang W, *Semin Immunol*, 2007). These cells constitute a distinct lineage of Th cells, with key role in protection against extracellular bacterial and fungal infections. While Th cell subsets are necessary for providing immunity against infectious pathogens, their aberrant response is to blame in several medical problems such as autoimmune diseases, allergies and malignancies. Therefore, a Th cell type could be either “good” or “bad” depending on the immunological context. Studies in humans as well as in animal models of MS suggest that Th1 and Th17 cells are mostly pathogenic, while Th2 and Treg cells are anti-inflammatory.

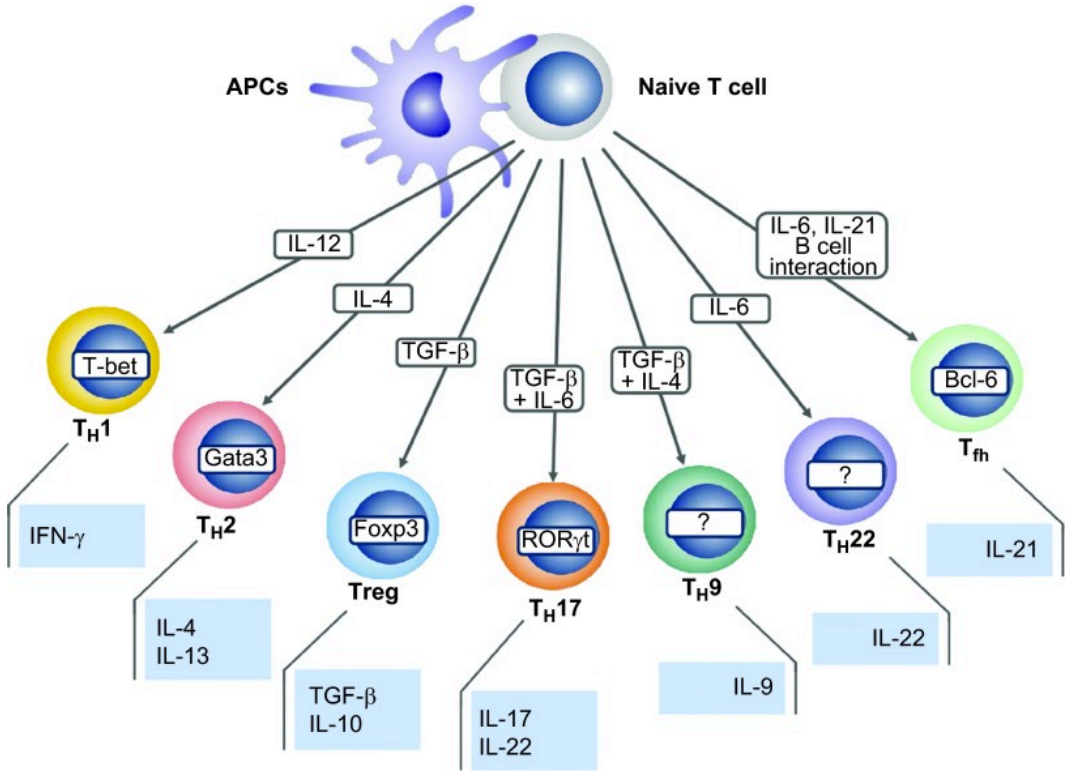

Figure 6. Different T helper cell subsets. Upon activation, naïve precursor T cell differentiates into effector T cell subsets, producing different cytokines and mediating distinct effector functions (Picture adapted from Wu RQ et al*., Int J Oral Sci*, 2014).

Autoreactive Th1 and Th17 cells in multiple sclerosis and its animal model

Th1 cells were thought originally to be the main pathogenic T cells in EAE and MS. It was postulated that during EAE, in the peripheral lymphoid organs, T precursor myelin-reactive T cells are induced to differentiate into myelin-reactive Th1 cells when an antigen that crossreacts with a myelin antigen is presented to a T cell by an APC in the context of IL-12 and co-stimulatory molecules. Th1 cells that react with myelin antigens, such as PLP, MBP and MOG, cross the BBB where the myelin antigens are represented to the T cell by APCs in the brain (microglia cells), and an inflammatory cascade is triggered with the release of inflammatory mediators that cause damage to the myelin sheath and ultimately the underlying axon. This conclusion was based partly on the observation that IFN-γ was detected in MS lesions (Traugott U and Lebon P, *Ann Neurol*, 1988) and in the CNS of EAE mice at the peak of disease and disappeared in CNS lesions during recovery (Olsson T, *J Neuroimmunol*, 1992; Issazadeh S et al., *J Neurosci*

Res 1995). As described previously, the differentiation of Th1 cells is dependent on IL-12. IL-12 is a heterodimeric protein composed of p40 and p35 subunits (Gately MK et al., *Annu Rev Immunol*, 1998). Since p40 knockout (KO) mice or wild-type mice treated with antibodies to p40 are entirely resistant to EAE (Leonard JP et al., *J Exp Med*, 1995; Becher B et al., *J Clin Invest*, 2002), this further had supported the paradigm that Th1 cells were responsible for inducing the disease.

The concept of Th1 driven organ-specific autoimmunity was challenged when it was found that mice deficient for p35, the second subunit of IL-12, were not protected from EAE but developed more severe disease (Becher B et al., *J Clin Invest*, 2002). IL-23 is a recent discovered cytokine that shares p40 subunit with IL-12 in combination with p19 subunit (Oppmann B et al., *Immunity*, 2000). Whereas IL-12p35 KO mice are more susceptible to EAE, IL-23p19 KO mice are absolutely protected from the disease (Cua DJ et al., *Nature*, 2003). It was also demonstrated that IL-23 could supports the differentiation of Th17 (Langrish CL et al., *J Exp Med,* 2005). Moreover, IL-17 was found highly expressed in tissue sites of many autoimmune diseases including MS lesions (Lock C et al., *Nat Med*, 2002). High levels of IL-17 producing CD4+ T cells were detected also in the peripheral blood and in the cerebrospinal fluid of RRMS patients. Moreover, the onset of EAE was significantly delayed and the severity of disease was reduced in IL-17 -/- mice, even though the clinical incidence appeared similar compared with wild type animals (Komiyama et al. 2006). The cumulative data suggested an important role of IL-17 and Th17 cells in inducing tissue inflammation and autoimmunity, but their contribution in EAE pathogenesis is still poorly understood.

Both Th1 and Th17 cells infiltrate the CNS during EAE but their relative proportions varied among different mouse strains (Langrish CL et al., *J Exp Med* 2005; Korn T et al., *Nat Med* 2007). In C57Bl/6 mice, autoreactive Th1 cells predominate in the inflamed CNS at disease peak, whereas in SJL mice, Th17 cells are more numerous (Langrish CL et al., *J Exp Med*, 2005; Korn T et al., *Nat Med* 2007). Immunization of mice with distinct MOG epitopes elicits T cell responses with a different Th1 to Th17 ratio, depending on the avidity of T cells

for their cognate antigen (Stromnes IM et al., *Nat Med*, 2008). These data suggest that the relative contribution of Th1 and Th17 responses in CNS inflammation might vary depending on the strain of mice and immunization strategy.

Another important feature of EAE is that the pathology induced by Th1 and Th17 cells is distinct. Th1-mediated CNS inflammation is characterized by infiltrating macrophages, whereas neutrophils predominated when Th17 cells are used to induce disease (Kroenke MA, *J Exp Med*, 2008). Moreover, Th1 and Th17 cells have a comparable capacity to induce EAE, although with different regional localization of CNS lesions and different clinical disease (Stromnes IM et al., *Nat Med*, 2008). Transfer of Th17 cells induces mainly brain inflammation in recipient mice, which developed atypical EAE, while transfer of Th1 cells leads to the development of classical EAE with only spinal cord (SC) inflammation. Interestingly, transfer of MOG-specific T cells containing different proportions of Th1 and Th17 cells directs the localization of CNS inflammation: a high Th17/Th1 cell ratio of CNS-infiltrating T cells, inflammation occurs in the brain parenchyma whereas in the presence of a lower Th17/ Th1 ratio inflammation is located in the SC (Stromnes IM et al., *Nat Med*, 2008). Studies in MS patients and normal human donors have provided evidence that Th1 and Th17 cells are active or expanded during diseases, but their contribution to pathology has, understandably, been more difficult to define, thus much of the focus in recent literature has been on the relative role of Th1 and Th17 in EAE and MS.

Lymphocyte migration into the brain represents a critical event in the pathogenesis of MS and its animal model, EAE. MS and EAE pathogenesis is mediated by myelin-specific T cells, which are activated in the periphery and translocate into the CNS followed by permeabilization of the BBB (Furtado GC et al., *J Immunol* 2008; O'Connor RA, *J Immunol*, 2008). Among pro-inflammatory myelin-specific T cells, Th1 and Th17 cells are key players in the induction of brain autoimmunity, but the different molecular mechanisms controlling their dynamics from inflamed vessels to CNS parenchyma are not well understood. Upon entering the CNS, the T cells are reactivated by local and infiltrating activated APCs, which present MHC-II-associated peptides, resulting in subsequent inflammatory process and eventually in demyelination and axonal

damage. In this process is very important how T cells move and interact with others immune cells, in fact the responses to potential antigen inside the CNS require long-range migration of cells, short-range communication and direct cell-cell contact with APCs. Moreover, the communication between cells and their environment is of the significant importance since influence different processes as proliferation, survival and motility, as well as regulate effector functions.

In vivo imaging techniques allow to study T leukocytes trafficking in the central nervous system

Epifluorescence intravital microscopy (IVM) and multiphoton microscopy enable imaging of leukocyte trafficking in the CNS. Providing qualitative and quantitative *data* concerning the molecular mechanisms that control leukocyte migration, IVM technique is suitable for the understanding of leukocyte-endothelial cells interactions, particularly slow rolling, tethering, arrest and adhesion strength in CNS vessels. This technique could also help to identify the role of selectins and integrins in the recruitment of different cell subsets and is ideal for the study of leukocyte trafficking during EAE. Particularly, a vertebral window over the pial vessels of the lumbar column at L1-L5 enables to follow T cell migration at the main site of inflammation of EAE (**Fig. 7A, B, C, D**). Multiphoton microscopy is more suited for studies on transmigration and motility mechanisms inside tissue parenchyma (**Fig. 7E, F**) (Zenaro E et al., *Immunology and cell biology*, 2013).

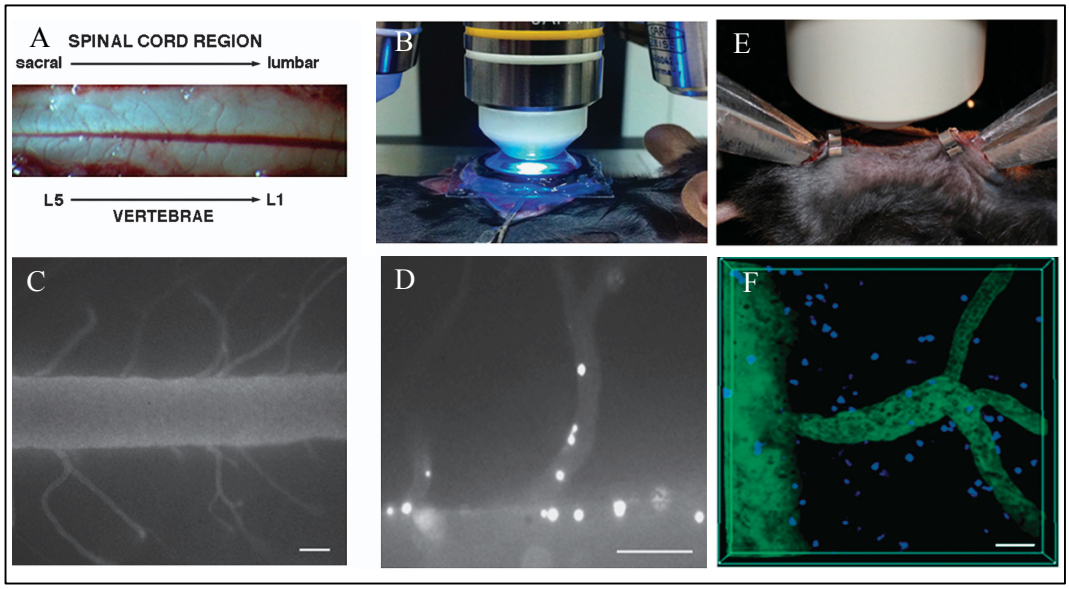

Figure 7. IVM and TPLM experimental settings. The main site of inflammation in MOG-induced EAE was exposed and laminectomy over L1-L5 was carefully performed both in IVM and TPLM experiments **(A)**. The preparation for IVM was placed under microscope on a water immersion objective with long focal distance (**B**). Pial vessels of the exposed SC were visualized at IVM by using fluorescent dextrans (**C**). Digital videotapes at IVM of the interacted cells with the inflamed endothelium (**D**). The preparation for TPLM fitted on a customized microscope stage was placed under microscope without coverglass to permit the direct immersion of the objective (**E**). Pial vessels and exogenous infiltrated T cells in the SC parenchyma were visualized at TPLM by using fluorescent dies **(F)** (Picture adapted from Zenaro E et al., *Immunol. Cell Biol.*, 2013).

Two photon laser microscopy technique: principles and applications in the study of the dynamic nature of immune cells

Two-photon laser microscopy (TPLM) allows visualizing immune processes within the living animal by providing dynamic views of sub-cellular structures and cells in a tissue context *in vivo*. TPLM is an ideal tool for long-term intravital imaging because of its low phototoxicity, superior penetration depth and high resolution (Matz MV et al., *Nat Biotech*, 1999). The difference between two-photon microscopy and one-photon microscopy, such as confocal and fluorescent microscopes, involves the excitation process. During conventional (one-photon) excitation a fluorescent molecule absorbs a photon with a specified energy. In contrast, during two-photon excitation, a fluorescent molecule is excited simultaneously by two photons that sum up their energy to activate it. After non-radiative relaxation, a fluorescent molecule emits fluorescence, which is common

in both conventional and two-photon excitation (**Fig. 8A**). In this situation, two photons merge their energy and excite a single fluorochrome. As two-photons excite one fluorochrome, each photon used in one-photon microscopy harbors half of the energy used in conventional microscopy. Therefore, the wavelength used in two-photon microscope is twice as long as in one-photon microscopy.

Specialized lasers had to be developed for practical realization of TPLM. Indeed, the most widely used light sources are characterized by high repetition rate, ultrafast pulsed lasers, such as titanium-sapphire and Nd:YLF lasers (So P TC, *Encyclopedia of life sciences*, 2002). Generated photons are then focused by the objective lens of the microscope, leading to their maximal accumulation at the focal point (**Fig. 8B**).

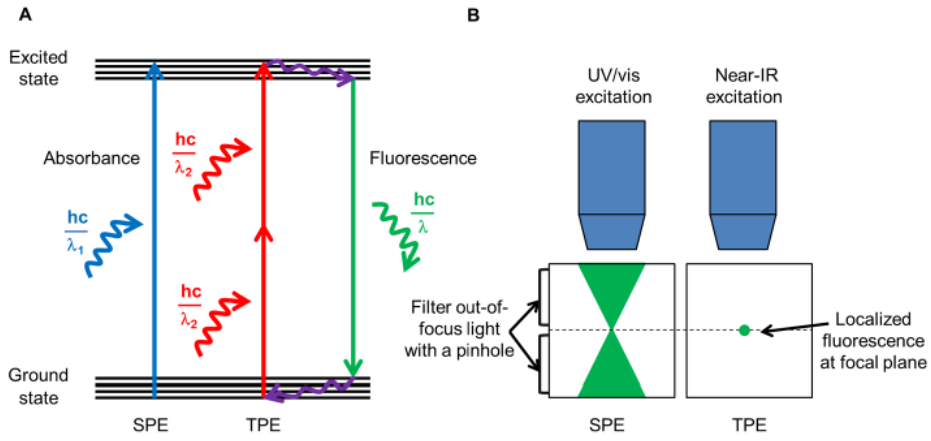

Figure 8. Comparison between conventional single photon excitation (SPE) versus two-photon excitation (TPE).
During conventional excitation, a photon activates a fluorescence molecule (*blue arrow*), whereas during two-photon excitation, two photons can sum up their energy to activate a fluorescence molecule (*red arrows*). After nonradiative relaxation (*green arrow*), a fluorescence molecule emits fluorescence, which is common in both conventional and two-photon excitation **(A)**. Conventional laser can excite a fluorescence molecule on its way causing an emitted cone of fluorescent light within the sample. In TPLM, fluorescent molecules can be activated only at the focus plane leading to less phototoxicity and less photobleaching (**B**) (Picture adapted from Bennewitz MF et al., *Intravital*, 2014).

Since the two-photon effect occurs only at a focal point, there is no out-of-focus signal to be rejected. This explains why a two-photon microscope does not need a

pinhole, while confocal microscopy requires it for removing the signal generated from outside the focal plane. TPLM allows studying the behavior of cells, in particular the immune cells, their dynamics, morphology, motility and signaling processes, while minimizing perturbation of the system under study.

The study of cell migration needs to consider the fact that cells migrate in a densely packed extracellular matrix environment, surrounded by interstitial cells, other leukocytes or resident neural cells, as well as fixed tissue elements such as blood vessels along with a dynamic context of immunoregulatory mediators that might be diffusing freely or are immobilized to the underlying stroma (Sumen C et al., *Immunity*, 2004). Particularly, leukocyte migration into the tissues depends on the composition and architecture of matrix protein cross-interactions. The matrix composition controls cell adhesion and migration, and its sensitivity to proteolytic enzymes will determine the ability of the cell to remodel the matrix and migrate through it.

TPLM has revealed the dynamic nature of immune cells within living lymphoid and target organs, in particular this technology has elucidated the dynamics of the autoreactive effector T cells in the course of EAE. Recent data have shown that myelin-specific T cells injected in an adoptive transfer model of rat EAE display a motility behavior suggesting that CNS cells present antigens and activate T cells inside SC parenchyma (Kawakami N et al., *J. Exp. Med*, 2005; Odoardi F et al., *Proc. Natl. Acad. Sci*., 2007). In fact, Bartholomäus and colleagues have recently demonstrated that rat T cells reactivate in the subarachnoid space (SAS) in the presence of leptomeningeal macrophages and that the efficiency of the reactivation in the presence of antigen is mandatory for subsequent invasion in CNS parenchyma of Lewis rat (Bartholomäus I et al., *Nature* 2009). However, and the molecular mechanisms implicated in the motility behavior of T cells inside CNS parenchyma and the interactions with neural cells in common mouse EAE models remain unknown. Moreover, the molecular mechanisms controlling Th1 and Th17 cells trafficking inside CNS parenchyma during neurological diseases is largely unknown.

Materials and Methods

Mice

8-10 weeks of age C57BL/6 female mice were used to active EAE induction. 2D2 TCR transgenic mice were used to Th1 and Th17 cells production. These mice used in this study were with C57BL/6 genetic background. All animals were housed and used in according to the current European Community rules.

Production MOG_{35-55} specific Th1 and Th17 cells

We used 2D2 TCR transgenic T cells that recognize MOG35-55 peptide (Bettelli E et al., *J Exp Med*, 2003) to obtain sufficient numbers of Th1 and Th17 cells. We used a modified protocol by Domingues and colleagues, which the obtainment of large numbers of Th1 and Th17 cells free of contaminating IL-17 and IFN-γ producing cells in Th1 and Th17 polarizations, respectively (Domingues HS et al., *PLoS One*, 2010). 2D2 TCR transgenic mice were sacrificed and spleen cells were isolated. 20 x 10^6 2D2 total erythrocyte-lysed spleen cells per well were cultured for 7 days in the presence of 20 μg/ml antigenic peptide MOG (MOG_{35-55}) in RPMI 1640 supplemented with 100 mM Na pyruvate, 200 mM in 0,85% NaCl solution ultraglutamine 1, 10000 U/ml penicillin, 10000 U/ml streptomycin and 10% fetal calf serum (FCS). For Th1 and Th17 polarization the following cytokines and antibodies were further added in the culture. Th1: IL-12 (1 ng/ml), anti-IL-4 (10 μg/ml). Th17: TGF-β (5 ng/ml), IL-6 (20 ng/ml), IL-23 (2 ng/ml), anti-IL-4 (10 μg/ml), anti-IFN-γ (10 μg/ml). Th1 cells were supplemented with IL-2 (20 U/ml) and Th17 cells with IL-7 (10 ng/ml) at day 4 of culture. After 72 hours, MOG-specific Th1 and Th17 cells were isolated by Ficoll-gradient centrifugation. MOG-specific Th1 and Th17 cells (approximately 30 x 10^6 cell/plate) were re-stimulated in the presence of irradiated splenic APCs (120 x 10^6 cell/plate) for 3 days with a proportion of 1:4. Then, cytokines and MOG were added in the culture as described previously. After, activated MOG-specific Th1 and Th17 cells were isolated by Ficoll-gradient centrifugation and IL-2 (20 U/ml) and IL-7 (10 ng/ml) was added, respectively.

Detection of intracellular and extracellular cytokines

For intracellular cytokines staining cells were stimulated for 4 hours with Phorbol 12-myristate 13- acetate (PMA) (50 ng/ml), ionomycin (1 µg/ml) and brefeldin A (10 µg/ml). Permeabilized cells were labeled with FITC-conjugated rat anti-mouse IFN-γ and PE-conjugated rat anti-mouse IL-17. As control, cells were stimulated with the same conditions, but without brefeldin A.

For extracellular staining, the following rat anti-mouse monoclonal antibodies were used: anti-α4 (clone PS/2), anti-CD44 (clone MJ64), anti-L-sel (clone MEL-14), anti-LFA-1 (clone TIB-213), anti-PSGL-1 (clone 2PH1), anti-α4β7 (clone DATK-32). Samples were collected and analyzed by fluorescence-activated cell sorting technology (FACS).

Active EAE induction

C57BL/6 mice were immunized with 150 µg/mouse of MOG_{35-55} peptide in 200 µl/mouse of emulsion consisting of equal volumes of Dulbecco's Phosphate Buffered Saline (PBS) and CFA, supplemented with 1 mg/mouse of *Mycobacterium tubercolosis* (strain H37Ra). CFA contains heat-killed *Mycobacterium tubercolosis* that stimulates the innate immune system. Immunization was made sub-cutaneously in the flank (100 µl/flank). Mice also received 40 ng of pertussis toxin (PTX) with intravenous injection at the time of immunization (day 0) and 48 hours later (day +2). Toxicity may vary by lot of toxin depends on its Adenylate Cyclase activity. The optimum dosage of each lot of PTX was determined based on EAE clinical symptoms appearance and disease severity. Mice were checked for clinical symptoms daily and signs of EAE were translated into clinical score as follows: 0= no disease, 1= tail weakness; 2= paraparesis; 3= paraplegia; 4= paraplegia with forelimb weakness or paralysis; 5= moribund or dead animals.

Epifluorescence intravital microscopy

IVM: experimental procedures

Lymphocytes were labeled with either green CMFDA (5-chloromethylfluorescein diacetate) (Molecular probes) or orange CMTMR (5-(and-6)-(((chloromethyl)benzoyl)amino)tetramethylrhodamine). Mouse was anesthetized with an intraperitoneal (i.p.) injection of ketamine (100 mg/kg body weight)/xylazine (15 mg/kg) and prepared for the SC exposure. The back of the animal was shaved and a midline dorsal incision of the skin was made to expose the lumbar column, the main site of inflammation. Skin was retracted and pulled to the side with small retractor clamps on either side to maintain the spine exposed. The paravertebral muscles were carefully incised and laminectomy over L1-L5, the main site of inflammation in MOG-induced EAE, to expose the SC. This procedure allowed us to leave an intact dura to protect the SC. Bleeding was controlled by making softly pressure on the area with gel foam or by using small vessel cauterizer. (Davalos D et al*., J Neurosci Methods*, 2008; advances in intravital microscopy book) (**Fig. 7A**). At the end of microsurgery, a 24mm x 24mm coverslip was applied on the exposed SC. A round camera with 11mm internal diameter was attached on the coverslip and filled with water (**Fig. 7B**).

IVM: imaging acquisition

The preparation was placed on an Olympus BX50WI microscope and a water immersion objective with long focal distance (focal distance 3.3 mm, NA 0.5 ∞) was used. Blood vessels were visualized by using fluorescent dextrans. 2 x 10^7 fluorescent labeled cells/condition were slowly injected into the tail vein. The images were visualized by using a silicon-intensified target videocamera (VE-1000 SIT) and a Sony SSM-125CE monitor and recorded employing a digital VCR (**Fig. 7C, D**).

IVM: integrins blockade experiments

In order to identify a potential role of integrins in the molecular mechanisms responsible for Th1 and Th17 cell trafficking on the inflamed pial vessels of the SC, labeled cells were treated with blocking monoclonal antibodies anti-LFA-1

integrin (clone TIB-213), anti-α integrin (clone PS/2) and anti α4β7 (clone DATK32). Cells were incubated at 37° C for 10 minutes with a concentration of blocking mAbs at 100 μg/ml. Then cells were intravenously administrated in 200 μl of PBS together with additional 100 μg/ml mAb.

IVM: image analysis

Video analysis was performed by playback of digital videotapes. Vessel diameter (D), hemodynamic parameters and the velocities of rolling were determined by using a PC based system (74). The velocities of ≥ 20 consecutive freely flowing cells/venule were calculated, and from the velocity of the fastest cell in each venule (V_{fast}), we calculated the mean blood flow velocities (V_m): $V_m=V_{fast}/(2-\varepsilon^2)$. The wall shear rate (WSR) was calculated from $WSR=8xV_m/D$ (s^{-1}), and the wall shear stress (WSS) acting on rolling cells was approximated by WSR x 0.025 (dyn/cm^2), assuming a blood viscosity of 0.025 Poise. Lymphocytes that remained stationary on venular wall for ≥ 30 s were considered adherent. At least 100 consecutive cells/venule were examined. Rolling and firm arrest fractions were determined as the percentage of cells that rolled or firmly arrested within a given venule in the total number of cells that entered that venule during the same period.

IVM: statistics

Statistics on the comparison of rolling and adhesion events between Th1 and Th17 during the different phases of the disease were calculated using Mann-Whitney test, which is a non parametric test with confidence interval of 95%. The reduction of rolling and adhesion events after antibody treatment was evaluated as percentage compared to control cells (100% of interactions). Statistics were calculated by using a one sample t test to the hypothetical control value fixed at 100. It's a two tailed test. A confidence interval of 95% was assumed. *Data* are expressed in mean ± standard error mean (SEM).

Two photon laser microscopy

TPLM: surgical procedures

Th1 or Th17 cells were labeled for 45 min at 37°C with 40 mM 7-amino-4-chloromethylcoumarin (CMAC) or carboxyfluorescein succinimidyl ester (CFSE). 2×10^7 of Th1 or Th17 cells were transferred intravenously (i.v.) injection in a C57BL/6 recipient mouse at different disease phases as shown. 48 hours after mouse was anesthetized with an intraperitoneal (i.p.) injection of ketamine (100 mg/kg body weight)/xylazine (15 mg/kg) and prepared for the SC exposure. A midline dorsal incision was made to expose the lumbar column over L1-L5, as described in intravital microscopy surgical procedures. Muscles were dissected from the sides of the vertebral bone and a small retraction of the paravertebral muscles allowed the insertion of the fine tips of the clamping of a spinal column stabilization device. We used an adapted method by Davalos et al. fitted on a customized microscope stage in the mechanical facility at the University of Verona. This method presents excellent stability by combining a customized spinal stabilization device (Narishige STS-A Compact Spinal Cord Clamps and Narishige MA-6N head holding adaptor on a steel base that will be adapted to fit on the microscope's stage) with a method of deep anesthesia minimizing respiratory-induced movements. This method allows optimal SC immobilization and eliminates the impact of respiratory movements for two photon microscopy studies (Davalos D et al., *J Neurosci Methods*, 2008). Few drops of artificial cerebrospinal fluid (CSF) were added on SC without cover glass to permit the direct immersion of the microscope objective (**Fig. 7E**). Blood vessels were stained by i.v. injection of fluorescent Qtracker quantum dots 655 (Qdots-655) immediately before imaging (**Fig. 7F**).

TPLM: integrin blockade experiments

In order to identify a potential role of integrins in the adhesion mechanisms responsible for Th1 and Th17 cell motility behavior into the SC parenchyma, blocking monoclonal antibodies anti-LFA-1 integrin (clone TIB-213) and anti-α4 integrin (clone PS/2) were locally administrated. Antibodies (100 μg/ml) were administered in 200 μl of artificial CSF on the exposed SC and incubated for 30-

60 min before the imaging to permit adequate local tissue diffusion (Kim JV et al., *Nature* 2009).

TPLM: imaging acquisition

The mouse was positioned on stabilizing device and maintained at 37°C using a thermostatic blanket system and placed on a customized upright Leica TCS SP5 AOBS confocal-multiphoton system. CMAC- or CFSE-labeled Th1 and Th17 cells and Qdots-655-labeled vessels were excited with a mode-locked Ti:Sapphire Chameleon Ultra II laser (Coherent Inc) and visualized with an Olympus XLUMPlanFI 20× objective (water immersed, numerical aperture, 0.95). For imaging, we used simultaneous laser excitation at 750-800 nm. Fluorescence emission from the three different fluorescent dyes was separated passing through panchromatic electronic barrier filters and detected as red (560–650 nm), green (490–560 nm), and blue (400-500 nm) signal.

Stacks of images were acquired using Leica acquisition software. To create time-lapse sequences, we scanned volumes of tissue in which each plane consists of an image of 100 × 120 μm (x and y = 2 pixel/μm). Z-stacks were acquired by taking 21 sequential steps at 2.5 μm spacing at 27-35-s intervals for up to 30 min. To increase signal contrast, we averaged 2 video frames for each z-slice. Multidimensional rendering was performed with Imaris (Bitplane).

TPLM: data analysis

Sequences of image stacks (**Fig.9A, B**) were transformed into volume-rendered three-dimensional movies and cell movement analysis was obtained using Imaris software (**Fig. 9C, E**). Three-dimensional spatial position of each cell was detected based on centroid fluorescence intensity. Tracks for each cell consist of serial sets of xyz coordinates of single cell centroid (**Fig. 9F**). Once the cell tracks were created they were exported from Imaris to calculate several parameters that can be used to describe the migration behavior of cells quantitatively (**Fig. 9G**). Cells were tracked over time manually and tracks greater than 3 min (≥12 time points) were included in the analysis. Intra-tissue tracking of robust number of cells was performed: i) fields with at least 20 fluorescent leukocytes were

considered for analysis; ii) a mean of 4 fields/mouse were examined; iii) at least 100 manually tracked cells were considered for each experimental condition.

The following parameters were calculated (**Fig. 10**): *cell velocity* was analyzed either as instantaneous velocity (**Fig. 10D**) or track velocity, the former providing a basic parameter derived from the displacement of the cell centroid between adjacent time periods whereas the latter is obtained from the median or mean instantaneous velocity computed from all time intervals throughout a track. The *displacement* of a cell moving with a constant velocity from an initial position but randomly changing direction is on average linearly proportional to the square root of the elapsed time (**Fig. 10C, E**). The most accurate current method to detect migration patterns is the *mean displacement plot*, in which the average displacement of a population of cells over specific time intervals is plotted against the square root of time. The slope of the resulting curve can be used to determine the *motility coefficient* of a cell population (**Fig. 10E**) and measures the volume an average cell scans per unit time. The *arrest coefficient* is another useful parameter, representing the proportion of time during tracking in which a cell does not move (threshold <2 μm/min). The arrest coefficient was calculated from cell tracks, so the reported value represents a percentage of cells in the entire population. For example, the arrest coefficient is generally high when T cells are in stable contact with other cells or swarm in a chemoattracting microenvironment. The *meandering index* was also calculated, based on the ratio of displacement from origin by track length, to provide another index of the directness of cell movement. A meandering index of 0.7-1 generally indicates that cell migration has a strong directional bias (**Fig. 10F**) (Zenaro E et al., *Immunol Cell Biol*, 2013).

TPLM: statistics

Statistics were calculated using non parametric Mann-Whitney test with confidence interval of 95%. *Data* on Th1 and Th17 motility behavior during the different phases of EAE are expressed in mean ± standard deviation (SD). Compared *data* between Th1 and Th17 cells before and after blocking antibody treatments were expressed in mean ± standard error mean (SEM). In the plot of displacement and chemotactic index we applied linear regression and compared

slopes.

EAE induction and antibody treatment

8 to 10 weeks old C57Bl/6J females were immunized sub-cutaneously in the flanks and in the tail base with 150 μg of MOG_{35-55} peptide in 200 μl emulsion consisting of equal volumes of PBS and CFA (Difco Laboratories), supplemented with 1 mg/mouse of *Mycobacterium tuberculosis* (strain H37Ra; Difco Laboratories). Mice received 40 ng of pertussis toxin (Alexis Biochemicals) intravenously (i.v.) at the time of immunization and 48 hours later. Clinical scores were recorder daily as previously described. For therapeutic anti-LFA-1 and anti-α4β7 treatment, mice were injected intrathecally with two intracisternal injections of 10 μl containing 50 μg of anti-LFA-1 antibody (M17/4 clone) and anti-α4β7 (DATK32 clone) or control anti-Ras monoclonal antibody. Mice were injected the day after disease onset, 4 and 3 days later for anti-LFA-1 and anti-α4β7 treatment, respectively. For intracisternal injection each mouse was anesthetized with a ketamine-xilazine solution and the atlanto-occipital membrane was punctured with Hamilton syringe by a 27-gauge needle and the antibody solution was administered as previously describe (Furlan R et al., *Methods Mol Biol,* 2003). Clinical scores *data* were expressed in mean ± standard error mean (SEM). Statistics were calculated using non parametric Mann-Whitney test.

Neuropathology

EAE mice were sacrificed 3 days after the first intrathecal antibody injection and SCs were collected and frozen. 20 μm sections were obtained for histological examination by hematoxylin/eosin and luxol fast blue staining for the presence of inflammatory infiltrates and demyelination, respectively (Butti E et al., *Gene Ther, 2008*). Microglia was stained using an anti–mouse ionized calcium binding adaptor molecule-1 antibody (Iba-1) (Wako) as described previously *(*Zenaro E et al., *Nat Med,* 2015*)*.

Total cord area, posterior column area, gray matter area and lateral, anterolateral, anterior column area were traced. Areas (mm^2) were manually outlined and calculated by an automated quantification system using ImageJ v1.49 software

(NIH). Results from quantification of neuropathological findings on an average of 4-6 cross sections of SC per mouse taken at different levels of lumbar and thoracic regions are expressed as percentage on white matter area or total area respectively (McGavern DB et al., *Neurosci Res,* 1999). The numerical density of Iba-1+ immunoreactive microglia was quantified by determination of the total number of positive elements and reported as number of positive elements per mm^2. Activation state of microglia was determined quantifying the area covered by the cell soma and expressed as percentage of Iba-1+ cells on total area as previously reported by Zenaro E and coworkers. A lowering microgliosis results in terms of reduction of the area covered by cell soma of Iba-1+ cells *(*Zenaro E et al.*, Nat Med,* 2015*)*. The activated microglia shows a globoid, thus smaller morphology. However, the portion of area covered by these globoid cells, results more extensive than the area covered by microglial ramified cells. This is probably due to a reduction in the complexity of cells but in an increasing of cell soma dimensions. A support of that, cell body size parameter was found positive correlated with microglial activation. Indeed, the cell body to cell size ratio emerged as novel method to evaluate the activation state of microglia cells (Hovens IB et al., *Neuroimmunol Neuroinflammation*, 2014). Accordingly, an other parameter used, in particular with fluorescent microglia, is the domain volume (μm^3) that results significantly higher in the activated microglia compared to the control cells (Plog BA et al., *J Neurosci Methods*, 2015).

All images were captured using a Leica microscopy DM6000B and the Leica Application Suite software. All *data* were expressed in mean ± standard error mean (SEM). Statistics were calculated using non parametric Mann-Whitney test.

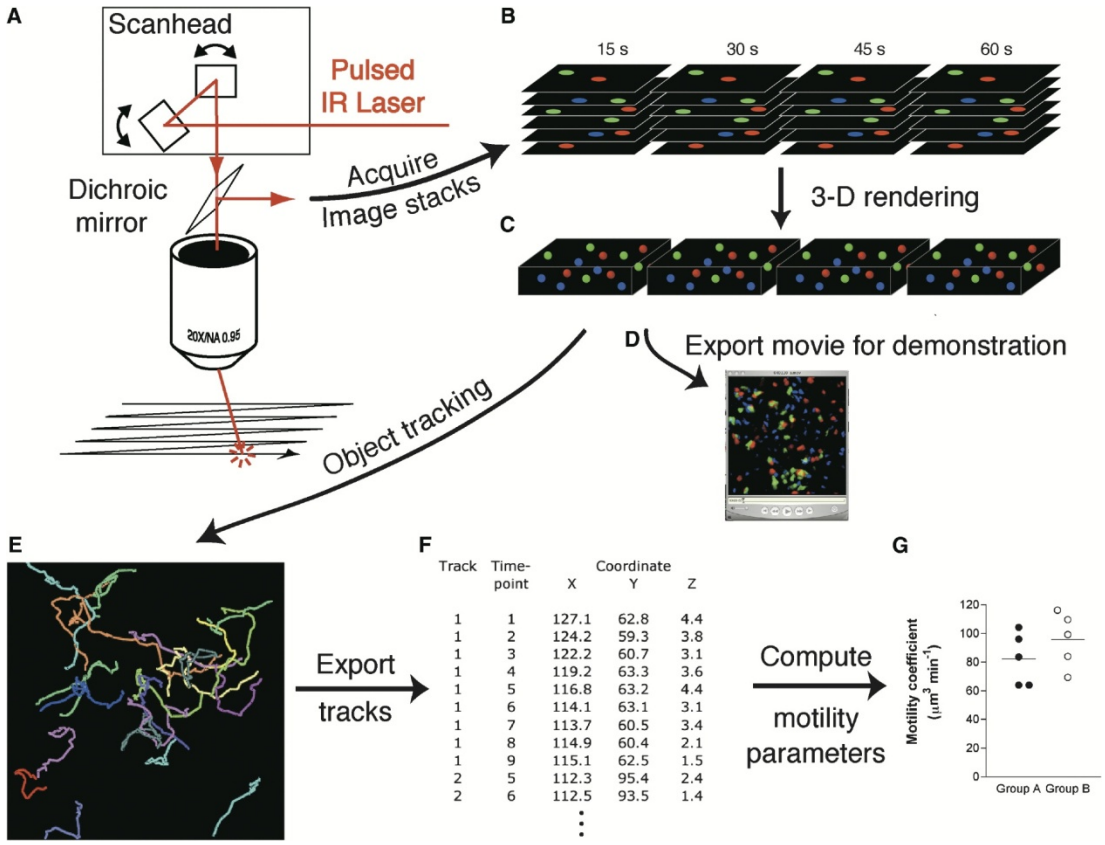

Figure 9. Acquisition of the *in vivo* cell motility by TPLM: steps demonstration. A pulsed bundle of infrared (IR) laser light is raster scanned via a microscope objective with high numerical aperture into a thick specimen by fast, synchronized movement of a pair of mirrors. Fluorescent signals are generated by the multiphoton excitation in a ~1μm deep section at the focal plane (**A**). The specimen stacks of optical sections are serially reacquired at defined time intervals (in this example, 15 s are required to acquire one z stack composed of six optical sections) (**B**). Each z stack is rendered as a three-dimensional volume (**C**), and two-dimensional projections of image stacks are exported as movie files for the off-line analysis (**D**). Determination of cell centroids to represent cell position allows automated or manual tracking of migration paths (**E**). Tracks consisting of serial sets of xyz coordinates of single cell centroids are exported as numerical databases, and are used to compute parameters of cell motility with specialized software for 2D or 3D cell tracking (**G**) (Picture adapted from Sumen C et al., *Immunity*, 2004).

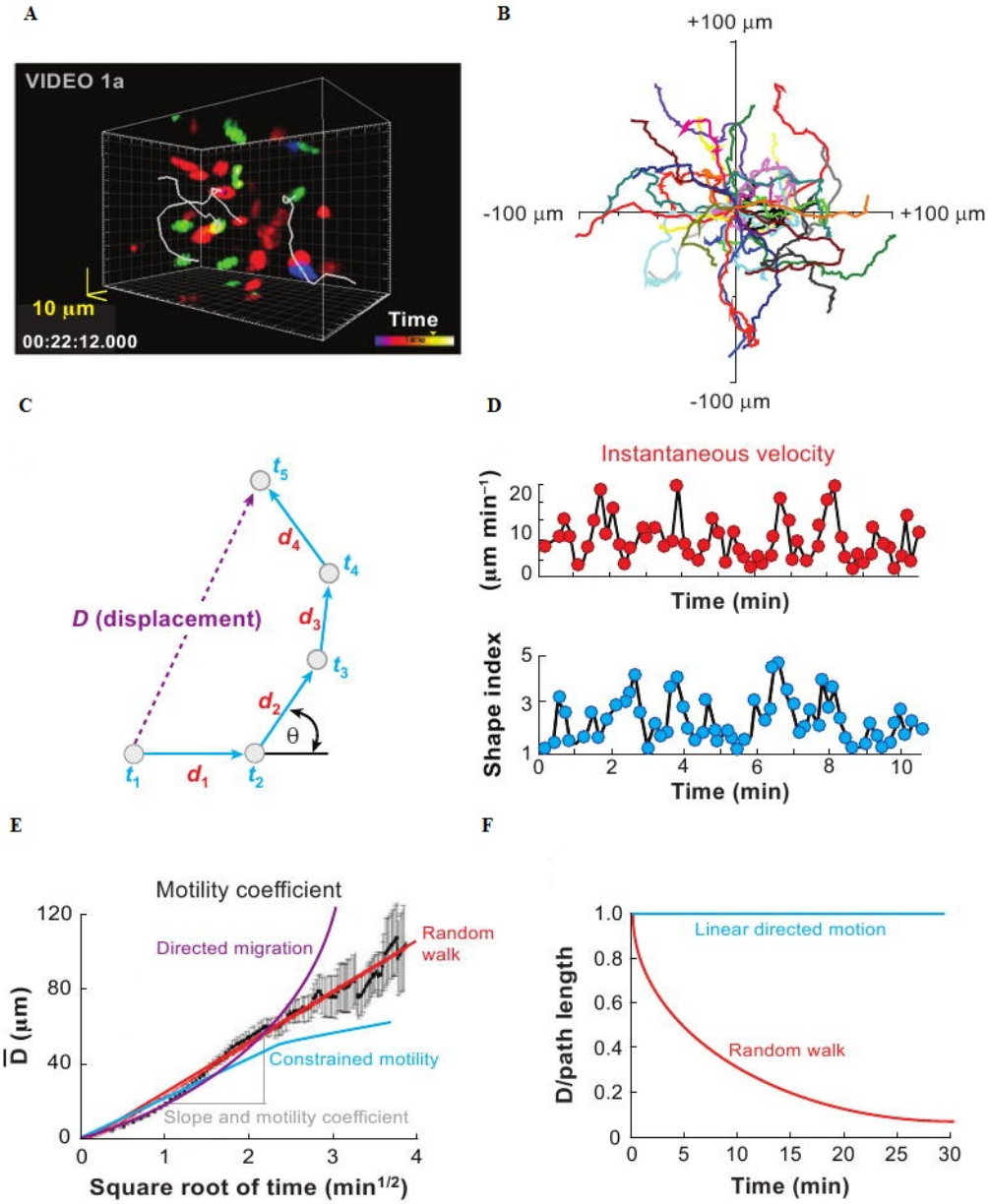

Figure 10. Analysis of the *in vivo* cell motility by TPLM: basics of motility parameters. Visualization of the 3D locations of fluorescently labeled cells at a single time point with tracks of three cells as demonstration (**A**). Plot representation of 2D tracks of several cells, rendering after normalizing their starting coordinates to the origin (**B**). A track of a cell at five successive time points, t_1, t_2, etc is showed. Instantaneous velocities are calculated from the net distance d traveled during each time interval Δt, and the turn angle θ is the angle through which the cell turns between time steps. The displacement D is the straight-line distance of the cell from its origin at any given time. Path length is given by the sum of d_1, d_2, d_3, etc. Persistence time (or length) is the time for which a cell continues to move without turning appreciably, as is illustrated for

time points t_2–t_4 (**C**). The instantaneous velocity of T cells sways in a characteristic manner over time, accompanied by changes in shape index (long axis/short axis) as the cell elongates while moving fast (**D**). If cell motility follows a random walk the plot of mean displacement from origin of multiple cells is expected to follow a straight line when plotted as a function of square root of time. The slope of this line can be used to derive a motility coefficient M, analogous to the diffusion coefficient for Brownian motion. Deviations from a straight-line relationship may be indicative of directed migration (*upward curvature*) or migration constrained by physical or biological barriers (*plateau*) (**E**). The measure defined as the ratio between displacement and path length from origin, namely chemotactic index, remains constant with a value of unity for linear-directed motion but decreases progressively with time if cells follow a random walk (**F**) (Picture adapted from Cahalan MD and Parker I, *Ann Rev Immunol*, 2008).

Results

Characterization of Th1 and Th17 cytokine production and their adhesion molecule expression

By using flow cytometry analysis, we first evaluated the purity of Th1 and Th17 cells preparation in term of cytokines production. We obtained bulk numbers of Th1 and Th17 cells free of contaminating IL-17 and IFN-γ producing cells in Th1 and Th17 cells, respectively. In Th1 cultures we achieved more than 50% of T cells that produced IFN-γ and in Th17 cultures 40% of cells produced IL-17 (**Fig. 11**). We next investigated the following adhesion molecule expression on Th1 and Th17 cells: α4 integrin chain, α4β7 integrin, LFA-1, CD44, L-selectin and PSGL-1 (**Fig. 12**). Th17 cells showed a significantly lower percentage of expression for L-selectin when compared to Th1 cells suggesting a higher state of activation. α4β7 integrin expression was higher on Th17 cells compared to Th1 cells (**Fig. 12A**). Interestingly the mean intensity fluorescence (MIF) of LFA-1 was statistically higher on Th1 cells (**Fig. 12B**). These data show a different integrin expression pattern in Th1 and Th17 cells, suggesting they may use different mechanisms during their migration and motility in the inflamed tissues.

Epifluorescence intravital microscopy results

Th1 and Th17 cells differently interact with inflamed CNS endothelium during EAE

We analyzed the intravascular interactions of fluorescently labeled exogenous Th1 and Th17 at different phases of EAE, in particular at the preclinical phase (7 dpi;), disease onset (11-14 dpi) and chronic phase (22-25 dpi; considered as 5 days after clinical course stabilization). Autoreactive Th1 and Th17 cells were intravenously injected immediately before imaging. We first collected morphological *data* on the vessel diameters during the different phases of the disease. The morphological results showed a significant enlargement of the pial vessels of the SC at disease peak in comparison to the other phases analyzed (**Fig. 13, Table I**). Results among the hemodynamic parameters analysis showed a great reduction in particular on the wall shear stress (WSS) at the onset of EAE compared to the other phases (**Table I**). In order to investigate the migration of

Th1 and Th17 cells in the CNS, we performed IVM experiments at different time points after EAE induction. In particular, we investigated Th1 and Th17 cell adhesion during the preclinical phase, disease onset and chronic phase. At the preclinical phase of the disease Th1 cells showed higher capacity to roll on vessel endothelium (26.5% *versus* 19.4%, *P=0.0172) and perform firm arrest in pial venules (4.4% versus 1.4%, **P=0.0026) when compared to Th17 cells. However, Th17 cells appeared more adhesive when compared to Th1 cells presenting higher capacity to roll (30.8% *vs* 21.0% respectively, *P=0.0412) and adhere (3.8% *vs* 2.2% respectively, *P=0.0419) in pial SC vessels during the EAE onset. IVM experiments performed during the chronic phase showed that Th1 and Th17 cells displayed a pair capacity to firm arrest in the pial venules (2.3% *vs* 2.8 % respectively, P=0.3705) with a major tendency for Th1 cells to roll when compared to Th17 (25.5% *vs* 20.0% respectively, *P=0.0131) (**Fig. 14**, **Table II)**. Basal frequency of T cell rolling and adhesion after transfer in naïve mice resulted from a previous work published by our laboratory's group shown that non activated cerebral endothelium does not support lymphocyte interactions both of resting cells freshly isolated from peripheral lymphonodes and autoreactive encephalitogenic T cells (Piccio L, *J Immunol*, 2002).

LFA-1 controls Th1 but not Th17 cell adhesion in inflamed CNS vessels

We next investigated the role of LFA-1 in Th1 and Th17 cell trafficking in the CNS during EAE (**Fig. 15**). For this purpose, we pretreated T cells with blocking anti-LFA-1 antibody (clone TIB213). LFA-1 blockade in the preclinical phase of disease reduced Th1 cell rolling events by 56% (**P=0.0085) and drastically reduced firm adhesion in pial vessels (inhibition of 87.5%, **P=0.0060) (**Table III)**. However, LFA-1 blockade at EAE onset led to a minor but significant reduction of Th1 cells rolling (inhibition of 41%, ***P=0.0004) and adhesion (inhibition of 38%, *P=0.0175) on SC vessels (**Table III**) without any effect in the chronic phase (**Table III**). Interestingly the pre-treatment with anti-LFA-1 mAb did not significantly affect interactions between Th17 cells and vessels endothelium in SC during all EAE phases (**Table IV**). These data suggest different molecular mechanisms controlling the recruitment of Th1 and Th17 cells

in the SC venules during EAE, and that LFA-1 plays a selective role in the migration of Th1 cells during the earlier phases of EAE (preclinical phase and disease onset), whereas Th17 cell recruitment in the SC seems to be independent from LFA-1.

α4 integrins differently control the recruitment of Th1 and Th17 cells in the CNS during EAE

In order to understand the role of α4 integrins in the recruitment of Th1 and Th17 cells, we pretreated T cells with blocking anti-α4 chain (clone PS/2) or anti-α4β7 integrin (clone DATK32) antibodies before the cell injection (**Fig. 16**). In the preclinical phase of disease, blockade of α4 chain in Th1 cells led to a significant inhibition of rolling and adhesion events (**P=0.0025 and *P=0.0167 for rolling and adhesion respectively) (**Table III**), whereas the adhesive interactions of Th17 cells were not affected by α4 blocking (**Table IV**). At the onset of EAE we observed a massive reduction of rolling (73% of inhibition, ***P=0.0002) and firm adhesion (81% of inhibition, **P=0.0013) in Th1 cells (**Table III**). Interestingly, α4 chain inhibition in Th17 cells drastically reduced stable adhesion by 95% (***P<0.0001) without significant effect on rolling (**Table IV**). Treatment with anti-α4 chain antibody during the chronic phase of the disease significantly inhibited Th1 cell rolling (35% of inhibition *P<0.05) and completely abrogated firm arrest (***P<0.0001) (**Table III**). α4 blockade in Th17 cells during the chronic phase did not affect rolling but reduced the arrest by 65% (**P=0.0010) (**Table IV**). These data suggest different molecular mechanisms used by Th1 and Th17 cells to interact with endothelium in CNS vessels during EAE stages. In the preclinical phase of EAE α4 integrins (probably VLA-4) play a selectively role in the migration of Th1 cells without interfering with Th17 recruitment, whereas at the latest stages of the disease (onset and the chronic phase) α4 integrins blocking prevents rolling and adhesion of Th1 cells, but affects only arrest in Th17 cells, suggesting different roles for α4 integrins in the control of Th1 and Th17 cells recruitment the CNS during EAE.

α4β7 specifically controls Th17 cell adhesion in inflamed CNS vessels during EAE

In order to investigate a potential specific role for α4 integrins in the Th1 and Th17 cells recruitment during EAE, we next investigated the potential role of α4β7 expressed on Th1 and Th17 cells in CNS trafficking during EAE (**Fig. 16**). At the onset of the disease, Th17 cells treated with a blocking anti-α4β7 antibody (clone DATK32) reduced adhesion events of 74% (**P=0.0075) without any effect on rolling in SC vessels (**Table IV**). Similarly, treatment of Th17 cells with anti-α4β7 in the chronic phase of EAE, led to a reduction of 60% of stable adhesion events (***P<0.0001) while rolling was not affected (**Table IV**). These results parallel the data obtained from IVM experiments obtained after α4 chain blockade and underline the role of α4β7 in stable adhesion of Th17 cells in the SC inflamed endothelial venules. In contrast to the results obtained with Th17 cells, α4β7 had no role in Th1 cell rolling and adhesion in the SC during EAE (**Table III**). Together these data suggest that VLA-4 is a major player in Th1 cells migration in the CNS during EAE, whereas α4β7 integrin has a more prominent role in Th17 cell trafficking.

Two photon laser microscopy results

Th1 and Th17 cells massively infiltrate the CNS at disease peak

We analyzed the intraparenchymal behavior of fluorescently labeled exogenous Th1 and Th17 at the following time points: pre-clinical phase (9 days post-immunization, dpi), T cells were injected 7 dpi and imaging was performed 48 hours later; disease peak (13-14 dpi), T cells were transplanted the day after the onset of disease (11-12 dpi) and imaging was performed 48 hours later; chronic phase of EAE (22-25 dpi), T cells were injected after 3 days of chronic course stabilization and their motility behavior was evaluated by imaging after 48 hours.

We first performed studies using TPLM to determine Th1 and Th17 cell infiltration at different time points after mice immunization with MOG_{35-55} peptide. Our results showed a massive cellular infiltration at the peak of EAE in comparison with the other phases (**Fig. 17**).

Th1 and Th17 cells behave in a similar manner in the preclinical phase of EAE

At the preclinical phase of the disease (mean clinical score 0 ± 0 (S.D.)) we found a very low number of T cells migrated into the SC. We did not observe significant differences in velocity and motility parameters between Th1 and Th17 cells: both were moving fast (around 8 μm/min) and displayed relative high levels of motility coefficient and low meandering index (around 0.5) suggesting random movements of these cells inside the SC without significant interactions with local cells (**Fig. 18A, B, C**).

Th1 and Th17 cells present different motility behavior at EAE peak

A different situation was observed at the disease peak (mean clinical score 4.5 ± 0.5 (S.D.)). We found a massive infiltration of Th1 and Th17 cells compared to the preclinical phase of EAE. Both T cells displayed a reduction in the movement when compared to the preclinical phase of EAE. However, Th1 cells displayed a significant higher velocity (4.9 μm/min) when compared to Th17 cells (3.7 μm/min) (**Fig. 18D**). Also, the motility coefficient was significantly higher in Th1 cells when compared to Th17 cells (**Fig. 18F**). Interestingly the higher value of meandering index in the Th1 cells (0.52) suggests a more straight (directed) movement of Th1 cells compared to Th17 cells (0.40) (**Fig. 18E**). We distinguished two different behavioral patterns in Th1 cells and Th17 cells: approximately 80-85% of cells were rapidly moving, while the rest 10-15% was not moving and was anchored around a fixed point closed to vessels wall suggesting a potential physical contact with other cells. In the portion of moving Th1 cells, it was possible to distinguish between cells that were following the vessels wall (30%) and cells (45%) moving inside the parenchyma. However, Th17 showed the same behavior with the 30% of cells walking beside the vessels wall and the 40% of cells moving in the parenchyma. Examining in depth we could distinguish two different behaviors between Th1 and Th17 cells in the way they were moving inside the parenchyma. Th1 cells were moving straight covering long distances deep in SC suggesting that they were meandering following a chemotactic gradient, while Th17 cells seemed to move around in a specific volume of tissue in a “stop and go” way. These observations were

confirmed analyzing the fraction of cells moving deep in the parenchyma. The plot of displacement *versus* time (**Fig. 19C**) displayed a significant higher sloop in Th1 cells migration suggesting that Th1 cells were moving covering wider space in the parenchyma compared to Th17 cells. Chemotactic index of Th1 cells displayed a stable value around 0.8 during the time of observation, while Th17 cells were inclined to decrease the ratio (**Fig. 19D**). These data suggested that Th1, unlike to Th17 cells, were meandering straight following a chemotactic gradient in a directed migration. Interestingly arrest index resulted significantly higher in Th17 cells (0.11) when compared to Th1 cells (0.07). Instantaneous velocity showed how Th1 cells meandered straight through the tissue in a steady movement, while Th17 cells displayed a "stop-and-go" mode when they migrated deep in the parenchyma (**Fig. 19E**). Representative tracks of motility behavior of Th1 and Th17 are displayed in **Fig. 19B**.

The different motility behavior between Th1 and Th17 cells during the peak of the disease indicates potential different molecular mechanisms used by these cells to migrate in SC parenchyma. Moreover, the massive cellular infiltration during the peak of EAE made this disease phase a powerful experimental approach to investigate how blocking of VLA-4 and LFA-1 integrins could affect motility behavior of Th1 and Th17 cells into the SC during EAE.

Th1 and Th17 cells behave similarly displaying a severe reduction in dynamics in the chronic phase of EAE.

A completely different behavior of Th1 and Th17 cells was found in the chronic phase of EAE (mean clinical score 2.1 ± 0.7 (S.D.)). TPLM experiments performed at the chronic phase of EAE showed a significant reduction of mean velocity, meandering index and motility coefficient of both Th1 and Th17 cells (**Fig. 18G, H, I**). However, we did not observe any significant difference between Th1 and Th17 behavior. Both Th subsets were moving slower when compared to the other disease phases (around 3 μm/min) and the results obtained for the meandering index showed that both Th1 and Th17 cells did not have highly directional migration (around 0.3) (**Fig. 18H**). As observed at disease peak, we distinguished two different motility patterns in Th1: 75% of the cells were moving

and the rest (25%) displayed a stationary behavior. On the other hand, only the 10% of Th17 cells appeared in an "anchored" state. All together these data suggest an antigen-recognition process between T cells and potential APCs in the SC during the chronic phase of EAE. The idea that T cells were engaged in a physical contact with other cells was confirmed by computation of the arrest coefficient that resulted statistically higher for both Th1 and Th17 cells when compared to the same T cells at the peak phase of disease. No differences were found between Th1 and Th17 cells regarding the arrest coefficient and instantaneous velocity at the chronic phase of EAE (**Fig. 18G**).

LFA-1 blockade affects Th1 cell motility and cytoskeleton rearrangement

In order to investigate a potential role of LFA-1 in the migration movement of Th1 cells in the CNS parenchyma, we performed TPLM experiments at the clinical peak of EAE analyzing the motility behavior of these cells before and after administration of an anti-LFA-1 blocking antibody. Neutralization of LFA-1 activity led to a reduction of mean velocity (from 5.7 μm/min in control cells to 3.8 μm/min in treated cells) and motility coefficient in Th1 cells (**Fig. 20B, C**). Interestingly the portion of not moving cells was not significantly modified after antibody treatment (11.4% in the control untreated cells and 16.7% in treated cells) suggesting that Th1 cells were still moving but with a reduced velocity. The arrest coefficient analysis confirmed these observations since the value of control cells (0.25%) resulted not modified after LFA-1 blocking (0.30%) (**Fig. 20E**). However, the meandering index was drastically affected by LFA-1 blocking: untreated Th1 cells showed a mean ratio of 0.6 with the majority of cells moving in straight direction, whereas anti-LFA-1 treated Th1 cells displayed a drastic reduction in the meandering index (0.4) (**Fig. 20F**). These data suggest that LFA-1 activity controls the capacity of Th1 cells to move in a straight line following a chemotactic stimulus. In particular, the analysis performed on the portion of Th1 cells moving deep in the SC parenchyma, has shown a drastic modification of motility behavior in Th1 cells after LFA-1 blocking treatment. The plot of the dynamic displacement showed a significant reduction in the curve sloop after antibody treatment suggesting that Th1 cells in absence of LFA-1 activity were

not able to walk through long-range distances covering a wide portion of volume of tissue (**Fig. 20G**). Moreover, the chemotactic index resulted significantly affected because treated Th1 cells showed a clear tendency to reduce the ratio between displacement and path length during the time of analysis suggesting a role of LFA-1 in the capacity of Th1 cells to proceed straight following a chemotactic factor (**Fig. 20H**). Representative tracks of motility behavior of Th1 before and after administration of anti-LFA-1 are displayed in **Fig. 20A**.

In order to investigate an active involvement of LFA-1 in cytoskeleton rearrangement in Th1 cell directed migration we compared the morphology of Th1 cells before and after the anti-LFA-1 treatment. The initial response of a cell to a migration-promoting agent is to polarize and extend protrusions in the direction of migration. These protrusions can be large, broad lamelli-podia or spike-like filopodia and are quantified as number of vertices for each cell analyzed. The volume of treated Th1 cells was significantly smaller compared to the control cells and the number of vertices was drastically reduced after LFA-1 blockade (**Fig. 21A, B**), indicating that treated Th1 cells became rounded and reduce their volume because of the reduction of cytoskeleton rearrangement. Thus, these data show that LFA-1 blockade drastically affects the dynamics of Th1 cells in the SC parenchyma during EAE through the inhibition of cytoskeleton dynamics. In addition, the inhibition of LFA-1 leads to a velocity reduction in Th1 cells with consequent decreased displacement and interferes with their directed migration.

LFA-1 controls Th17 cells motility behavior in the CNS at EAE peak

Using TPLM approach we next investigated a potential role of LFA-1 in the motility behavior of Th17 cells in CNS parenchyma at EAE peak. Neutralization of LFA-1 activity affected the dynamics of Th17 cells leading to a reduction of mean velocity (from 3.5 μm/min in control cells to 2.6 μm/min in anti-LFA-1 treated cells) and motility coefficient (**Fig. 22B, C**). Differently to Th1 cells that reduced their velocity after antibody administration, Th17 cells massively reduced their velocity till stop. Indeed, the portion of not moving cells in the control (11.0%) was drastically increased after LFA-1 blocking (47.7%) leading to an

increased arrest coefficient that was significant higher in the treated Th17 cells (0.49%) when compared to control cells (0.30%) (**Fig. 22E**). Moreover, the meandering index was reduced in Th17 cells after antibody administration (0.26) when compared to untreated condition (0.36) (**Fig. 22F**). As shown before, while Th1 cells showed high levels of meandering index, Th17 cells were associated to lower values of this ratio indicating that the majority of t cells were not moving in a directed way but displayed a different migration pattern. For this reason, the reduced meandering index in Th17 cells after LFA-1 blocking was probably due to the portion of not moving cells and not to a change in the motility behavior of moving cells. The analysis performed on the portion of Th17 cells that were still moving deep in the SC parenchyma after antibody administration, suggested that LFA-1 did not affect the motility behavior in Th17 cells after LFA-1 blocking treatment: we did not indeed observe significant differences in displacement and chemotactic index in Th17 cells before and after LFA-1 blocking (**Fig. 22G, H**).
Representative tracks of motility behavior of Th17 before and after administration of anti-LFA-1 are shown in **Fig.22A**.
The volume and the number of vertices were not altered after antibody treatment (**Fig. 23A, B**), indicating that LFA-1 activity is not involved in the cytoskeleton rearrangement during Th17 motility and ii) the arrest of these cells during LFA-1 blockade is not due to a deficit in cytoskeleton dynamics.
Taken together these data clearly show that LFA-1 drastically controls the movement of Th17 cells in the SC parenchyma during EAE, increasing the percentage of not moving cells and without interfering in their cytoskeleton dynamics. The inhibition of LFA-1 led to a massive reduction in the velocity (50% reduction) of Th17 cells without interfering with the motility behavior of the rest of moving cells (50%).

Intrathecal injection of anti-LFA-1 antibody at disease onset inhibits EAE development

The data shown above suggest that efficient effector T cell motility in the SC parenchyma is regulated by CNS resident cells, which are important for their functionality and reactivation in the CNS. For this reason, we hypothesized that

interfering with local T cell dynamics in the SC may limit their pathogenicity and may impact EAE development in immunized mice. To test this hypothesis, we treated MOG_{35-55}-immunized EAE animals the day after disease onset and 4 days later by intrathecal injection of anti-LFA-1 antibody or control anti-Ras antibody. We found that local LFA-1 blockade significantly inhibited EAE development, when compared to mice treated with the control antibody (*P<0.05) (**Fig. 24A**). This clinical amelioration was associated with a significant reduction of both inflammatory cell infiltration (**P=0.0034) and demyelination (***P=0.0003) in anti-LFA-1 treated animals, compared to control animals (**Fig. 24B**). Furthermore, the massive microgliosis in the lumbar SC of control EAE mice was drastically attenuated in anti-LFA-1 treated animals (***P<0.0001) (**Fig. 24C**). To note, the second anti-LFA-1 injection 4 days after the first one further delayed the appearance of the clinical peak in EAE mice. However, 5-6 days after the second antibody injection, anti-LFA-1 treated mice showed a tendency toward disease worsening, compared to control mice that already developed the disease peak, suggesting that LFA-1 blocking probably did not eliminate pathogenic T cells from the SC parenchyma, but they were maintained in a more "quiescent" state in the SC parenchyma. Collectively, these results confirm that interfering with local effector T cell dynamics in the CNS parenchyma may reduce their pathogenic potential and may represent a useful therapeutic strategy to control autoimmune disease progression.

α4 integrin blockade does not affect Th1 cells intraparenchymal motility behavior in the CNS at the peak of EAE

We next evaluated a potential role of α4 integrin in Th1 cells movement in the SC parenchyma at EAE peak. We performed TPLM experiments evaluating the effect of anti-α4 integrin blocking antibodies on the motility behavior of Th1 cells. We did not observe differences in the dynamics of Th1 cells before and after administration of blocking antibody regarding mean velocity, meandering index, motility and arrest coefficient (**Fig. 25A**, **B**, **C**, **D**). These data clearly indicate that α4 integrin is not involved in the motility behavior of Th1 cells at EAE peak.

α4 integrins control Th17 cells intraparenchymal motility behavior in the CNS at EAE peak

Neutralization of α4 integrin activity, differently from Th1 cells, affected the dynamics of Th17 cells leading to a drastic reduction of mean velocity (from 3.7 μm/min in control cells to 2.6 μm/min in treated cells) and motility coefficient (from 47 μm^2/min in control cells to 13 μm^2/min in treated cells (**Fig. 26A, C**). Moreover, the meandering index was significantly affected by α4 blockade, with anti-α4 treated Th17 cells displaying a drastic reduction in the meandering index (0.27) (**Fig. 26B**). Also, the portion of not moving cells was clearly increased after LFA-1 blocking leading to a raise in the arrest coefficient that was significant higher in the treated Th17 cells (0.35%) compared to control cells (0.15%) (***P<0.0001) (**Fig. 26D**). These data suggest a selective role for α4β7 integrin in the control of the motility behavior of Th17 cells inside SC parenchyma.

Intrathecal injection of anti-α4β7 antibody at disease onset ameliorates EAE severity

We hypothesized that α4β7 integrin blockade may specifically interfere with local dynamics of Th17 cell subset in the SC and may impact EAE development in immunized mice. To test this hypothesis, we treated MOG_{35-55}-immunized EAE animals the day after disease onset and 3 days later by intrathecal injection of anti-α4β7 antibody or control anti-Ras antibody. We found that local α4β7 blockade significantly inhibited EAE development, when compared to mice treated with the control antibody (*P<0.05) (**Fig. 27**). To note, the clinical amelioration remained stable during all observation time suggesting an important role for autoreactive Th17 cells not only in EAE induction but also in the maintenance of neuroinflammatory *milieu.*

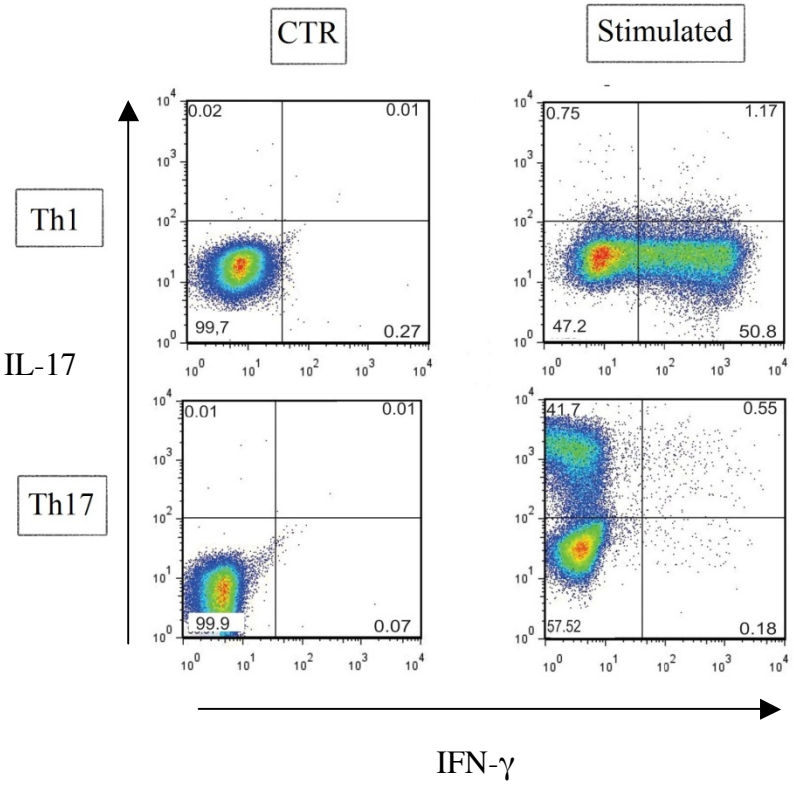

Figure 11. Intracellular staining of Th1 and Th17. Intracellular IL-17 and IFN-γ cytokine expression was analyzed by FACS.

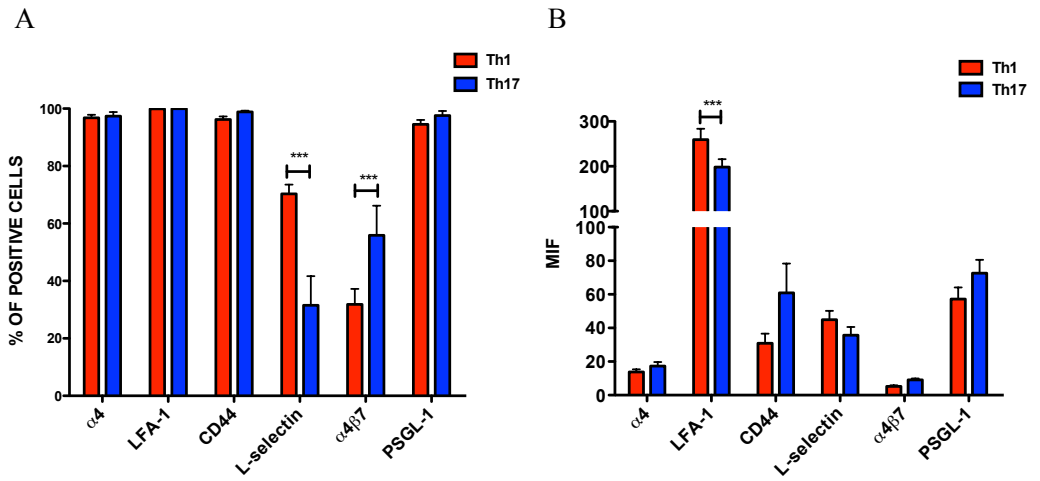

Figure 12. Adhesion molecule expression in Th1 and Th17 cells. Samples were analyzed by flow cytometry. Percentage of positive expression of adhesion molecules was evaluated. Th17 cells showed a significantly lower percentage of expression for L-selectin compared to Th1 cells, whereas α4β7 integrin expression was higher on Th17 compared to Th1 cells (**A**). MIF of LFA-1 was statistically significantly higher on Th1 cells (**B**). *Data* are expressed as mean ± SD. Statistics were calculated using Mann-Whitney test (*** P<0.0001).

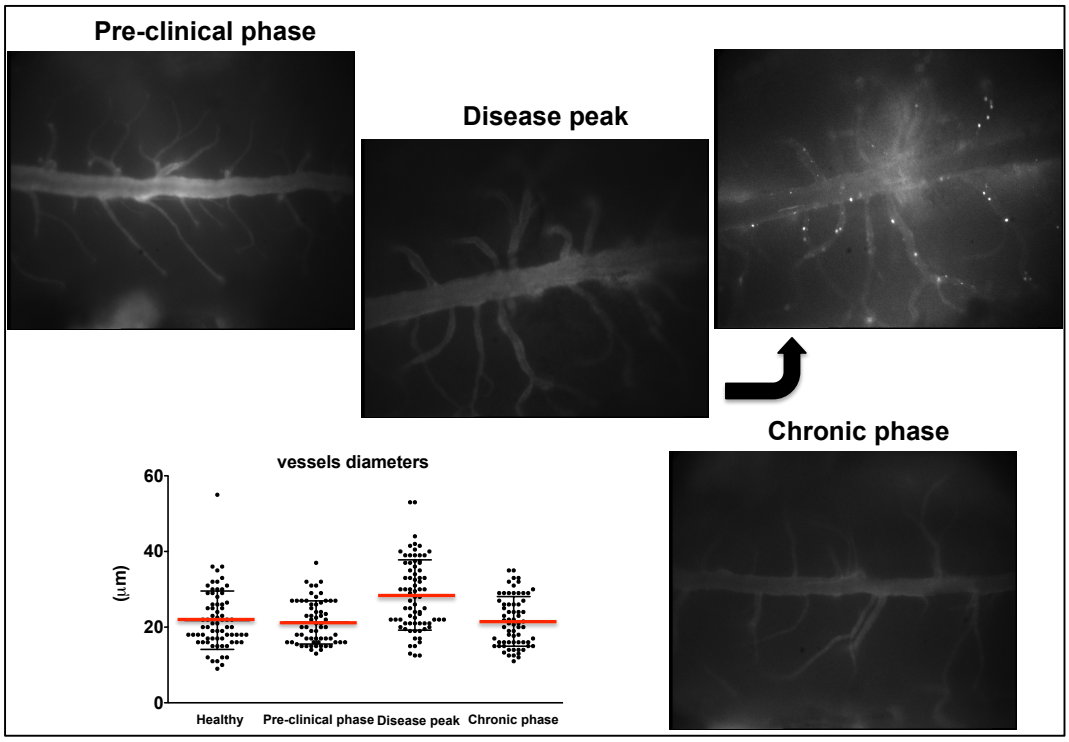

Figure 13. Vessel morphology during different EAE phases. Representative images of the spinal cord pial vessels during the pre-clinical phase, disease peak and chronic phase were taken at IVM to evaluate morphological changes in the course of pathology. Vessels were labeled with high molecular weight dextran. At the disease peak are reported two representative images taken before and after intravenously injection of labeled T cells. Graph reports the diameters, express in μm, of at least 75 vessels for each condition at different time point. Statistics were calculated using ANOVA one way test (*P<0.05).

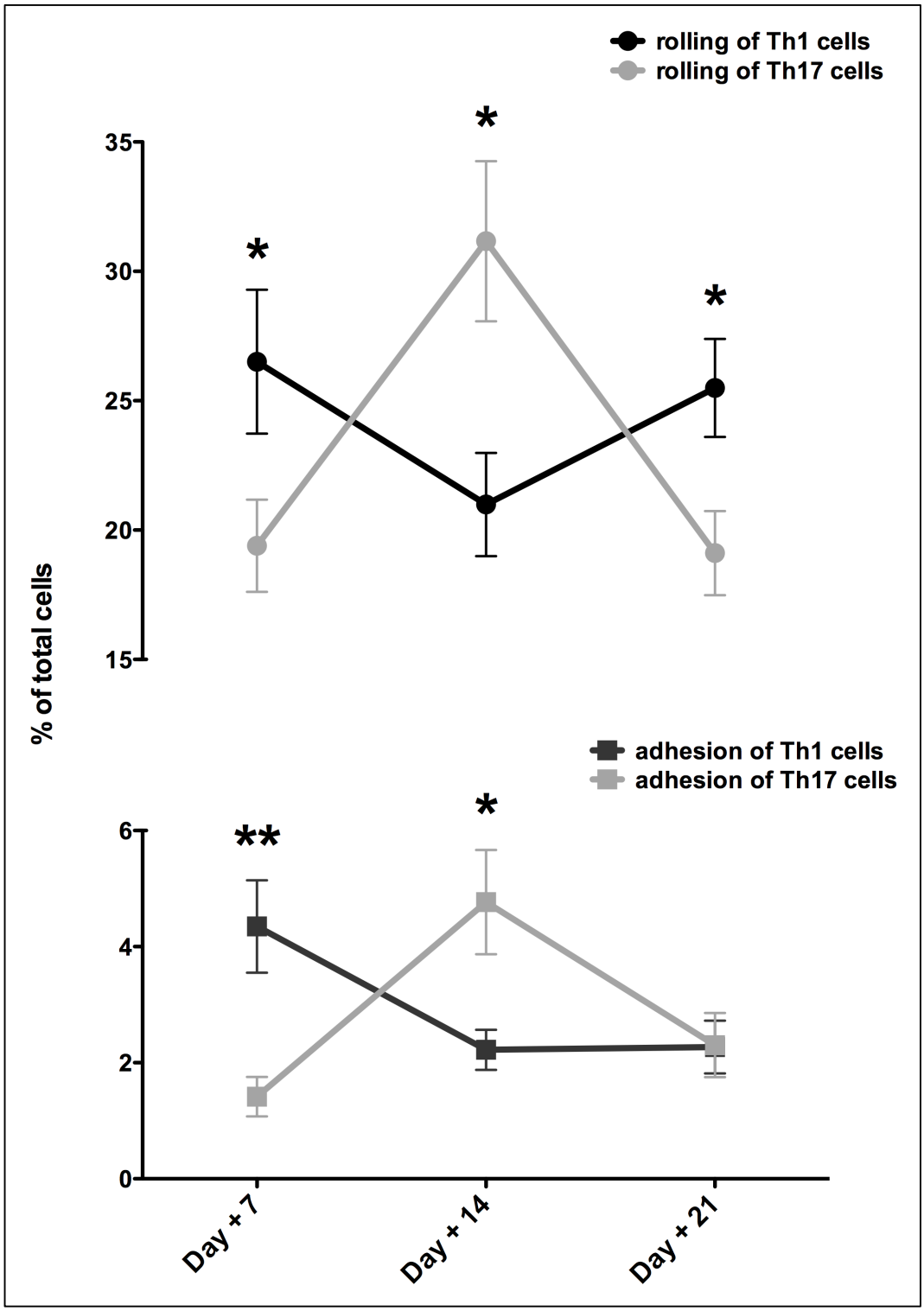

Figure 14. Time course of interactive events of Th1 and Th17 cells during different EAE phases. Two representatives graphs show the variations in the rolling and adhesion components for Th1 and Th17 cells during the course of the pathology. Graphs were obtained from the comparison of the interactive events of Th1 and Th17 at day 7, 14 and 21 post immunization and are expressed as

percentage on total cells. *Data* are expressed as mean ± SEM. Statistics were calculated using Mann-Whitney test (*P<0.05; **P<0.005).

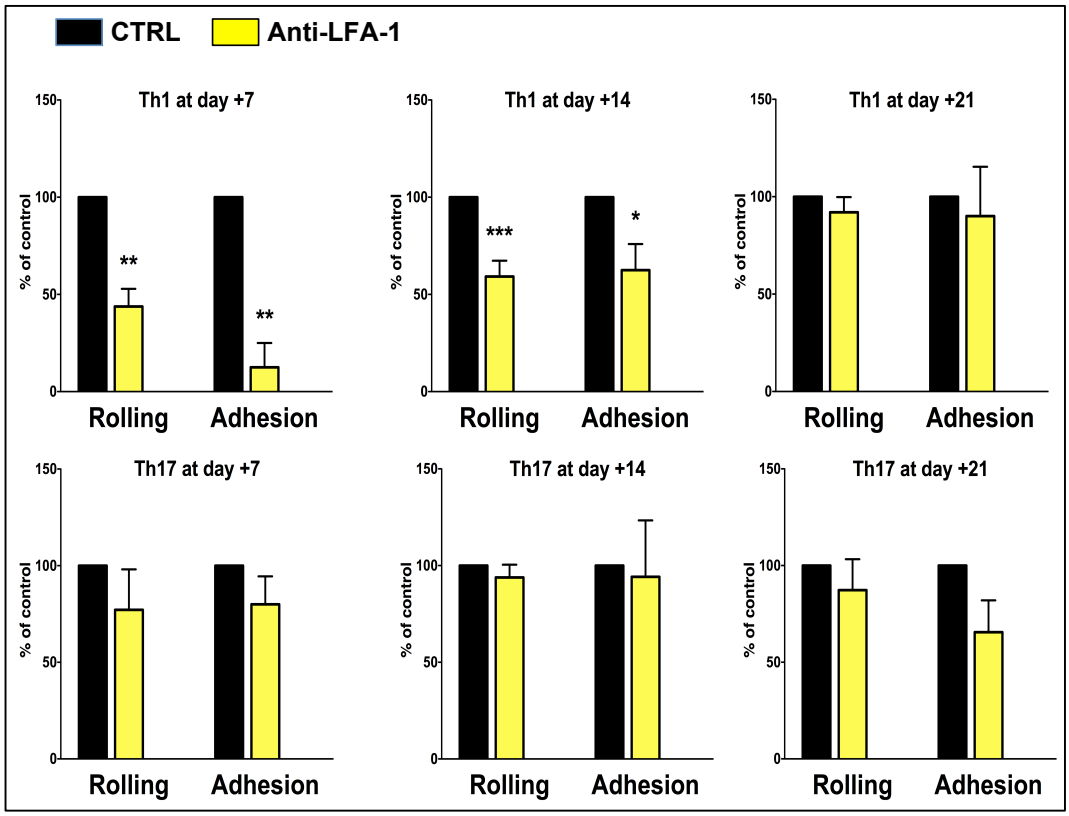

Figure 15. LFA-1 blocking affects early phases of Th1 interactions in the inflamed SC pial vessels during EAE. MOG_{35-55}-specific Th1 or Th17 cells were injected in EAE mice in the preclinical phase (7 dpi), at disease onset (14 dpi) and in the chronic phase (21 dpi) directly before imaging. A digital videotape of control cells interactions in the inflamed SC pial vessels was acquired. Afterwards, a tranche of anti-LFA-1 treated cells was injected. Digital videotape of treated cells was registered and manually analyzed. *Data* are expressed in mean ± standard error mean (SEM). Statistics were calculated with a one sample t test to the hypothetical control value fixed at 100. Two tailed test (*P<0.05; **P<0.005; ***P<0.0001).

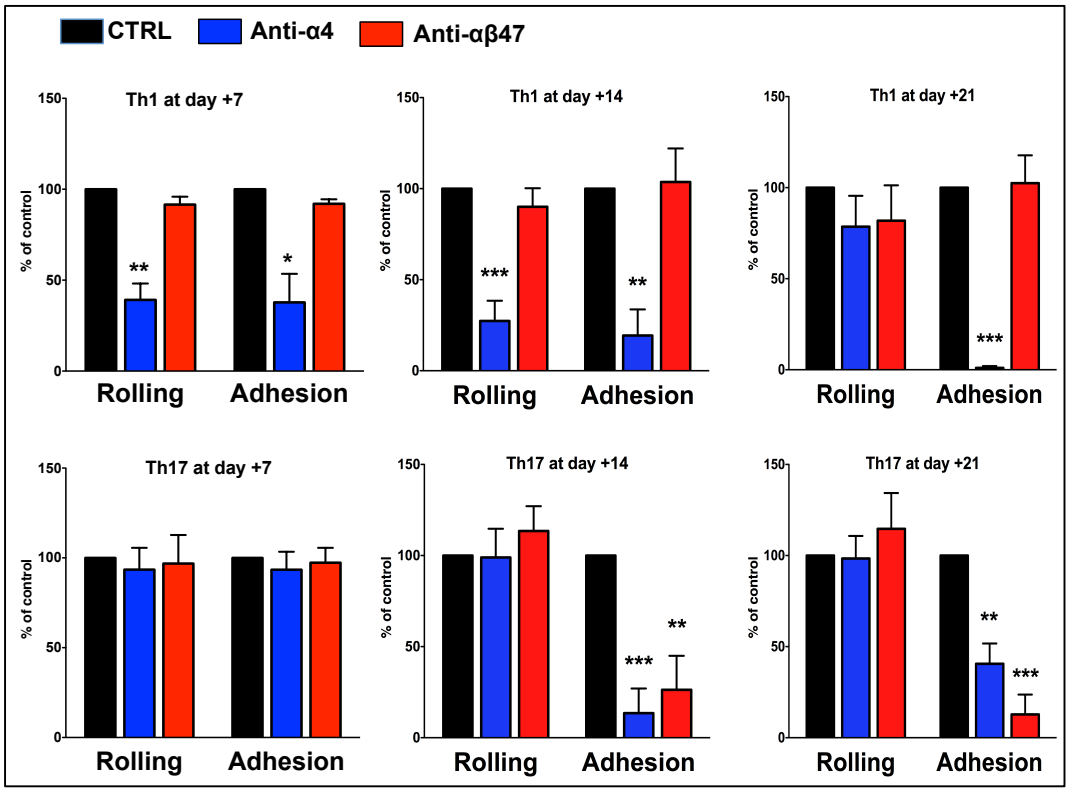

Figure 16. α4 integrins blockade differently affect Th1 and Th17 cell adhesion in inflamed SC vessels during EAE. MOG_{35-55}-specific Th1 or Th17 cells were injected in EAE mice in the preclinical phase (7 dpi), at disease onset (14 dpi) and in the chronic phase (21 dpi) directly before imaging. A digital videotape of control cells interactions in the inflamed SC pial vessels was acquired. Afterwards, a tranche of anti-α4 or anti-α4β7 treated cells was injected. Digital videotape of treated cells was registered and manually analyzed. *Data* are expressed in mean ± standard error mean (SEM). Statistics were calculated with a one sample t test to the hypothetical control value fixed at 100. Two tailed test (*P<0.05; **P<0.005; ***P<0.0001).

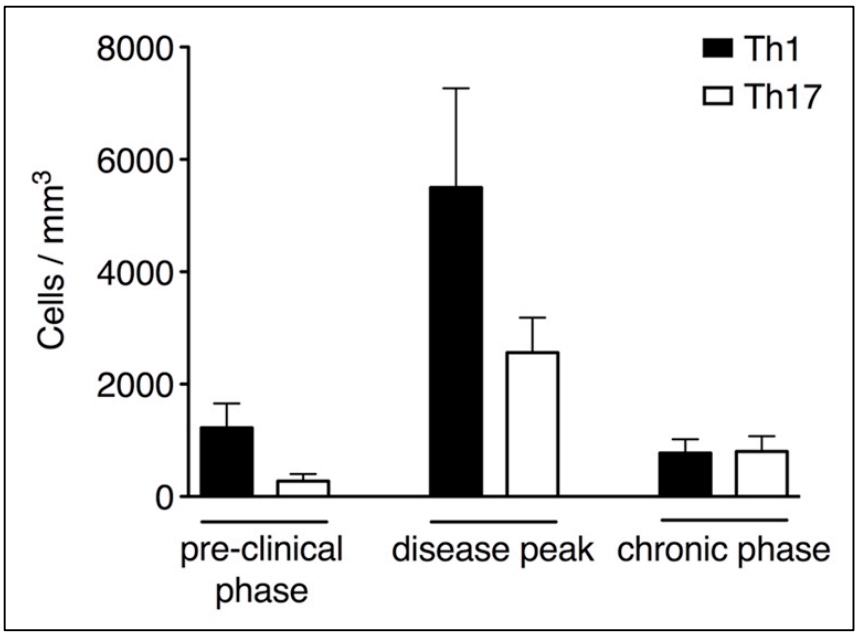

Figure 17. Quantification of Th1 and Th17 accumulation in the SC parenchyma at different disease stages. MOG_{35-55}-specific Th1 and Th17 cells were co-injected in EAE mice in the preclinical phase (7 dpi), at disease peak (11-14 dpi) or in the chronic phase (22-25 dpi). 48 hours later, TPLM imaging was performed. Cells were subsequently quantified by manual counting in field (volume) of acquisition. Data are the mean ± SEM of 6 different fields from 3 independent experiments.

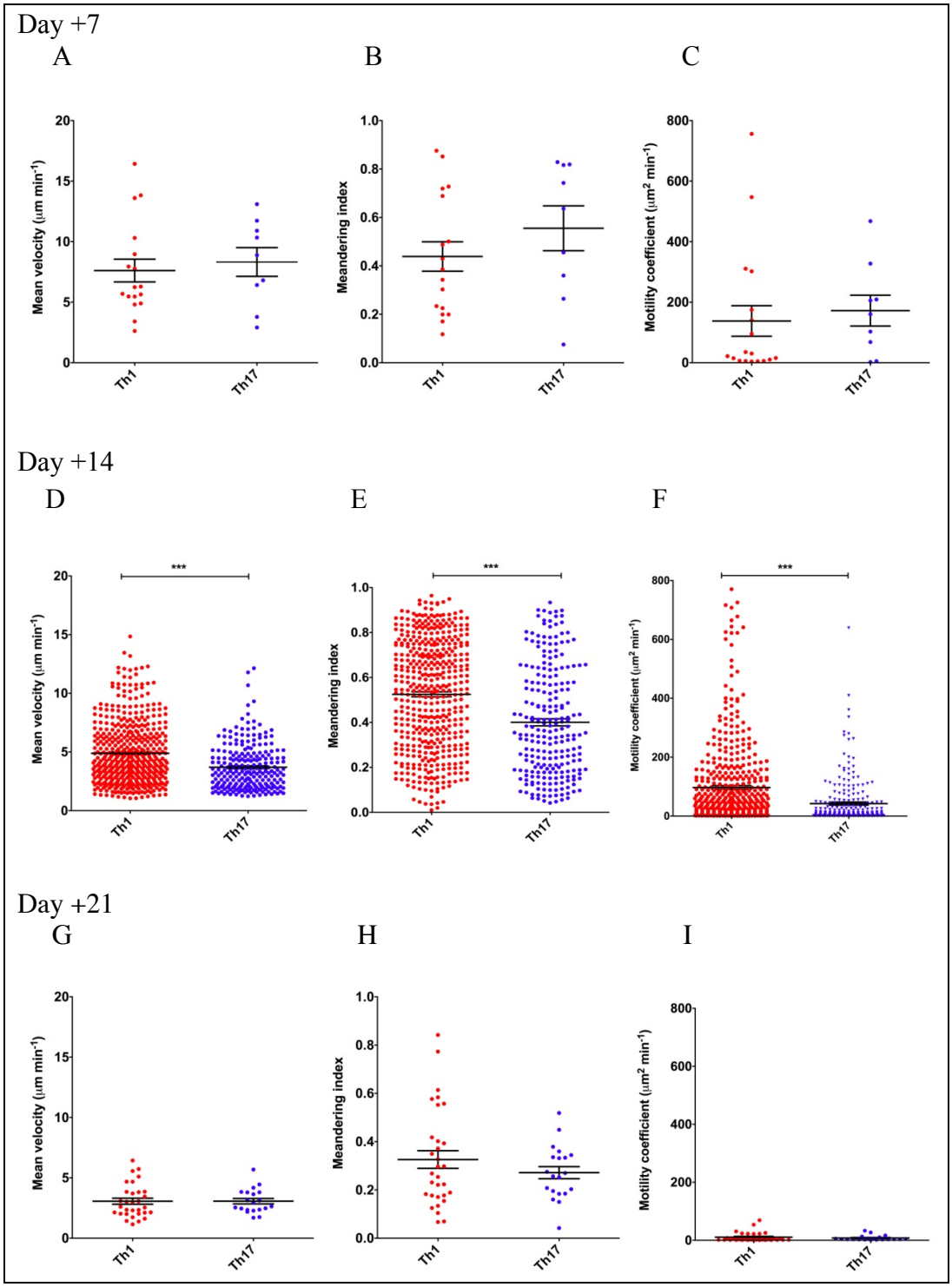

Figure 18. Th1 and Th17 cell dynamics during EAE phases in the SC parenchyma. Mice were immunized with MOG_{35-55} peptide and scored for EAE. MOG_{35-55}-specific Th1 and Th17 cells were co-injected in EAE mice in the preclinical phase (7 dpi), at disease peak (11-14 dpi) or in the chronic phase (22-25 dpi). 48 hours later, TPLM imaging was performed. (**A**) Mean velocity, **(B)** Meandering index and **(C**) Motility coefficient of Th1 and Th17 cells in the preclinical phase of the disease (7 dpi). (**D**) Mean velocity, **(E**) meandering index

and (**F**) motility coefficient of Th1 and Th17 cells at the peak of the disease (11-14 dpi). Massive infiltration of Th1 and Th17 was observed. (**G**) Mean velocity, **(H**) meandering index and (**I**) motility coefficient of Th1 and Th17 cells in the chronic phase of the disease (22-25 dpi). Data are expressed as mean ± SD. Statistics were calculated using Mann-Whitney test (***P< 0.0001).

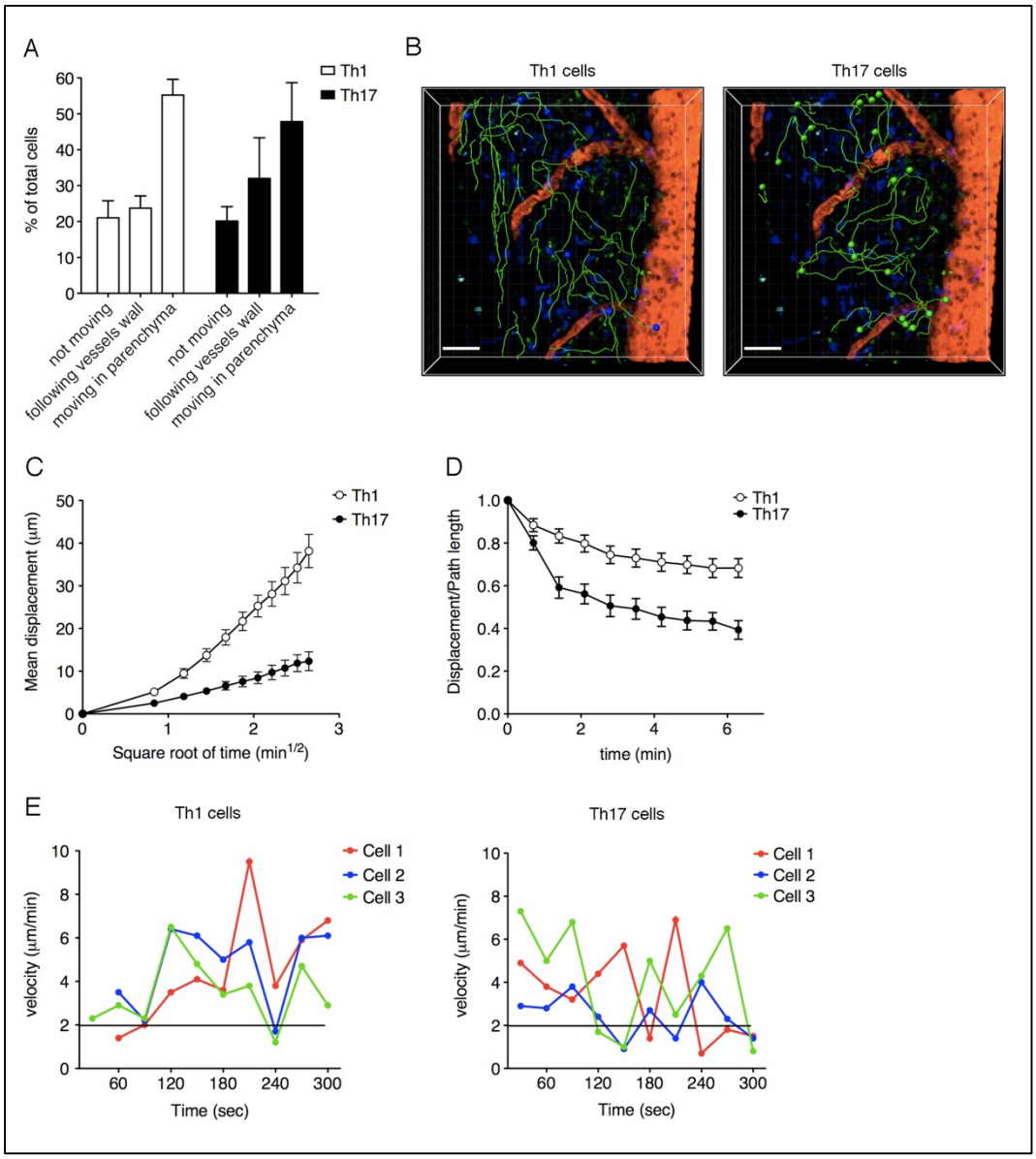

Figure 19. Comparison of autoreactive Th1 and Th17 dynamics in the SC parenchyma at EAE peak. MOG_{35-55}-specific Th1 and Th17 cells were co-injected in EAE mice at disease peak (11-14 dpi). 48 hours later, TPLM imaging was performed. Comparison of percentage of total Th1 and Th17 cells that were moving in the parenchyma, along vessels wall or not moving cells. Three-dimensional spatial position of each cell was detected based on centroid fluorescence intensity (**A**). Representative images of Th1 and Th17 cells moving in the deep SC parenchyma of EAE mice at disease peak. The images are all 3D reconstructions that include the vasculature (red), CMAC-labeled Th1 cell (blue) and CFSE-labeled Th17 cell (green). Green lines tracks motile T cells (scale bar: 50 µm). Cells were tracked over time (30 min of acquisition) manually **(B)**. Mean displacement **(C)** and chemotactic index (**D**) of Th1 and Th17 cells moving in the deep parenchyma of the SC. Instantaneous velocities of 3 representative Th1 (left panel) and Th17 cells (right panel) moving in the SC parenchyma. Cells moving

below 2 μm/min were considered stopped (**E**). Multidimensional imaging was performed by Imaris. *Data* are the mean ± SEM of 100 cells from 3 independent experiments. In (**C**) and (**D**) was applied a linear regression and compared the slopes.

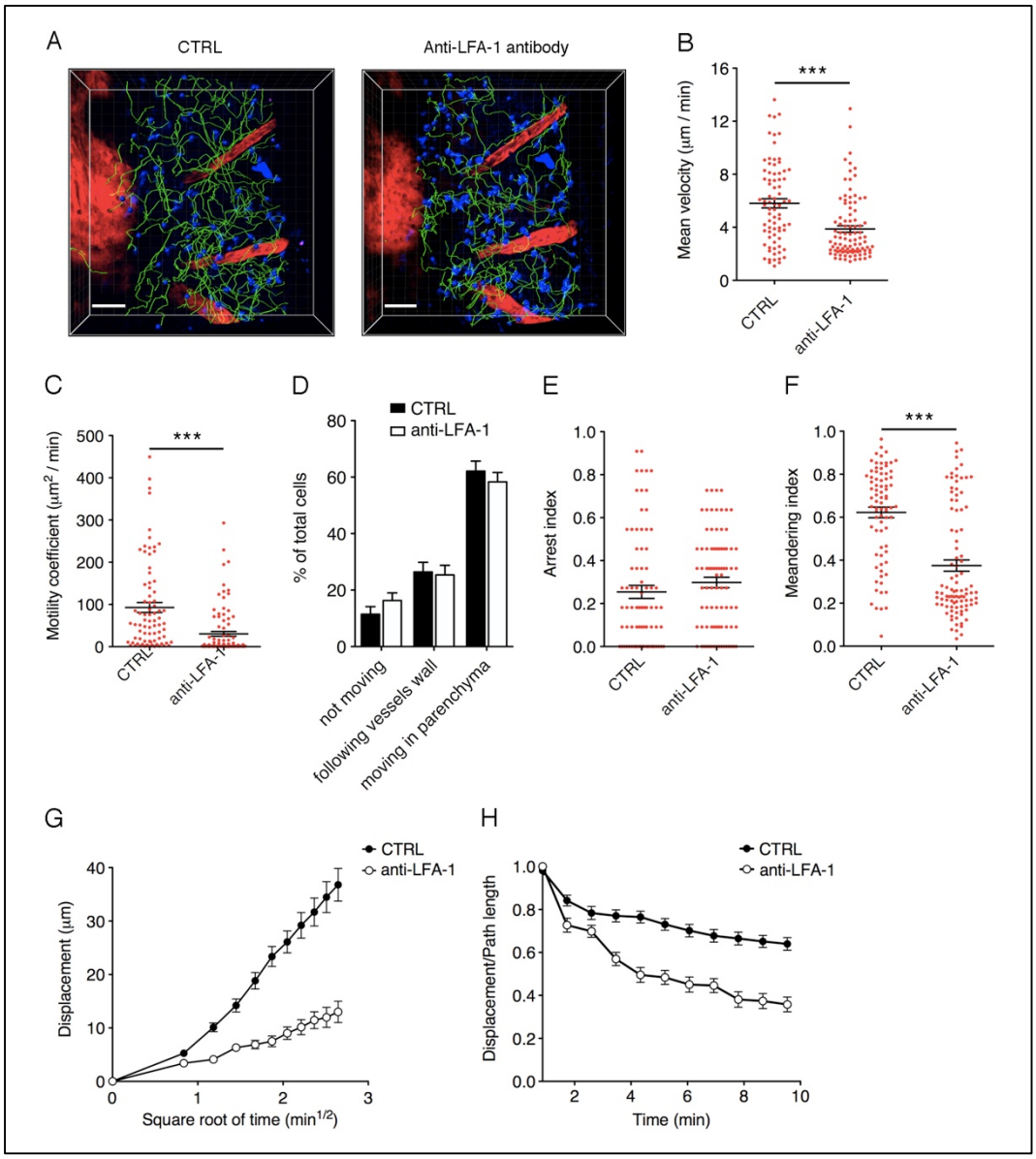

Figure 20. LFA-1 blocking strongly affects autoreactive Th1 cell dynamics in the SC parenchyma of EAE mice at disease peak. Th1 cell dynamics were analyzed in the SC of EAE mice at disease peak before (CTRL) and after application of anti-LFA-1 mAb on the exposed SC using TPLM approach. Representative images of Th1 moving in the SC parenchyma before and after antibody treatment. Cell tracks (green lines) are also shown (scale bar: 50 μm; red color: blood vessel) (**A**). Mean velocity (**B**), motility coefficient (**C**), dynamic properties (**D**), arrest coefficient (**E**) and meandering index (**F**) of the whole Th1 cell population in the SC parenchyma in the presence or absence of anti-LFA-1 antibody. Displacement (**G**) and ratio between displacement and path length during the time of analysis (**H**) of Th1 cells moving in the deep parenchyma of the SC. In all graphs, data are the mean ± SEM of 100 cells from 3 independent experiments. Statistics were calculated using Mann-Whitney test (***P<0.0001). In (**G**) and (**H**) was applied a linear regression and compared the slopes

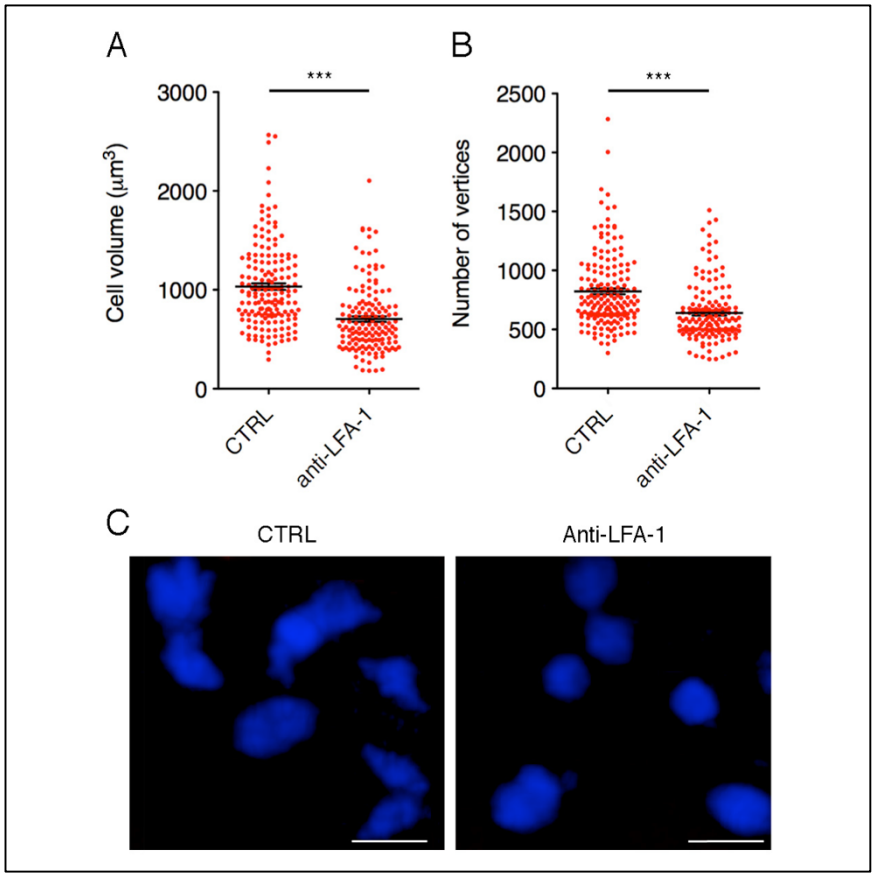

Figure 21. LFA-1 blockade affects Th1 cell morphology in the SC parenchyma at disease peak. Intraparenchymal Th1 cell morphology was determined before (CTRL) and after application of an anti-LFA-1 mAb antibody on the exposed SC. Cell volume (**A**) and number of vertices (**B**) of Th1 cells before and after LFA-1 inhibition Representative images of Th1 cells before and after anti-LFA-1 treatment. Note the presence of highly polarized cells before antibody application (left panel, white arrows) and the predominant round-like cell morphology induced by LFA-1 blocking (right panel) (scale bar: 10 µm; red color: blood vessel) (**C**). *Data* are the mean ± SEM of 100 cells from 3 independent experiments. Statistics were calculated using Mann-Whitney test (*** $P<0.0001$).

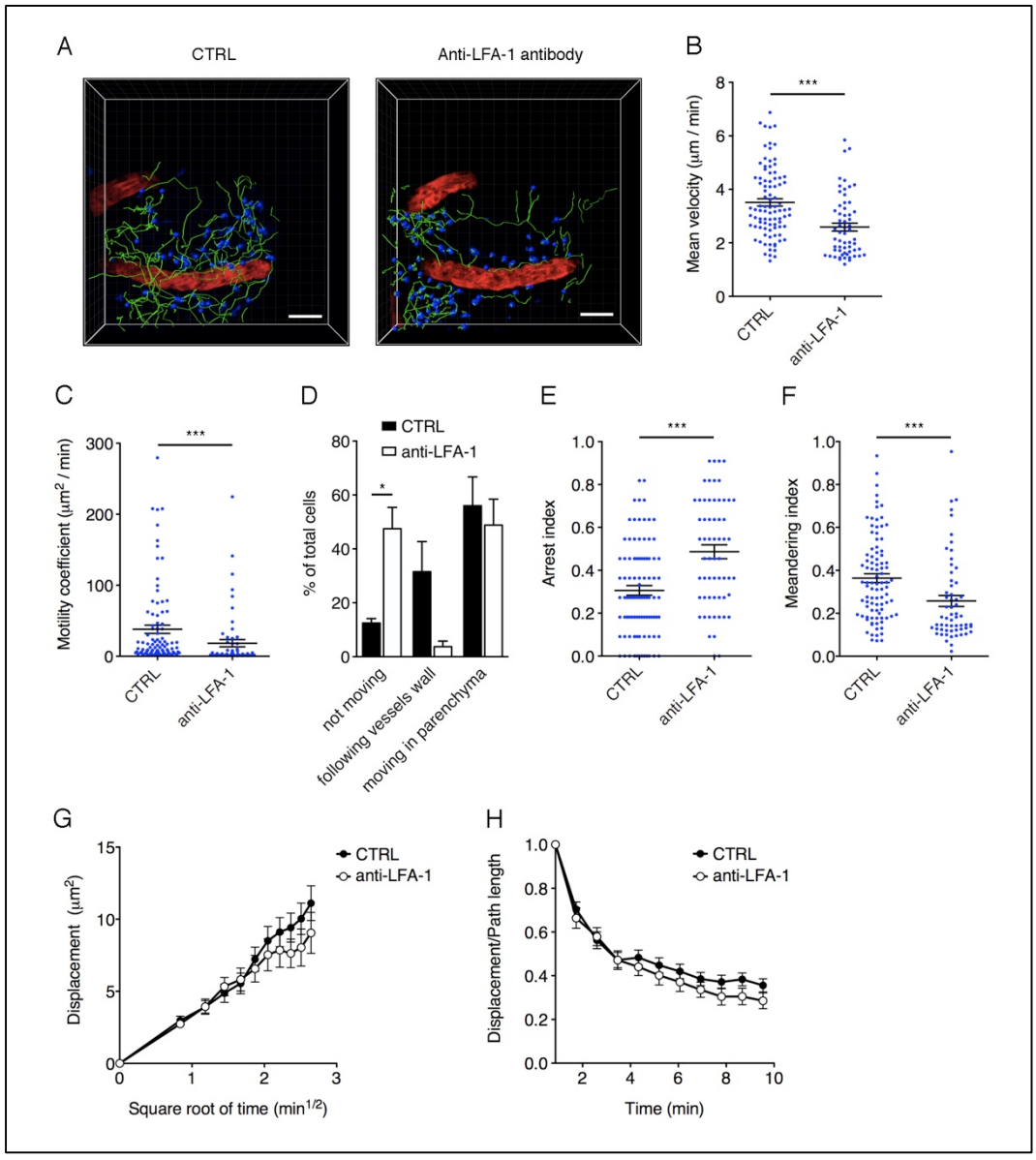

Figure 22. LFA-1 inhibition reduces autoreactive Th17 cell motility in the SC at disease peak. Th17 cell dynamics were analyzed in the SC of EAE mice at disease peak before (CTRL) and after application of anti-LFA-1 mAb on the exposed SC using TPLM. Representative images of Th17 cells moving in the SC parenchyma before (CTRL) and after antibody treatment. Cell tracks (green lines) are also shown (scale bar: 50 μm; red color: blood vessel) (**A**). Mean velocity (**B**), motility coefficient (**C**), dynamic properties (**D**), arrest coefficient (**E**) and meandering index (**F**) of Th17 cells are shown in the presence or absence of anti-LFA-1 antibody. Mean displacement (**G**) and chemotactic index (**H**) of Th17 cells moving in the SC parenchyma after antibody treatment. *Data* are the mean ± SEM of 100 cells from 3 independent experiments. Statistics were calculated using Mann-Whitney test (*P<0.05; ***P<0.0001). In (**E**) and (**F**) it was applied a linear regression and slopes were compared.

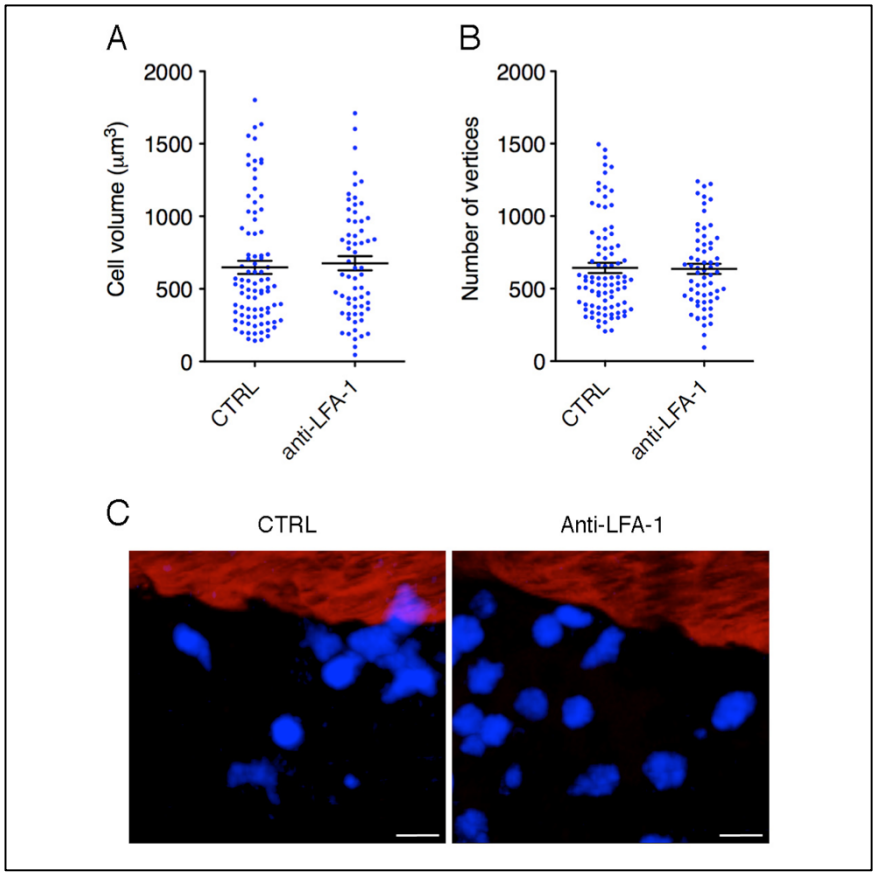

Figure 23. Morphology of Th17 cells in the SC parenchyma is not affected by anti-LFA-1 treatment. The cell volume (**A**) and the number of vertices (**B**) of intraparenchymal Th17 cells were calculated before and after anti-LFA-1 mAb treatment of the SC of EAE mice at disease peak. LFA-1 blocking had no effect on Th17 cell cytoskeletal organization, compared to control condition. Representative images of Th17 cells before (left panel) and after anti-LFA-1 treatment (right panel) (scale bar: 10 μm; red color: blood vessel) (**C**). *Data* are the mean ± SEM of 100 cells from 3 independent experiments. Statistics were calculated using Mann-Whitney test.

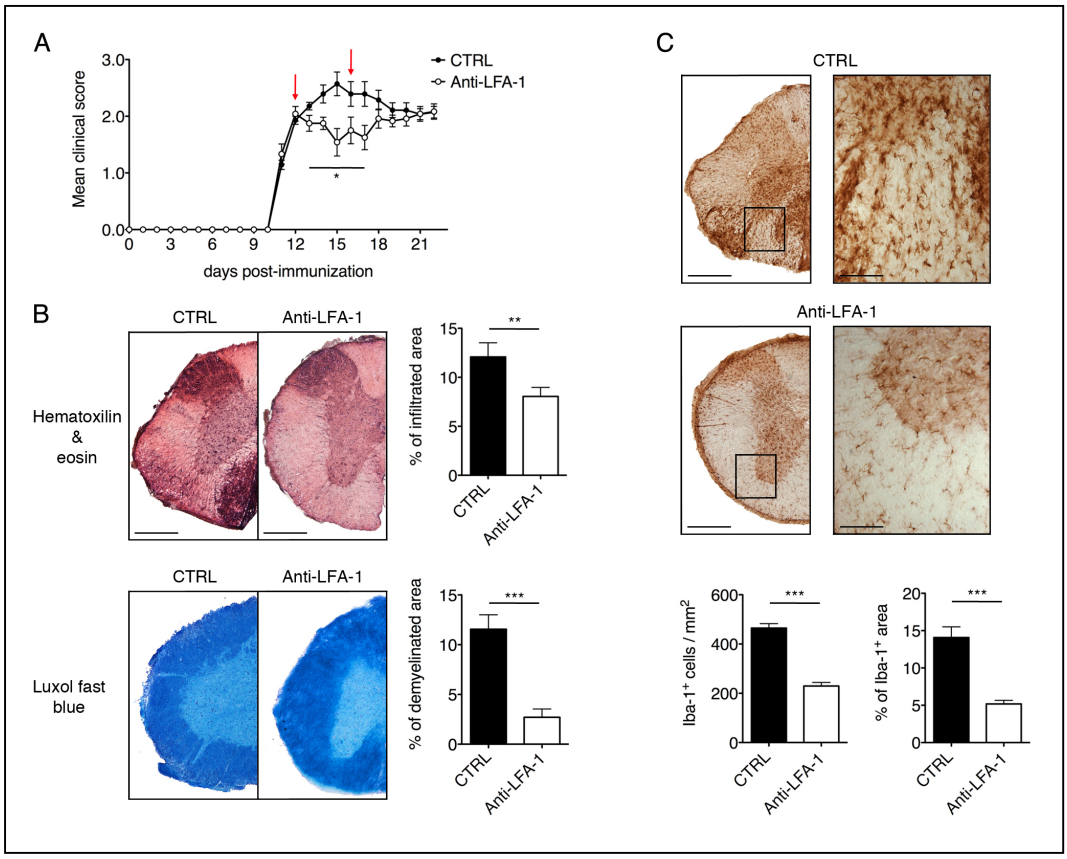

Figure 24. Intrathecal injection of an anti-LFA-1 blocking antibody ameliorates EAE severity. C57Bl/6 mice were immunized with MOG_{35-55} peptide and injected in the cisterna magna the day after disease onset (12 dpi) and 4 days later (red arrows) with 10 µl of PBS containing 50 µg of anti-human Ras (CTRL) or anti-LFA-1 blocking antibody. Mice were followed until 40 dpi and scored daily for disease activity. Data are the mean ± SEM of 16 mice/conditions from 4 independent experiments. Statistics were calculated using Mann-Whitney test (*P<0.05) (**A**). Neuropathology of EAE mice treated with anti-LFA-1 blocking antibody. Mice were sacrificed 3 days after the first antibody injection (14 dpi), and SCs were analyzed for the presence of inflammatory infiltrates and demyelination with hematoxylin/eosin and luxol fast blue staining respectively (4-6 cross sections of SC per mouse, *n* = 3 mice). Representative consecutive SC sections of anti-Ras (CTRL) or anti-LFA-1-treated animals are shown. Quantitative analysis of infiltrated cells and demyelination area for each condition are expressed as mean ± SEM. Statistics were calculated using Mann-Whitney test (**P < 0.005; ***P < 0.0001). All panels shown are 5x magnification, scale bar = 200 µm (**B**). Quantitative analysis of microglial cells for each condition to determine the total number of Iba-1+ cells and the area occupied by cell soma (4-6 cross sections of SC per mouse, *n* = 3 mice). Representative images of $Iba1^+$ microglia in mice treated with an isotype control or anti-LFA-1 antibody. Error bars indicate SEM (***P<0.0001). Left, 5x magnification; right, 10x magnification, scale bar = 200 µm (**C**).

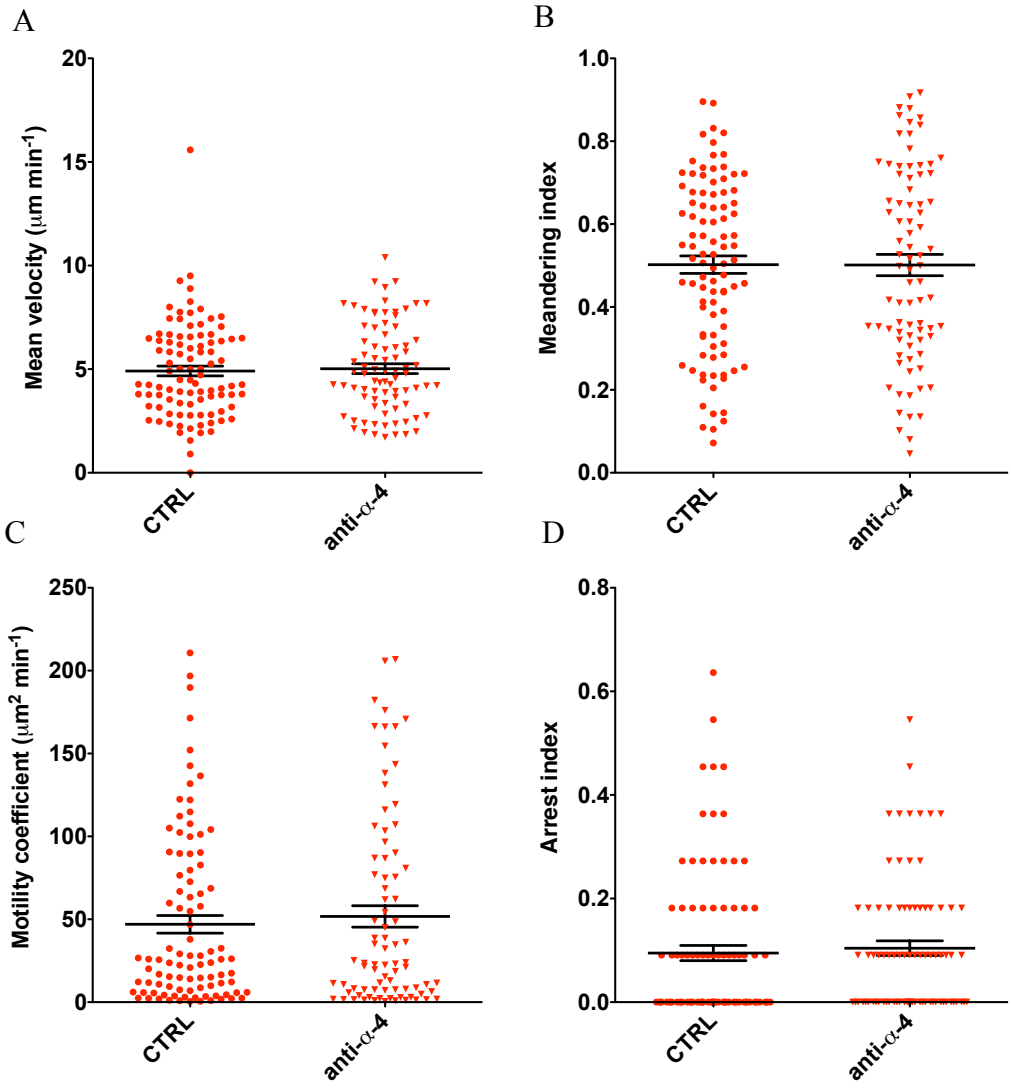

Figure 25. α4 integrins do not affect Th1 cells intraparenchymal motility behavior in the CNS at the peak of EAE. Th1 cell dynamics were analyzed in the SC of EAE mice at disease peak before (CTRL) and after application of anti-α4 mAb on the exposed SC using TPLM. (**A**) Mean velocity, (**B**) meandering index, (**C**) motility coefficient and (**D**) arrest index. *Data* are expressed as mean ± SEM. Statistics were calculated using Mann-Whitney test.

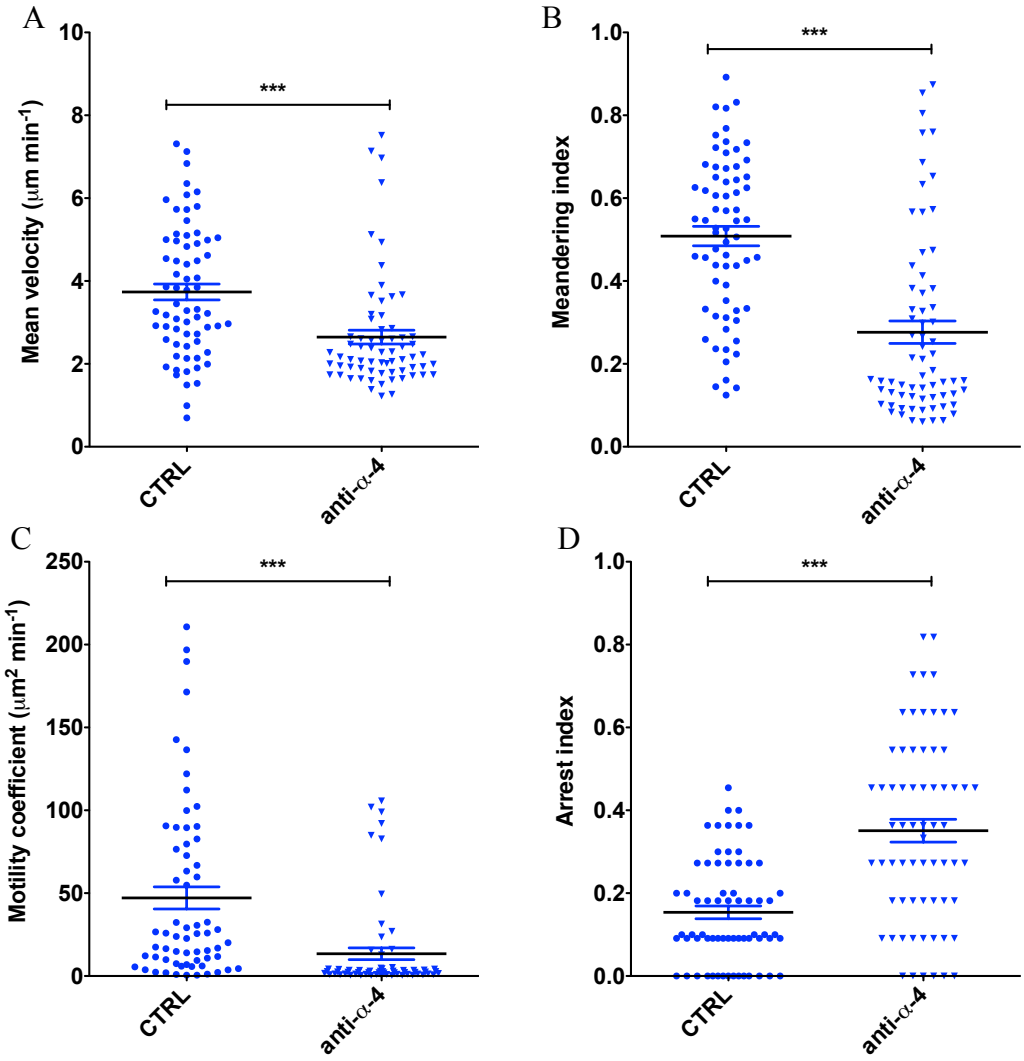

Figure 26. α4 integrins control Th17 cells intraparenchymal motility behavior in the CNS at the peak of EAE. Th17 cell dynamics were analyzed in the SC of EAE mice at disease peak before (CTRL) and after application of anti-α4 mAb on the exposed SC using TPLM. (**A**) Mean velocity, (**B**) meandering index, (**C**) motility coefficient and (**D**) arrest index. *Data* are expressed as mean ± SEM. Statistics were calculated using Mann-Whitney test (***P<0.0001).

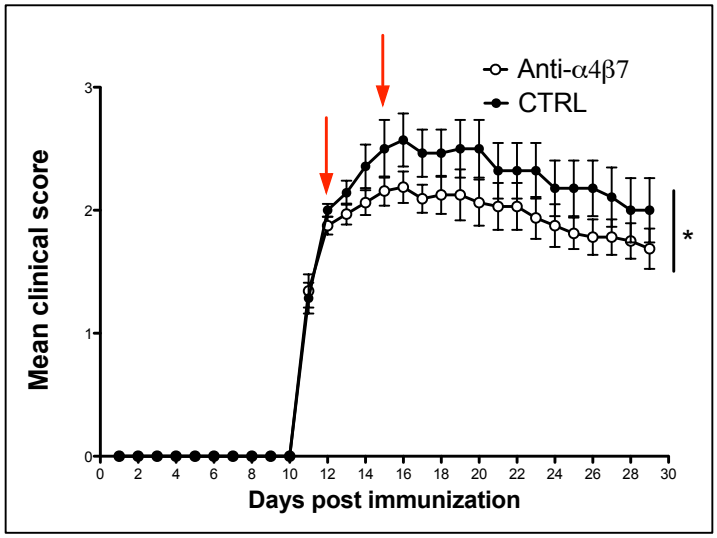

Figure 27. Intrathecal injection of anti-α4β7 blocking antibody reduces EAE progression in MOG_{35-55}- immunized mice. C57Bl/6 mice were immunized with MOG_{35-55} peptide and injected in the cisterna magna the day after disease onset (12 dpi) and 3 days later (red arrows) with 10 µl of PBS containing 50 µg of anti-human Ras (CTRL) or anti-α4β7 blocking antibody. Mice were followed until 40 dpi and scored daily for disease activity. Data are the mean ± SEM of 16 mice/conditions from 2 independent experiments. Statistics were calculated using Mann-Whitney test (*P<0.05).

	Diameter (μm)	V_{max} (μm/s)	V_m (μm/s)	WSS (dyne/cm^2)	V_{roll} (μm/s)
Preclinical	24.6 ± 6.8	1701 ± 349	1097 ± 115	9.3 ± 3.9	31.3
	24.6 ± 6.8	1528 ± 500	1027 ± 415	9.4 ± 6.6	31.1
Onset	31.8 ± 10.3	1616 ± 382	882 ± 207	4.8 ± 1.1	33.6
	31.8 ± 10.3	1099 ± 222	598 ± 113	3.2 ± 0.4	45.6
Chronic	22.0 ± 6.2	1558 ± 316	1133 ± 206	10.7 ± 5.3	45.8
	22.0 ± 6.2	1654 ± 280	1055 ± 148	9.8 ± 4.1	53.3

Table I. Diameter, hemodynamics, and rolling velocities of Th1 and Th17 cells in the SC at the different phases of EAE. The diameters of pial vessels maximum velocity (Vmax), mean blood flow velocity (Vm), wall shear stress (WSS) and rolling velocities for the injected T cells were calculated during the different phases of EAE. The velocity of rolling cells was measured by digital frame-by-frame analysis of videotapes. Vroll are presented as median. Data are expressed as arithmetic mean ± SD.

		Score	Nr. animals/ /venules	% Rolling	% Adhesion
Preclinical	**Th1**	0 ± 0	3/13	26.5 ± 2.8	4.4± 0.8
	Th17	0 ± 0	3/13	19.4 ± 1.8	1.4 ± 0.3
Onset	**Th1**	2.2±0.3	3/14	21.0 ± 2.0	2.2 ± 0.3
	Th17	2.2±0.3	3/14	26.1 ± 2.1	3.8 ± 0.6
Chronic	**Th1**	2 ± 0	3/16	25.5 ± 1.9	2.3 ± 0.4
	Th17	2 ± 0	3/16	20.0 ± 1.8	2.8 ± 0.7

Table II. Percentage of rolling and adhesion events of Th1 and Th17 cells in the SC at the different phases of EAE. The velocity of rolling cells was measured by digital frame-by-frame analysis of videotapes. Data are mean ± SEM for the percentages of rolling and arrest.

		Score	Nr. animals/ venules	% Rolling	% Adhesion
Preclinical	**CTR**	0 ± 0	3/13	28.5 ± 3.8	6.8 ± 1.4
	anti-α4	0 ± 0	3/13	12.2 ± 4.0	2.5 ± 0.8
	CTR	0 ± 0	3/18	31.4 ± 8.0	4.3 ± 1.7
	anti-LFA-1	0 ± 0	3/18	12.3 ± 3.0	0.6 ± 0.6
Onset	**CTR**	2.3±0.6	3/14	10.2 ± 2.5	1.4 ± 0.6
	anti-α4	2.3±0.6	3/14	3.4 ± 1.8	0.2 ± 0.2
	CTR	2 ± 0	3/15	34.1 ± 5.8	6.3 ± 0.9
	anti-α4β7	2 ± 0	3/15	29.1 ± 3.6	6.0 ± 0.5
	CTR	2.5±0	3/19	25.9 ± 2.7	2.1 ± 0.5
	anti-LFA-1	2.5±0	3/19	15.1 ± 2.2	1.0 ± 0.3
Chronic	**CTR**	1.7±0.6	3/16	17.3 ± 4.8	2.1 ± 1.1
	anti-α4	1.7±0.6	3/16	11.3 ± 1.8	0.0 ± 0.0
	CTR	2±0	2/18	31.7±1.2	1±0.5
	anti-α4β7	2±0	2/18	30.8±1.8	0.85±0.4
	CTR	2.2±0.3	3/15	22.4 ± 3.1	1.5 ± 0.6
	anti-LFA-1	2.2±0.3	3/15	19.6 ± 2.3	1.5 ± 0.5

Table III. Percentage of rolling and adhesion events of Th1 cells treated with blocking antibodies. Data are arithmetic mean ± SEM for the percentages of rolling and arrest.

		Score	Nr. animals /venules	% Rolling	% Adhesion
Preclinical	**CTR**	0 ± 0	3/13	13.3 ± 1.8	1.6 ± 0.7
	anti-α4	0 ± 0	3/13	11.0 ± 1.2	1.5 ± 0.5
	CTR	0 ± 0	3/15	19.5 ± 3.6	1.1 ± 0.4
	anti-LFA-1	0 ± 0	3/15	14.5 ± 4.5	1.3 ± 0.8
Onset	**CTR**	2 ± 0	3/14	30.4 ± 4.2	1.8 ± 1.4
	anti-α4	2 ± 0	3/14	30.8 ± 6.9	0.4 ± 0.4
	CTR	2 ± 0	3/24	38.7 ± 4.4	5.0 ± 1.3
	anti-α4β7	2 ± 0	3/24	40.4 ± 2.5	2.4 ± 1.0
	CTR	2 ± 0	3/10	22.7 ± 4.0	5.5 ± 1.5
	anti-LFA-1	2 ± 0	3/10	20.7 ± 3.7	4.1 ± 1.1
Chronic	**CTR**	2 ± 0	3/16	13.8 ± 1.8	1.4 ± 0.4
	anti-α4	2 ± 0	3/16	14.5 ± 3.6	0.7 ± 0.2
	CTR	2 ± 0	3/12	27.3 ± 4.9	5.0 ± 1.3
	anti-α4β7	2 ± 0	3/12	26.4 ± 6.2	0.6 ± 0.5
	CTR	1.5±0.7		24.5 ± 2.8	3.7 ± 1.2
	anti-LFA-1	1.5±0.7	3/15	23.4 ± 5.7	2.6 ± 0.7

Table IV. Percentage of rolling and adhesion events of Th17 cells treated with blocking antibodies. Data are arithmetic mean ± SEM for the percentages of rolling and arrest.

Discussion

Lymphocytes are constantly in motion, trafficking passively in the blood, migrating in lymphoid or non-lymphoid target organs where they can be activated by migrated or resident APCs. Several prerequisites must be met for leucocytes to reach a target site. Initially, they need to adhere to the activated endothelium in post-capillary venules, a process that is governed by the multistep adhesion cascade. This cascade consists of selectin-mediated tethering and rolling, firm adherence facilitated by activated integrins, and transendothelial migration. Auto-reactive T cells trafficking in the CNS represents a critical event in the pathogenesis of EAE, the animal model of MS. In this study, we have tested the involvement of αLβ2 (LFA-1), α4β1 (VLA–4) and α4β7 integrins in Th1 and Th17 cells trafficking in MOG_{35-55} peptide immunized mice during EAE.

Our results have shown that Th17 cells display higher levels of α4 integrins and lower L-selectin expression compared to Th1 cells, suggesting these cells are more activated and may have increased propensity to migrate to sites of inflammation (Chen J et al*, J Immunol, 2006:* Ley K et al*, Nat Rev Immunol, 2004*). Mean fluorescence intensity of LFA-1 was significantly higher on Th1 cells compared to Th17 cells, whereas α4β7 integrin expression was significantly higher on Th17 cells compared to Th1 cells. Our flow cytometry data suggest a potential different integrin pattern used by Th1 and Th17 cells during their migration into the inflamed tissues.

By using IVM we compared Th1 and Th17 cell adhesion in the SC venules during EAE phases: preclinical phase, disease onset and chronic phase. We observed that Th1 cells show higher capacity to roll and arrest on CNS endothelium in pial venules when compared to Th17 cells at the preclinical phase of EAE. This data suggest that Th1 cells have a higher capacity to migrate inside the SC during early disease when compared to Th17 cells. These data are in agreement with previous studies showing that Th1 effector cells infiltrate the non-inflamed CNS to initiate inflammation that facilitates subsequent recruitment of Th17 cells in a transfer EAE model (O'Connor R. et al*, J Immunol,* 2008). However, at disease onset Th17 cells displayed equal capacity to roll but significantly higher adhesive capacity in inflamed SC venules compared to Th1 cells, suggesting a major role

of Th17 cell trafficking during clinical disease. During the chronic phase of EAE we observed that Th1 cells were more engaged in adhesive interactions compared to Th17 cells, suggesting a role for these cells in disease progression. These data suggest different roles and molecular mechanisms used by Th1 and Th17 cells to migrate into the SC and contribute to disease induction and progression. It was previously shown that human and murine Th1 and Th17 cells express different patterns of integrins and chemokine receptors that can selectively drive these cells into the brain or SC. For example, CXCR3 and CCR5 are preferentially express on Th1 cells whereas CCR6 is highly expressed on Th17 cells (Prendergast CT et al. *Endocr. Metab. Immune Disord Drug Targets, 2009*). Moreover, parenchymal inflammation in the brain but not SC is dependent on the presence of a high Th17:Th1 ratio suggesting that Th1 and Th17 migration capacity and vascular factors may determine lesion localization (Stromnes IM et al., *Nat Med, 2008*).

The results obtained by IVM performed using blocking anti-integrin antibodies, showed that VLA-4 is the major adhesion molecule involved in Th1 cell adhesion in SC venules during all disease phases, whereas LFA-1 had a minor role only during the preclinical phase and disease onset. Our data are in agreement with previous results showing a major role for VLA-4 in the migration of Th1 cells in the SC and that α4 blockade inhibits the development of the disease interfering with the migration of Th1 cells both in the brain and in the SC in a transfer EAE model (Glatigny S, *J Immunol,* 2011; Rothhammer V et al*., J Exp Med,* 2011).

α4β7 blockade prevented firm adhesion of Th17 cells in the SC vessels during clinical EAE, suggesting a prominent role for this integrin in Th17 cell adhesion. Mice transferred with encephalitogenic Th17 cells developed atypical EAE in the presence of anti-α4 treatment, showing signs of cerebral rather than SC disease with severe gait ataxia or hemiparesis, suggesting that α4 blockade inhibited Th17 cell-dependent pathology in the SC but not in the brain. (Rothhammer V et al*, J Exp Med,* 2011). Previous studies have also shown that Th17 cells are recruited to the CNS in a LFA-1 dependent manner (Yamazaki T et al*, J Immunol,* 2008; Rothhammer V et al*., J Exp Med,* 2011). In fact, Rothhammer and colleagues have shown that CD11a (the αL subunit of LFA-1) blockade combined with α4 inhibition totally prevented Th17 cell entrance in the brain and blocked disease

development (Rothhammer V et al*, J Exp Med,* 2011). A role for α4β7 integrin was previously shown by Kanwar and coworkers using a chronic form of EAE in which the administration of anti-α4 integrin antibody as well as β7 blockade reduced EAE (Kanwar RJ et al., *J Neuroimmunol*, 2000). Also, blockade of Mucosal Addressin Cell Adhesion Molecule-1 (MAdCAM-1), the main α4β7integrin ligand, prevented development of disease in a chronic-non remitting form of EAE actively induced by immunization with MOG_{35-55} peptide. MAdCAM-1 expression was found on specialized high endothelial venules (HEV) as well as at chronic inflammation sites (Rossi B et al., *J Leuk Biol*, 2010). In our IVM study we did not determine the role of MAdCAM-1 and further studies are needed to clarify the role of this molecule in T cell adhesion in CNS microcirculation. Moreover, our data showing a role for β7 integrin chain were obtained in a chronic EAE model induced with MOG_{35-55} peptide, whereas the role of α4β7 integrins and MAdCAM-1 in relapsing-remitting EAE is unclear (Engelhardt B et al., *J Clin Invest*, 1998).

Surprisingly, our data showed that Th17 cell adhesion in inflamed SC pial vessels is independent of LFA-1 and α4 at the preclinical phase of disease. T cell adhesion during early disease needs to be further investigated to identify the molecular mechanisms specifically involved in the recruitment of encephalitogenic Th17 cells during early phase of EAE. Previous studies have shown that melanoma cell adhesion molecule (MCAM) (CD146) is involved in rolling, adhesion and transmigration of T cells in the inflamed CNS during EAE (Larochelle C, *Brain*, 2012). Moreover, our laboratory has also shown that endothelial selectins and their mucin ligands such as PSGL-1 and TIM-1 are involved in Th1 and Th17 cell migration into the inflamed brain (Piccio L et al., *J Immunol*, 2002; Rossi B et al., *J Leuk Biol* 2010; Angiari S et al., *Immunity* 2014; Angiari S and Constantin G, *Trends Mol Med*, 2014). Thus, we speculate that endothelial selectins and other molecules from the immunoglobulin superfamily may be responsible for the early recruitment of Th17 cells in the inflamed CNS.

The activation and trafficking of T cells in autoimmune diseases is not fully understood. In recent years TPLM has been used extensively to study the motility behavior of T cells inside lymphoid and non-lymphoid tissues during autoimmune

responses. TPLSM is advantageous because it achieves deep tissue penetration and high resolution with low phototoxicity, making it ideal to visualize immune system cells in living animals and to provide dynamic views of leukocytes. For example, TPLSM has shown that following extravasation in the LNs, T cells initially move at high velocity, displaying a random walk or directed migration pattern to facilitate antigen surveillance (Miller MJ et al., *Proc Natl Acad Sci USA*, 2003; Calahan MD and Parker I, *Ann Rev Immunol*, 2008; Rossi B and Constantin G, *Front Immunol*, 2016). If migrating T cells come into direct contact with APCs in the lymph nodes, their dynamic behavior undergoes changes such as reduced motility or organization into clusters, leading to cell activation and proliferation. These TPLM results have helped to explain how lymphocytes optimize their chances of encountering rare cognate antigens and initiate adaptive immune responses by their fast and stochastic motility (Bousso P, *Nat Rev Immunol,* 2008; Rossi B and Constantin G, *Front Immunol*, 2016).

The reactivation of primed T cells in the CNS is necessary for the initiation of inflammatory responses and requires physical contact between T cells and local APCs, which present MHC-II associated peptides, resulting in inflammation, demyelination and axonal damage (Goverman, J. 2009. *Nat. Rev. Immunol.* 2009). In the last decade, TPLSM has revealed the motility behavior of migrating T cells in the CNS, and their reactivation inside the SC parenchyma, which is the main site of CNS inflammation in most EAE models in mice. Importantly, T cells interact with APCs in the subarachnoid space during the early stages of EAE, and these contacts seem critical for T cell reactivation and expansion in the CNS (Bartholomäus I et al., *Nature* 2009; Kivisäkk P, *Annals Neurol*, 2009). It was demonstrated that CD4+ T-cell motility is actively promoted in the SC during EAE (Siffrin V et al., *Brain*, 2009), facilitating an efficient and rapid screening of the mainly professional APCs, integrating relevant stimulatory, costimulatory and regulatory signals (Serafini B et al*., Am J Pathol* 2000*;* Serafini B et al., *J Neuropathol Exp Neurol*, 2006). The MHC-II^{+} APCs located in the CNS during EAE mainly comprise perivascular macrophages and DCs, which induce local reactivation of primed myelin-reactive T cells resulting in CNS inflammation and EAE progression (Rossi B and Constantin G, *Front Immunol*, 2016).

Previous TPLM studies have shown that autoreactive effector T cells move seemingly unhindered and fast through the CNS with two distinct migratory patterns: a major proportion of the autoimmune T cells moved rapidly, randomly and in a "stop and go" mode through the compact white and grey matter, while the rest of the cells were attached and moved around a fixed anchor point (Kawakami N et al., *J. Exp. Med*, 2005). However, how T cell subsets move inside the inflamed CNS and the molecular mechanisms involved in the dynamics of autoreactive T cells in the CNS parenchyma during the disease are largely unknown. In our experiments for this PhD thesis we studied Th1 and Th17 cell dynamics in SC at different time points during EAE: the preclinical phase, the disease peak and the chronic phase of disease. Moreover, we characterized, for the first time, the role of integrins in the motility behavior of Th1 and Th17 cells in SC parenchyma during EAE.

At the preclinical phase of EAE, we found a low number of T cells entering the CNS, with Th1 cells being in higher number comparing to Th17 cells (ratio 2/1 between Th1 and Th17 cells). The higher accumulation of Th1 in the SC parenchyma in TPLM settings was supported by IVM experiments showing a greater capacity to adhere in the meningeal vessels exerted by Th1 cells when compared to Th17 cells in the preclinical phase of disease. Moreover, in a transfer EAE model it was previously shown that only Th1 cells access the non inflamed CNS and that Th17 cells appear in the CNS after Th1 cells induce the EAE lesion. These data suggest that Th1 cells initiate EAE upon passive transfer and promote subsequent recruitment of Th17 cells to the CNS (O'Connor RA et al., *J Immunol*, 2008). Notably, in our experiments T cells were not uniformly distributed along the volume of tissue analyzed, but both Th subsets accumulated in small groups in discrete SC areas, suggesting preferential points of entrance and microenvironmental positioning for this cells in the preclinical phase of EAE. Interestingly, we observed that Th1 cells were distributed deeply in the parenchyma without clustering organization, whereas a high percentage of Th17 cells were moving in the perivascular area following the vessels wall. We did not observe significant differences in velocity and motility parameters between Th1 and Th17 lymphocytes, suggesting some common migration mechanisms inside

the inflamed SC at this stage of disease. Both Th1 and Th17 cells were moving fast and displayed a relative high levels motility coefficient suggesting random movements of these cells inside the SC parenchyma, suggesting low engagement with APCs. Our data are supported by previous studies showing that the first T cells entering the CNS immediately after transfer are in a very few numbers when compared to a second massive inflammatory cells accumulation coinciding with the onset of clinical symptoms. Indeed, it has been previously shown that the majority of the T cells during the preclinical phase of EAE remain confined within secondary immune organs (such as spleen) and blood before they invade the SC (Flügel A et al., *Immunity*, 2001). Moreover, the first T cells entering the CNS are able to produce high amounts of pro-inflammatory cytokines independent on antigen recognition (supporting the random movements displayed by Th1 and Th17 cells in ours TPLM experiments). These cells are able to create an immune permissive setting the stage for the second inflammatory wave, which contains antigen-specific cells as well as non-specific recruited immune cells (Flügel A et al., *Immunity*, 2001). However, these "pioneer T cells" do not cause any immediate clinical or histological changes, but rather seem to prepare the CNS tissue for the second wave of invading effector cells, which coincides with the onset of clinical symptoms (Wekerle et al., *Trends Neurosci*, 1986; Hickey et al., *J Neurosci*, 1991).

At disease peak we found a massive infiltration of Th1 and Th17 cells compared to the preclinical phase of EAE. We found similar density of Th1 and Th17 cells the SC suggesting an equal capacity of these cells to invade the inflamed CNS at disease peak. Both T cells displayed a reduction in the movement compared to the preclinical phase, nevertheless Th1 cells displayed a higher velocity and motility when compared to Th17 cells. Both Th subsets presented two different motility behavior: the majority of cells were rapidly moving, while the rest was stationary around a fixed point closed to vessels wall suggesting a potential physical contact with perivascular phagocytes/APCs (Odoardi F et al., *Proc Natl Acad Sci U.S.A*., 2007; Pesic M. et al, *Clin investigation*, 2013; Bartholomäus I et al., *Nature*, 2009). Our data are supported by previous TPLM studies on spinal cord slices obtained at the onset of EAE in a rat model (Kawakami N et al., *J Exp Med*,

2005). These results showed that MBP-specific effector T cells move through the CNS with two distinct migratory patterns: ~65% of the cells moved rapidly and randomly through the compact white and gray matter, whereas the remaining ~35% appeared tethered to a fixed point, suggesting the formation of immune synapses (Kawakami N et al., *J Exp Med*, 2005). In fact, pretreatment of the spinal cord tissue with neutralizing anti-MHC-II monoclonal antibodies significantly reduced the number of arrested autoreactive T cells (Kawakami N et al., *J Exp Med*, 2005). In contrast to the MBP-specific T cells, OVA-specific T cells did not form synapse-like contacts in the spinal cord in this model but invaded the CNS and moved rapidly through the tissue. More recent *in vivo* TPLM studies based on laminectomy in the lumbar spinal cord of a rat EAE model were used to visualize T cells within the meningeal areas and the adjacent white matter (Odoardi F et al., *Proc Natl Acad Sci U.S.A.*, 2007). These studies revealed that an intravenous infusion of soluble MBP during the acute EAE phase caused rapid antigen uptake by APCs in the CNS, resulting in the deceleration of MBP-specific T cells, a higher frequency of T cell immobilization, a stronger activating state and the enhanced production of inflammatory cytokines (Odoardi F et al., *Proc Natl Acad Sci U.S.A.*, 2007). In this EAE model, BBB leakage allowed the uptake of circulating antigen that was quickly processed by CNS cells expressing MHC-II, which were preferentially located in meningeal areas and in the vicinity of vessels, i.e. the regions mainly infiltrated by T cells. However, effector and resting memory T cells specific for the non-CNS antigen OVA were also recruited to EAE lesions and moved there without contacting APCs. As shown for the MPB-specific T cells, the OVA-specific T cells were activated and arrested following the intravenous infusion of ovalbumin, which increased the severity of disease symptoms. This suggested that effector T cells home towards acute EAE lesions and can be reactivated locally by exogenous antigen regardless of the specificity of the intruding T cell population (Odoardi F et al., *Proc Natl Acad Sci U.S.A.*, 2007).

In our experiments, 30% of moving Th1 and Th17 cells at disease peak was walking beside the vessels wall and the 40-45% of cells was moving in the parenchyma. Previous TPLM experiments demonstrated that CD4+ T-cell

compartmentalization in the parenchyma along CNS vessels is dependent on CXCR4 functioning, whereas classical adhesion molecules seem to have no major function in this process (Siffrin V et al., *Brain*, 2009). Pretreatment with a CXCR4 antagonist led to a shift of CD4+ T cells from a perivascular motility pattern to intraparenchymal invasion, resulting in disorganization of the vessel cuffs. These data suggest that the compartmentalization of CD4+ T-cells in vessels proximity is actively promoted, and can facilitate efficient and rapid screening of perivascular professional APCs (Siffrin V et al., *Brain*, 2009). We also observed that Th1 cells were mainly moving in a straight direction covering long distances deep in the SC parenchyma in a constant motion following the same direction, while Th17 cells moved in a specific volume of tissue displaying a stop-and-go motility type. In particular, Th1 cells seemed to move preferentially along the axis of the SC in the same direction on the main SC central vein. Similar observation was recently made by Kim and colleagues who reported that effector T cells migrate preferentially along the rostrocaudal SC axis with confined lateral movement in the thoracic area during EAE (Kim JV et al., *J Immunol Methods*, 2010).

TPLM experiments performed during the chronic phase of EAE showed a significant reduction of Th1 and Th17 cell movement with lower mean velocity, meandering index and motility coefficient associated to higher arrest coefficient. We did not observe any significant difference between Th1 and Th17 movement and both subsets were moving slower when compared to the other disease phases. These data suggest that stationary T cells were engaged in contacts with APCs and that antigen-dependent phenomena contribute to disease progression.

Previous TPLM studies have shown that migration of T cells is guided by stromal cells/extracellular matrixes (ECMs) exhibiting unique fibrous structures such as stromal cell networks (Bajénoff M et al., *Immunity*, 2006), and collagen fibers (Boissonnas A et al., *J Exp Med*, 2007). Leukocytes including T cells exhibit amoeboid migration and the three biomechanical factors determining this type of motility include: 1) integrin-mediated adhesion, 2) actin polymerization-driven leading edge protrusion, and 3) myosin II-mediated contractility (Lämmermann T et al., *Curr Opin Cell Biol*, 2009). It is unclear whether stromal cell networks like

those found in the lymph nodes are also present in the CNS parenchyma, but activated T cells can move in a similar manner in the CNS and lymph nodes, suggesting analogous stromal structures are present in the CNS (Wilson EH et al., *Immunity*, 2009). Accordingly, TPLSM analysis in an experimental model of toxoplasmic encephalitis indicated the presence of a reticular system associated with areas of parasite replication and local CNS inflammation, but not in normal brain tissues (Wilson EH et al., *Immunity*, 2009). $CD4^+$ T-cell motility is actively promoted in the spinal cord during EAE (Herz JM et al., *J Neuroinflammation,* 2011), and $CD4^+$ T cells can gain access to CNS parenchyma and partially migrate along inflammation-induced ECMs, which are similar to those seen in lymph nodes (Herz JM et al., *J Neuroinflammation,* 2011). These observations suggest that pre-existing scaffolds guide lymphocyte migration in lymphoid tissues, but specialized structures are induced during CNS inflammation and guide T cell migration, potentially facilitating the screening of APCs and integrating relevant stimulatory, costimulatory and regulatory signals (Wilson EH et al., *Immunity*, 2009; Herz JM et al., *J Neuroinflammation,* 2011).

The molecular mechanisms controlling T cell motility within the inflamed CNS are poorly understood (Mrass P and Weninger W, *Immunol Rev*, 2006). In this context, we studied the role of integrins in both Th1 and Th17 cell migration into the SC parenchyma during EAE. Integrins are α-β-heterodimeric transmembrane glycoprotein receptors that mediate cell-ECM and cell-cell adhesion events through binding ECM proteins such as fibronectin. We used a TPLM approach to investigate the potential role of integrins in Th1 and Th17 cell dynamics during CNS inflammation. Blocking antibody anti-LFA-1 administration on the exposed SC at disease peak significantly altered the dynamics of Th1 and Th17 cells leading to a reduction in their velocity and motility. However, LFA-1 blockade differently modified the behavior of Th1 and Th17 cells. Th1 cells significantly reduced speed without stopping their movement and their directed migration in the parenchyma was profoundly altered after LFA-1 blockade. Also, the analysis of cellular morphology showed a drastic reduction in the volume and capacity of Th1 cells to extend cellular protrusions during their movement, suggesting that LFA-1 is actively involved in the cytoskeleton rearrangement necessary for Th1

cell amoeboid migration inside the inflamed CNS. LFA-1 blocking also drastically increased the number of not moving Th17 cells although the constrained migration of cells moving in the parenchyma was not affected by LFA-1 inhibition. Moreover, Th17 cells did not displayed morphological modifications in term of volume and number of vertices in both moving and not moving fractions ruling out the involvement of LFA-1 in cytoskeleton dynamics in Th17 cells. Together, these data suggest a different role of LFA-1 in the motility of Th1 compared to Th17 cells in the SC parenchyma during EAE and that LFA-1 is pivotal for T cell motility in the SC under inflammatory conditions at EAE peak.

Notably, α4 integrin blockade had no role in Th1 cells motility, but drastically reduced the dynamics of Th17 cells inside the SC parenchyma leading to a significant decrease in the velocity of these cells. Importantly, the arrest coefficient was significantly higher after α4 integrin blockade suggesting that a great portion of cells completely stopped their movements. Overall, these data suggest a selective involvement for the α4 integrins in Th17 cell motility in the SC under inflammatory conditions at EAE peak. Future experiments are needed to clarify the contribution of α4β1 and α4β7 in Th1 and Th17 migration inside the SC during EAE. Interestingly, MAdCAM-1, the α4β7 ligand, has been reported to be expressed on astrocytes surrounding blood vessels and on dendritic cells potentially mediating T cell migration and costimulation inside the CNS (Cannella B, *J Neuroimmunol,* 1991; Szabo MC et al, *J Immunol* 1997; Lehnert K et al., Eur J Immunol 1998; Kanwar JR et al., *Immunol Cell Biol,* 2000).

The inhibition of intra-tissue motility of activated T cells into CNS could represent a point of therapeutic intervention in autoimmune diseases of the CNS. An important result of our study was the significant impact of anti-LFA-1 or anti-α4β7 antibodies intrathecal injection on EAE development. Our data clearly indicate that local administration of blocking anti-integrin antibodies after disease onset prevents EAE worsening, suggesting that interference with intra-CNS motility of activated T cells may represent a potential therapeutic approach in autoimmune diseases such as MS. However, integrin LFA-1 is involved in the generation of functional immunological synapse during antigen presentation in

secondary lymphoid organs and this process may also be important during T cell reactivation by CNS APCs (Kawakami N et al., *J Exp Med*, 2005; Springer TA et al., *Curr Opin Cell Biol*, 2012). Thus, we speculate that LFA-1 inhibition in the SC of EAE mice may limit not only T cell movement but also T cell reactivation in the CNS parenchyma. On the other hand, LFA-1 was shown to be also important for neuronal functionality, and to mediate direct T cell-neuron contacts through binding to neuronal ICAMs (Tian L et al., *Blood*, 2008; Dove A et al., *Nat Biotechnol*, 2000). In particular, using TPLM it was previously demonstrated that Th17 cells form synapse-like contacts with neurons in an LFA-1/ICAM-1 dependent manner leading to neuronal dysfunction and axonal damage during EAE (Siffrin V et al., *Immunity,* 2010). LFA-1 binding is also implicated in the sequestration and accumulation of activated T cells in the leptomeningeal milieu, a crucial process leading to CNS invasion by leukocytes during EAE (Schläger CH et al., *Nature*, 2016). Therefore, we cannot exclude that anti-LFA-1 intrathecal treatment may affect other immunological processes inside the CNS, like the motility and pathogenic behavior of other immune cell populations and immune-cell mediated neuronal damage, and further studies are required to clarify the of anti-LFA-1 treatment in CNS local inflammatory responses during EAE. In light of these considerations, further neuropathological investigations after anti integrin treatments will clarify the potential manifolds mechanisms at the basis of clinical disease amelioration. Indeed, the number of inflammatory infiltrates stained with hematoxylin/eosin was reduced probably due to a less activated milieu, including T cell reactivation blockade, that reduced the attraction of other pro-inflammatory immune components. Therefore, we don't expect neither a reduction exclusively of infiltrating T cells nor an interference only with Th17 cells.

Integrins involved in leukocyte adhesion cascade (β1 and β2), have been proven to be valuable therapeutic targets in the treatment of several inflammatory and autoimmune diseases. Natalizumab was the first humanized monoclonal antibody targeting the α4-integrin subunit (Steinman L, *Nat Rev Drugs Discov*, 2005) approved by the Food and Drug Administration (FDA) for the treatment of MS and Crohn's disease. The treatment with this drug caused severe side effects in

some patients leading to the development of progressive multifocal leukoencephalopathy (PML) due to infection with JC virus (Yousry TA et al., *N Engl J Med,* 2006). Vedolizumab, a humanized anti α4β7 integrin antibody has recently emerged as efficient therapy for inflammatory bowel diseases with an excellent safety profile. Notably no cases of PML were reported in patients treated with Vedolizumab, suggesting this antibody, which acts more selectively on leukocyte trafficking has lower risk of PML compared to Natalizumab (Sands Bruce, *Dig Dis*, 2017). In recent years, several anti-LFA-1-inhibitory compounds with various structural motifs have been described in patent literature. Antibodies against LFA-1 have been developed for the treatment of ischemia and stroke, but the occurrence of severe side effects in late clinical phases lead to the discontinuation of several drug candidates (e.g., β2-targeting antibody Erlizumab) (Dove A et al., *Nat Biotechnol,* 2000). Efalizumab, an αL-selective antibody, previously approved by the FDA for the treatment of psoriasis, was removed in 2009 from the market after several cases of PML (Woolacott H et al., *Health Technol Assess*, 2006). PML after anti-integrin treatment is due to the systemic immunosuppressive action of anti-integrin interfering with T cell trafficking necessary to fight against opportunistic infections. In the light of these considerations, intrathecal therapies may represent an efficient route of administration with lower risk of PML. Among side collateral effects of intrathecal route of administration, literature reports neurocognitive impairment in 20-40% of survivors of childhood acute lymphoblastic leukemia after regional treatment with intrathecal Methotrexate (Krull KW et al., *Leuk Lymphoma*, 2013). The same intrathecal chemotherapy agent causes cognitive impairment in children with medulloblastoma (Riva D et al., *Neurology*, 2002. Notably, Methotrexate is the most well-known antifolate included in many cancer therapies, but its substantial toxicity impacts its wider use, especially in pediatric oncology. Recently, Pompe and coworkers assessed, in a preliminary study, the feasibility and toxicity of intraventricularly administered Methotrexate in children with infant and /or metastatic medulloblastoma. Interestingly, this other CNS regional treatment was feasible and mostly well tolerated, to date (Pompe RS et al., *Eur J Cancer*, 2015). Other alterations in CNS functions and social behavior after

intrathecal therapies do not emerge from recent literature. At the state of art, we suggest that intrathecal injection of therapies interfering with effector T cell dynamics in the CNS will not impair systemic immunity and may complement existing MS therapies leading to faster resolution of the CNS immune attack and potentially interfering with chronic disease course.

References

Abbas AK, Murphy KM, Sher A. Functional diversity of T helper lymphocytes. *Nature* 1996; 383:787-93.

Alon R, Feigelson SW, Manevich E, Rose DM, Schmitz J, Overby DR, Winter E, Grabovsky V, Shinder V, Matthews BD, Sokolovsky-Eisenberg M, Ingber DE, Benoit M, Ginsberg MH. Alpha4beta1-dependent adhesion strengthening under mechanical strain is regulated by paxillin association with the alpha4-cytoplasmic domain. *J Cell Biol*. 2005; 171(6):1073-84.

Angiari S, Donnarumma T, Rossi B, Dusi S, Pietronigro E, Zenaro E, Della Bianca V, Toffali L, Piacentino G, Budui S, Rennert P, Xiao S, Laudanna C, Casasnovas JM, Kuchroo VK, Constantin G.TIM-1 glycoprotein binds the adhesion receptor P-selectin and mediates T cell trafficking during inflammation and autoimmunity. *Immunity* 2014; 40(4):542-53.

Angiari S, Constantin G. Regulation of T cell trafficking by the T cell immunoglobulin and mucin domain 1 glycoprotein. *Trends Mol Med*. 2014; 20(12):675-84.

Ascherio A and Munger K. Epidemiology of multiple sclerosis: from risk factors to prevention. *Semin Neurol* 2008; 28:17–28.

Bajénoff M, Egen JG, Koo LY, Laugier JP, Brau F, Glaichenhaus N, Germain RN. Stromal cell networks regulate lymphocyte entry, migration, and territoriality in lymph nodes. *Immunity* 2006; 25:989-1001.

Bajénoff M, Egen JG, Qi H, Huang AYC, Castellino F, Germain RN. Highways, byways and breadcrumbs: directing lymphocyte traffic in the lymph node. *Trends Immunol* 2007; 28:346-52.

Bajénoff M, Glaichenhaus N, Germain RN. Fibroblastic reticular cells guide T lymphocyte entry into and migration within the splenic T cell zone. *J Immunol* 2008; 181:3947-54.

Bartholomäus I, Kawakami N, Odoardi F, Schläger C, Miljkovic D, Ellwart JW, Klinkert WE, Flügel-Koch C, Issekutz TB, Wekerle H, Flügel A. Effector T cell interactions with meningeal vascular structures in nascent autoimmune CNS lesions. *Nature* 2009; 462:94-8.

Bazzoni G and Hemler ME. Are changes in integrin affinity and conformation overemphasized? *Trends Biochem Sci* 1998; 23:30–34.

Becher B, Durell BG, Noelle RJ. Experimental autoimmune encephalitis and inflammation in the absence of interleukin-12. *J Clin Invest* 2002; 110:493–97.

Ben-Nun A, Wekerle H, Cohen IR. The rapid isolation of clonable antigen-specific T lymphocyte lines capable of mediating autoimmune encephalomyelitis. *Eur J Immunol* 1981; 11:195–99.

Bettelli E, Pagany M, Weiner HL, Linington C, Sobel RA, Kuchroo VK. Myelin oligodendrocyte glycoprotein-specific T cell receptor transgenic mice develop spontaneous autoimmune optic neuritis. *J Exp Med* 2003; 197:1073-81.

Bettelli E, Baeten D, Jäger A, Sobel RA, Kuchroo VK. Myelin oligodendrocyte glycoprotein–specific T and B cells cooperate to induce a Devic-like disease in mice. *J Clin Invest* 2006; 116(9): 2393-2402.

Boissonnas A, Fetler L, Zeelenberg IS, Hugues S, Amigorena S. In vivo imaging of cytotoxic T cell infiltration and elimination of a solid tumor. *J Exp Med* 2007; 204: 345-56.

Born J, Lange T, Kern W, McGregor GP, Bickel U, and Fehm HL. Sniffing neuropeptides: a transnasal approach to the human brain. *Nat Neurosci*. 2002; 5:514–16.

Bousso P. T-cell activation by dendritic cells in the lymph node: lessons from the movies. *Nat Rev Immunol,* 2008; 8:675-84.

Brower DL, Brower SM, Hayward DC, Ball EE. Molecular evolution of integrins: genes encoding integrin beta subunits from a coral and a sponge. *Proc Nat Acad Science* 1997; 94(17): 9182-7.

Brucklacher-Waldert V, Stuerner K, Kolster M, Wolthausen J, Tolosa E. Phenotypical and functional characterization of T helper 17 cells in multiple sclerosis. *Brain* 2009; 132:3329-41.

Butti E, Bergami A, Recchia A, Brambilla E, Del Carro U, Amadio S, Cattalini A, Esposito M, Stornaiuolo A, Comi G, Pluchino S, Mavilio F, Martino G, and Furlan R. IL4 gene delivery to the CNS recruits regulatory T cells and induces clinical recovery in mouse models of multiple sclerosis. *Gene Ther*. 2008; 15: 504-15.

Cahalan MD, Parker I. Choreography of cell motility and interaction dynamics imaged by two-photon microscopy in lymphoid organs. *Annu Rev Immunol* 2008; 26:585-626.

Cannella B, Cross AH, Raine CS. Relapsing autoimmune demyelination: A role for vascular addressins. *J Neuroimmunol* 1991; 35: 295–300.

Cannella B and Raine CS. The adhesion molecule and cytokine profile of multiple sclerosis lesions. *Ann. Neurol* 1995, 37: 424-35.

Carman CV, Springer TA. Integrin avidity regulation: are changes in affinity and conformation underemphasized? *Curr Opin Cell Biol* 2003; 15: 547-56.

Chen J, Fujimoto C, Vistica BP, He J, Wawrousek EF, Kelsall B, Gery I. Active participation of antigen-nonspecific lymphoid cells in immune-mediated inflammation. *J Immunol* 2006; 177:3362-8.

Clegg DO, Wingerd KL, Hikita ST, Tolhurst EC. Integrins in the development, function and dysfunction of nervous system. *Front Biosci* 2003; 8:723-50.

Comabella M and Khoury SJ. Immunopathogenesis of multiple sclerosis, *Clinical Immunology* 2012; 142: 2–8.

Compston A, Coles A. Multiple Sclerosis. *Lancet* 2008; 372: 1502-17.

Confavreux C and Vukusic S. Natural history of multiple sclerosis. A unifying concept. *Brain* 2006; 129: 606-16.

Cua DJ, Sherlock J, Chen Y, Murphy CA, Joyce B, Seymour B, Lucian L, To W, Kwan S, Churakova T, Zurawski S, Wiekowski M, Lira SA, Gorman D, Kastelein RA, Sedgwick JD. Interleukin-23 rather than interleukin-12 is the critical cytokine for autoimmune inflammation of the brain. *Nature* 2003; 421:744–48.

Cuzner ML, Gveric D, Strand C, Loughlin AJ, Paemen L, Opdenakker G. The expression of tissue-type plasminogen activator, matrix metalloproteases and endogenous inhibitors in the central nervous system in multiple sclerosis: comparison of stages in lesion evolution. *J Neuropathol Exp Neurol* 1996; 55: 1194-1204.

Davalos D, Lee JK, Smith WB, Brinkman B, Ellisman MH, Zheng B, Akassoglou K. Stable in vivo imaging of densely populated glia, axons and blood vessels in the mouse spinal cord using two-photon microscopy. *J Neurosci Methods* 2008; 169:1-7.
Dityatev A and Fellini T. Extracellular matrix in plasticity and epileptogenesis. *Neuron Glia Biol* 2008; 4:235-47.

Domingues HS, Mues M, Lassmann H, Wekerle H, Krishnamoorthy G. Functional and pathogenic differences of Th1 and Th17 in experimental autoimmune encephalomyelitis. *PLoS One* 2010; 5: e15531.

Dove A. CD18 trials disappoint again. *Nat Biotechnol* 2000; 18:817-18.

Engelhardt B, Melanie Laschinger, Martina Schulz, Ulrike Samulowitz, Dietmar Vestweber, and Gabi Hoch. The development of experimental autoimmune encephalomyelitis in the mouse requires α4-integrin but not αβ47-integrin. *J Clin. Invest* 1998; 102(12) 2096-2105.

Flügel A, Berkowicz T, Ritter T, Labeur M, Jenne DE, Li Z, Ellwart JW, Willem M, Lassmann H, Wekerle H. Migratory activity and functional changes of green fluorescent effector cells before and during experimental autoimmune encephalomyelitis. *Immunity* 2001; 14:547-60.

Frohman EM, Racke MK, Raine CS. Multiple sclerosis – the plaque and its pathogenesis. *N Engl J Med* 2006; 354:942–55.

Friedl P and Gunzer M. Interactions of T cells with APCs. The serial encounter model. *Trends Immunol* 2001; 22(4): 187-91.

Furlan R, Pluchino S, Marconi PC, and Martino G. Cytokine gene delivery into the central nervous system using intrathecally injected nonreplicative viral vectors. *Methods. Mol. Biol.* 2003; 215: 279-89.

Furtado GC, Marcondes MC, Latkowski JA, Tsai J, Wensky A, Lafaille JJ. Swift entry of myelin-specific T lymphocytes into the central nervous system in spontaneous autoimmune encephalomyelitis. *J Immunol* 2008; 181:4648-55.

Gall CM and Lynch G. Integrins, synaptic plasticity and epileptogenesis. *Adv Exp Med Biol* 2004; 548:12-33.

Gately MK, Renzetti LM, Magram J, Stern AS, Adorini L, Gubler U, Presky DH. The interleukin-12/interleukin-12-receptor system: role in normal and pathologic immune responses. *Annu Rev Immunol* 1998; 16:495-521.

Germain RN, Bajénoff M, Castellino F, Chieppa M, Egen JG, Huang AY, Ishii M, Koo LY, Qi H. Making friends in out-of-the-way places: how cells of the immune system get together and how they conduct their business as revealed by intravital imaging. *Immunol Rev* 2008; 221:163-81.

Glatigny S, Duhen R, Oukka, Bettelli E. Cutting Edge: loss of a4 integrin expression differentially affects the homing of Th1 and Th17 cells. *J Immunol* 2011; 187:6176-179.

Ghilardi N, Ouyang W. Targeting the development and effector functions of Th17 cells. *Semin Immunol* 2007; 19:383-93.

Gold R, Linington C, Lassmann H. Understanding pathogenesis and therapy of multiple sclerosis via animal models: 70 years of merits and culprits in experimental autoimmune encephalomyelitis research. *Brain* 2006; 129:1953–71.

Harrington LE, Hatton RD, Mangan PR, Turner H, Murphy TL, Murphy KM, Weaver CT. Interleukin 17- producing CD4+ effector T cells develop via a lineage distinct from the T helper type 1 and 2 lineages. *Nat Immunol* 2005; 6:1123-32.

Herz J, Paterka M, Niesner RA, Brandt AU, Siffrin V, Leuenberger T, Birkenstock J, Mossakowski A, Glumm R, Zipp F and Radbruch H. In vivo imaging of lymphocytes in the CNS reveals different behaviour of naïve T cells in health and autoimmunity. *Journal of Neuroinflammation* 2011**;** 8:131.

Hickey WF, Hsu BL, Kimura H. T lymphocyte entry into the central nervous system. *J Neurosci Res* 1991; 28:254-60.

Hyduk SJ, Rullo J, Cano AP, Xiao H, Chen M, Moser M, Cybulsky MI. Talin-1 and kindlin-3 regulate alpha4beta1 integrin-mediated adhesion stabilization, but not G protein-coupled receptor-induced affinity upregulation. *J Immunol* 2011;15; 187(8):4360-8.

Horwitz AR and Parsons JT. Cell migration-movin'on. *Science* 1999; 286:1102-3.

Hovens IB, Nyakas C, Schoemaker RG. A novel method for evaluating microglial activation using ionized calcium-binding adaptor protein-1 staining: cell body to cell size ratio. *Neuroimmnol Neuroinflammation* 2014; 1(2):82-4.

Issazadeh S, Mustafa M, Ljungdahl A, Hojeberg B, Dagerlind A, Elde R, Olsson T. Interferon gamma, interleukin 4 and transforming growth factor beta in experimental autoimmune encephalomyelitis in Lewis rats: dynamics of cellular mRNA expression in the central nervous system and lymphoid cells. *J Neurosci Res* 1995; 40:579–90.

Ivanov II, McKenzie BS, Zhou L, Tadokoro CE, Lepelley A, Lafaille JJ, Cua DJ, Littman DR. The orphan nuclear receptor RORgammat directs the differentiation program of proinflammatory IL-17+ T helper cells. *Cell* 2006; 126:1121-33.

Kabat EA, Wolf A, Bezer AE. Rapid production of acute disseminated encephalomyelitis in Rhesus Monkeys by injection of brain tissue with adjuvants. *Science* 1946; 104:362–63.

Kader M, Wang X, Piatak M, Lifson J, Roederer M, Veazey R, Mattapallil JJ. Alpha4(+)beta7(hi)CD4(+) memory T cells harbor most Th-17 cells and are preferentially infected during acute SIV infection. *Mucosal Immunol* 2009; 2:439-49.

Kanwar JR, Harrison JEB, Wang D, Leung E, Mueller W, Wagner N, Krissansen GW. β7 integrins contribute to demyelinating disease of the central nervous system. *J Neuroimmunol* 2000; 103: 146-52.

Kanwar JR, Kanwar RK, Wang D, Krissansen GW. Prevention of a chronic progressive form of experimental autoimmune encephalomyelitis by an antibody against mucosal addressin cell adhesion molecule-1, given early in the course of disease progression. *Immunol Cell Biol* 2000; 78: 641-45.

Kapsenberg ML, Dendritic-cell control of pathogen-driven T-cell polarization. *Nature Reviews Immunology* 2003; 12: 984–93.

Kawakami N, Nägerl UV, Odoardi F, Bonhoeffer T, Wekerle H, Flügel A. Live imaging of effector cell trafficking and autoantigen recognition within the unfolding autoimmune encephalomyelitis lesion. *J Exp Med* 2005; 201:1805-14.

Kim JV, Kang SS, Dustin ML, McGavern DB. Myelomonocytic cell recruitment causes fatal CNS vascular injury during acute viral meningitis. *Nature* 2009, 457:191-5.

Kim JV, Jiang N, Tadokoro CE, Liu L, Ransohoff RM, Lafaille JJ, Dustin ML. Two-photon laser scanning microscopy imaging of intact spinal cord and cerebral cortex reveals requirement for CXCR6 and neuroinflammation in immune cell infiltration of cortical injury sites. *J Immunol Methods* 2010; 352: 89-100.

Kivisäkk P, Imitola J, Rasmussen S, Elyaman W, Zhu B, Ransohoff RM, Khoury SJ. Localizing central nervous system immune surveillance: meningeal antigen-presenting cells activate T cells during experimental autoimmune encephalomyelitis.
Ann Neurol 2009; 65(4):457-69.

Komiyama Y, Nakae S, Matsuki T, Nambu A, Ishigame H, Kakuta S, Sudo K, Iwakura Y. IL-17 plays an important role in the development of experimental autoimmune encephalomyelitis. J Immunol 2006; 177(1): 566-73.

Korn T, Reddy J, Gao W, Bettelli E, Awasthi A, Petersen TR, Backstrom BT, Sobel RA, Wucherpfennig KW, Strom TB, Oukka M, Kuchroo VK. Myelin-specific regulatory T cells accumulate in the CNS but fail to control autoimmune inflammation. *Nat Med* 2007; 13:423-31.

Krishnamoorthy G, Lassmann H, Wekerle H, Holz A. Spontaneous opticospinal encephalomyelitis in a double-transgenic mouse model of autoimmune T cell/B cell cooperation. *J Clin Invest* 2006; 116(9): 2385-92.

Kroenke MA, Carlson TJ, Andjelkovic AV, Segal BM. IL-12-and IL-23-modulated T cells induce distinct types of EAE based on histology, CNS chemokine profile, and response to cytokine inhibition. *J Exp Med* 2008; 205:1535–41.

Krull KR, Hockenberry MJ, Miketova P, Carey M, Moore I. Chemotherapy-related changes in central nervous system phospholipids and neurocognitive function in childhood acute lymphoblastic leukemia. *Leuk Lymphoma* 2013; 54(3): 535-40.

Lämmermann T and Sixt M. Mechanical modes of 'amoeboid' cell migration. *Curr Opin Cell Biol* 2009; 21:636–44.

Langrish CL, Chen Y, Blumenschein WM, Mattson J, Basham B, Sedgwick JD, McClanahan T, Kastelein RA, Cua DJ. IL-23 drives a pathogenic T cell population that induces autoimmune inflammation. *J Exp Med* 2005; 201:233–40.

Larochelle C, Cayrol R, Kebir H, Alvarez JI, Le´cuyer MA, Ifergan I, Viel E, Bourbonnie` re L, Beauseigle D,Terouz S, Hachehouche L, Gendron S, Jose´e Poirier J, Jobin C, Duquette P, Flanagan K, Yednock T, Arbour N, Prat A. Melanoma cell adhesion molecule identifies encephalitogenic T lymphocytes and promotes their recruitment to the central nervous system. *Brain* 2012; 135: 2906-24.

Lehnert K, Print CG, Yang Y, Krissansen GW. Mucosal addressin cell adhesion

molecule-1 (MAdCAM-1) costimulates T cell proliferation exclusively through integrin a4b7 (LPAM- 1), whereas VCAM-1 and CS-1 peptide use a4b1 (VLA-4): Evidence for 'remote' costimulation and induction of hyperresponsiveness to B7 molecules. *Eur J Immunol* 1998; 28: 3605-15.

Leonard JP, Waldburger KE, Goldman SJ. Prevention of experimental autoimmune encephalomyelitis by antibodies against interleukin 12. *J Exp Med* 1995; 181:381-86.

Ley K and Kansas GS. Selectins in T-cell recruitment to non-lymphoid tissues and sites of inflammation. *Nat Rev Immunol* 2004; 4:325-35.

Ley K, Laudanna C, Cybulsky MI, Nourshargh S. Getting to the site of inflammation: the leukocyte adhesion cascade updated. *Nat Rev Immunol* 2007; 7:678-89.

Lock C, Hermans G, Pedotti R, Brendolan A, Schadt E, Garren H, Langer-Gould A, Strober S, Cannella B, Allard J, Klonowski P, Austin A, Lad N, Kaminski N, Galli SJ, Oksenberg JR, Raine CS, Heller R, Steinman L. Gene-microarray analysis of multiple sclerosis lesions yields new targets validated in autoimmune encephalomyelitis. *Nat Med* 2002; 8:500–08.

Lucchinetti C, Brück W, Parisi J, Scheithauer B, Rodriguez M, Lassmann H. Heterogeneity of multiple sclerosis lesions: implications for the pathogenesis of demyelination. *Ann Neurol*, 2000; 47(6):707-17.

Luster AD, Alon R, Von Andrian UH. Immune cell migration in inflammation: present and future therapeutic targets. *Nat Immunol* 2005; 6: 1182-90.

Matz MV, Fradkov AF, Labas YA, Savitsky AP, Zaraisky AG, Markelov ML, Lukyanov SA. Fluorescent proteins from nonbioluminescent Anthozoa species. *Nat Biotech* 1999; 17:969–73.

McGavern DB, Murray PD, and Rodriguez M. Quantitation of spinal cord demyelination, remyelination, atrophy, and axonal loss in a model of progressive neurologic injury. *Neurosci. Res*. 1999; 58: 492-504.

McGeachy MJ, Chen J, Tato CM, Laurence A, Joyce-Shaikh B, Blumenschein WM, McClanahan TK, O'Shea JJ, Cua DJ. The interleukin 23 receptor is essential for the terminal differentiation of interleukin 17-producing effector T helper cells in vivo. *Nat Immunol* 2009; 10:314-24.

Mempel TR, Henrickson SE, Von Andrian UH. T-cell priming by dendritic cells in lymph nodes occurs in three distinct phases. *Nature* 2004; 427:154-9.

Mempel TR, Junt T, von Andrian UH. Rulers over randomness: stroma cells guide lymphocyte migration in lymph nodes. *Immunity* 2006; 25:867- 69.

Miller MJ, Wei SH, Parker I, Cahalan MD. Two-photon imaging of lymphocyte motility and antigen response in intact lymph node. *Science* 2002; 296:1869-73.

Miller MJ, Wei SH, Cahalan MD, Parker I. Autonomous T cell trafficking examined in vivo with intravital two-photon microscopy. *Proc Natl Acad Sci U S A* 2003; 100:2604-9.

Miossec P, Korn T, Kuchroo VK. Interleukin 17 and type 17 helper T cells. *N Engl J Med* 2009; 361:888–98.

Mrass P and Weninger W. Immune cell migration as a means to control immune privilege: Lessons from the CNS and tumors. Immunol Rev, 2006; 213:195–212.

Noonan CW, Kathman SJ, White MC. Prevalence estimates for MS in the United States and evidence of an increasing trend for women. *Neurology* 2002; 58:136-8.

O'Connor RA, Prendergast CT, Sabatos CA, Lau CW, Leech MV, Wraith DC, Anderton SM. Cutting edge: Th1 cells facilitate the entry of Th17 cells to the central nervous system during experimental autoimmune encephalomyelitis. *J Immunol* 2008; 181:3750–4.

Odoardi F, Kawakami N, Klinkert WE, Wekerle H, Flügel A. Blood-borne soluble protein antigen intensifies T cell activation in autoimmune CNS lesions and exacerbates clinical disease. *Proc Natl Acad Sci U S A* 2007; 104:18625-30.

Olsson T. Cytokines in neuroinflammatory disease: role of myelin autoreactive T cell production of interferon-gamma. *J Neuroimmunol* 1992; 40:211–18.

Oppmann B, Lesley R, Blom B, Timans JC, Xu Y, Hunte B, Vega F, Yu N, Wang J, Singh K, Zonin F, Vaisberg E, Churakova T, Liu M, Gorman D, Wagner J, Zurawski S, Liu Y, Abrams JS, Moore KW, Rennick D, de Waal-Malefyt R, Hannum C, Bazan JF, Kastelein RA. Novel p19 protein engages IL-12p40 to form a cytokine, IL-23, with biological activities similar as well as distinct from IL-12. *Immunity* 2000; 13:715–25.

Orrell RW. Multiple sclerosis: the history of a disease. *J R Soc Med* 2005; 98(6):289.

Orton SM, Herrera BM, Yee IM, Valdar W, Ramagopalan SV, Sadovnick AD, Ebers GC, Canadian Collaborative Study. Sex ratio of multiple sclerosis in Canada: a longitudinal study. *Lancet Neurol* 2006; 5: 932–36.

Park H, Li Z, Yang XO, Chang SH, Nurieva R, Wang YH, Wang Y, Hood L, Zhu Z, Tian Q, Dong C. A distinct lineage of CD4 T cells regulates tissue inflammation by producing interleukin 17. *Nat Immunol* 2005; 6:1133–41.

Pesic M, Bartholomäus I, Kyratsous NI, Heissmeyer V, Wekerle H, Kawakami N. 2-photon imaging of phagocyte-mediated T cell activation in the CNS. *J Clin Invest* 2013; 123:1192-1201.

Piccio L, Rossi B, Scarpini E, Laudanna C, Giagulli C, Issekutz AC, Vestweber D, Butcher EC, Constantin G. Molecular mechanisms involved in lymphocyte recruitment in inflamed brain microvessels: critical roles for P-selectin glycoprotein ligand-1 and heterotrimeric Gi-linked receptors. *J Immunol* 2002; 168: 1940-49.

Pillet MJ and Weissleder R. Intravital imaging. *Cell* 2011; 147:983-91.

Plog BA, Moll KM, Kang H, Iliff JJ, Dashnaw ML, Nedergaard M, Vates GE. A novel technique for morphometric quantification of subarachnoid hemorrhage-induced microglia activation. *J Neurosci Methods* 2014; 229:44-52.

Pompe RS, von Bueren AO, Mynarek M, von Hoff K, Friedrich C, Kwiecien R, Treulieb W, Lindow C, Deinlein F, Fleischhack G, Kuehl J, Rutkowski S. Intraventricular methotrexate as part of primary therapy for children with infant and/or metastatic medulloblastoma: Feasibility, acute toxicity and evidence for efficacy. *Eur J Cancer* 2015; 51(17):2634-42.

Porter JC, Bracke M, Smith A, Davies D, Hogg N. Signaling through integrin LFA-1 leads to filamentous actin polymerization and remodeling, resulting in enhanced T cell adhesion. *J Immunol* 2002; 168:6330-35.

Prendergast CT, Anderton SM. Immune cell entry to central nervous system. Current understanding and prospective therapeutic targets. *Endocr Metab Immune Disord Drug Targets*, 2009; 9:315–27.

Prineas JW. Handbook of Multiple Sclerosis (ed. Cook, S.D.), Marcel Dekker, Newark NJ 1996; 223–55.

Pugliatti M, Rosati G, Carton H, Riise T, Drulovic J, Vécsei L, Milanov I. The epidemiology of multiple sclerosis in Europe. *Eur J Neurol* 2006; 13:700–22.

Puré E, Cuff CA. A crucial role for CD44 in inflammation. *Trends Mol Med* 2011; 7 (5): 213–21.

Ransohoff RM, Kivisäkk P, Kidd G. Three or more routes for leukocyte migration into the central nervous system. *Nat Rev Immunol* 2003; 3(7):569-81.

Reboldi A, Coisne A, Baumjohann D, Benvenuto F, Bottinelli D, Lira S, Uccelli A, Lanzavecchia A, Engelhardt B, Sallusto F. C-C chemokine receptor 6–regulated entry of TH-17 cells into the CNS through the choroid plexus is required for the initiation of EAE. *Nat Immunol* 2009; 10(5): 514-23.

Riva D, Giorgi C, Nichelli F, Bulgheroni S, Massimino M, Cefalo G, Gandola L, Giannotta M, Bagnasco I, Saletti V, Pantaleoni C. Intrathecal methotrexate affects cognitive function in children with medulloblastoma. *Neurology* 2002; 59(1):48-53.

Rivers TM, Schwentker FF. Encephalomyelitis accompanied by myelin destruction experimentally produced in monkeys. *J Exp Med* 1935; 61:689–702.

Rossi B, Angiari S, Zenaro E, Budui SL, and Constantin G. Vascular inflammation in central nervous system diseases: adhesion receptors controlling leukocyte–endothelial interactions**.** *J Leukoc Biol,* 2010; 89(4): 539-56.

Rossi B, Constantin G. Live imaging of immune responses in experimental models of multiple sclerosis. *Front Immunol* 2016; 7:506.

Rothhammer V, Heink S, Petermann F, Srivastava R, Claussen MC, Hemmer B, Korn T. Th17 lymphocytes traffic to the central nervous system independently of α4 integrin expression during EAE. *J Exp Med* 2011; 208:2465-76.

Sands BE. Leukocyte anti-trafficking strategies: current status and future directions. *Dig Dis* 2017; 35:13-20.

Sakaguchi S, Sakaguchi N, Asano M, Itoh M, Toda M. Immunologic self-tolerance maintained by activated T cells expressing IL-2 receptor alpha-chains (CD25). Breakdown of a single mechanism of self-tolerance causes various autoimmune diseases. *J. Immunol* 1995; 155:1151-64.

Schläger C, Körner H, Krueger M, Vidoli S, Haberl M, Mielke D, Brylla E, Issekutz T, Cabañas C, Nelson PJ, Ziemssen T, Rohde V, Bechmann I, Lodygin D, Odoardi F, Flügel A. Effector T-cell trafficking between the leptomeninges and the cerebrospinal fluid. *Nature* 2016; 530(7590):349-53.

Serafini B, Columba-Cabezas S, Di Rosa F, Aloisi F. Intracerebral recruitment and maturation of dendritic cells in the onset and progression of experimental autoimmune encephalomyelitis. *Am J Pathol* 2000; 6:1991-2002.

Serafini B, Rosicarelli B, Magliozzi R, Stigliano E, Capello E, Mancardi GL, Aloisi F. Dendritic cells in multiple sclerosis lesions: maturation stage, myelin uptake, and interaction with proliferating T cells. *J Neuropathol Exp Neurol* 2006; 65:124-41.

Serrador JM, Nieto M, Sánchez-Madrid F. Cytoskeletal rearrangement during migration and activation of T lymphocytes. *Trends Cell Biol* 1999; 9:228-33.

Siffrin V, Brandt AU, Radbruch H, Herz J, Boldakowa N, Leuenberger T, Werr J, Hahner A, Schulze-Topphoff U, Nitsch R, Zipp F. Differential immune cell dynamics in the CNS cause CD4+ T cell compartmentalization. *Brain* 2009; 132:1247-58.

Siffrin V, Radbruch H, Glumm R, Niesner R, Paterka M, Herz J, Leuenberger T, Lehmann SM, Luenstedt S, Rinnenthal JL, Laube G, Luche H, Lehnardt S, Fehling HJ, Griesbeck O, Frauke Zipp F. In vivo imaging of partially reversible Th17 cell-induced neuronal dysfunction in the course of encephalomyelitis. *Immunity* 2010; 33: 424-36.

Smith A, Stanley P, Jones K, Svensson L, McDowall A, Hogg N. The role of the integrin LFA-1 in T-lymhocyte migration. *Immunol Rev* 2007; 218:135-46.

So P TC. Two-photon fluorescence light microscopy. *Encyclopedia of life sciences* 2002.

Sørensen TL, Tani M, Jensen J, Pierce V, Lucchinetti C, Folcik VA, Qin S, Rottman J, Sellebjerg F, Strieter RM, Frederiksen JL, Ransohoff RM. Expression of specific chemokines and chemokine receptors in the central nervous system of multiple sclerosis patients. *J Clin Invest* 1999; 103:807-15.

Springer TA, and **Dustin ML**. Integrin inside-out signaling and the immunological synapse. *Curr Opin Cell Biol*. 2012; 24:107-15.

Steinman L. Blocking adhesion molecules as therapy for multiple sclerosis: natalizumab. *Nat Rev Drug Discov* 2005; 4:510-18.

Stockinger B, Veldhoen M. Differentiation and function of Th17 T cells. *Curr Opin Immunol* 2007; 19:281-6.

Stromnes IM, Cerretti LM, Liggitt D, Harris RA, Goverman JM. Differential regulation of central nervous system autoimmunity by Th1 and Th17 cells. *Nat Med* 2008; 14:337–42.

Sumen C, Mempel TR, Mazo IB, von Andrian UH. Intravital microscopy: visualizing immunity in context. *Immunity* 2004; 21: 315-29.

Szabo MC, Butcher EC, McEvoy LM. Specialization of mucosal follicular dendritic cells revealed by mucosal addressin-cell adhesion molecule-1 display. *J Immunol* 1997; 158: 5584–8.

Tian L, Lappalainen J, Autero M, Hänninen S, Rauvala H and Gahmberg CG. Shedded neuronal ICAM-5 suppresses T-cell activation. *Blood*. 2008; 111:3615-25.

Traugott U and Lebon P. Multiple sclerosis: involvement of interferons in lesion pathogenesis. *Ann Neurol* 1988; 24:243-51.

von Andrian UH and Mackay CR. T-cell function and migration. Two sides of the same coin. *N Engl J Med* 2000; 343:1020-34.

Wekerle H, Linington C, Lassmann H, Meyermann R. Cellular immune reactivity within the CNS. *Trends Neurosci*, 1986; 9:271-77.

Wilson EH, Harris TH, Mrass P, John B, Tait ED, Wu GF, Pepper M, Wherry EJ, Dzierzinski F, Roos D, Haydon PG, Laufer TM, Weninger W, Hunter CA. Behavior of parasite-specific effector CD8+ T cells in the brain and visualization of a kinesis-associated system of reticular fibers. *Immunity* 2009; 30:300-11.

Woolacott N, Hawkins N, Mason A, Kainth A, Khadjesari Z, Vergel YB, Misso K, Light K, Chalmers R, Sculpher M, Riemsma R. Etanercept and efalizumab for the treatment of psoriasis: a systematic review. *Health Technol Assess* 2006; 10:1-233.

Worthylake RA, Burridge K. Leukocyte transendothelial migration: orchestrating the underlying molecular machinery. *Curr Opin Cell Biol* 2001; 13:569-77**.**

Wu X, Reddy DS. Integrins as receptor targets for neurological disorders. *Pharmacol Ther* 2012; 134:68-81.

Wucherpfenning KW and Strominger JL. Molecular mimicry in T cell-mediated autoimmunity: viral peptides activate human T cell clones specific for myelin basic protein**.** *Cell* 1995; 80(5): 695-705.

Yamazaki T, Yang XO, Chung Y, Fukunaga A, Nurieva R, Pappu B, Martin-Orozco N, Kang HS, Ma L, Panopoulos AD, Craig S, Watowich SS, Jetten AM, Tian Q, Dong C. CCR6 Regulates the Migration of Inflammatory and Regulatory T Cells. J Immunol 2008; 181(12): 8391-8401.

Yang XO, Nurieva R, Martinez GJ, Kang HS, Chung Y, Pappu BP, Shah B, Chang SH, Schluns KS, Watowich SS, Feng XH, Jetten AM, Dong C**.** Molecular antagonism and plasticity of regulatory and inflammatory T cell programs. *Immunity* 2008; 29(1): 44-56.

Zamvil SS and Steinmann L. The T lymphocytes in experimental allergic encephalomyelitis. *Annu Rev Immunol* 1990; 8:579-621.

Zenaro, E, Rossi B, Angiari S, and Constantin G. Use of imaging to study leukocyte trafficking in the central nervous system. *Immunol Cell Biol* 2013; 9: 271-80.

Zenaro E, Pietronigro E, Della Bianca V, Piacentino G, Marongiu L, Budui S, Turano E, Rossi B, Angiari S, Dusi S, Montresor A, Carlucci T, Nanì S, Tosadori G, Calciano L, Catalucci D, Berton G, Bonetti B and Constantin G. Neutrophils promote Alzheimer's disease-like pathology and cognitive decline via LFA-1 integrin. *Nat Med* 2015; 21: 880-86.